

**BONDING MATERIAL COATED CLAY FOR IMPROVING PAPER
PROPERTIES**

A Dissertation
Presented to
The Academic Faculty

by

Se-Young Yoon

In Partial Fulfillment
of the Requirements for the Degree
Doctor of Philosophy in the
School of Chemical and Biomolecular Engineering

Georgia Institute of Technology
May 2007

Copyright 2007 by Se-Young Yoon

BOND MATERIAL COATED CLAY FOR IMPROVING PAPER PROPERTIES

Approved by:

Dr. Yulin Deng, Advisor
School of Chemical & Biomolecular
Engineering
Georgia Institute of Technology

Dr. Jeff Empie
School of Chemical & Biomolecular
Engineering
Georgia Institute of Technology

Dr. Art Ragauskas
School of Chemical & Biomolecular
Engineering
School of Chemistry & Biochemistry

Dr. Jeff Hsieh
School of Chemical & Biomolecular
Engineering
Georgia Institute of Technology

Dr. Sujit Banerjee
School of Chemical & Biomolecular
Engineering
Georgia Institute of Technology

Date Approved: April 2, 2007

*To my parents, Jonglak Yoon and Yeonhee Kwon,
and
To my wife, Jinhee Lee, son, Donghyeok, daughter, Youngshin*

ACKNOWLEDGEMENTS

I would like to take this opportunity to thank those who have made this thesis possible. First of all, I would like to thank my advisor Dr. Yulin Deng for guiding me through my graduate studies at IPST and Georgia Tech. During the past six years, he has shown me not only scientific knowledge or logical way to solve the problem but also the passion and creativity for the research. I also greatly appreciate all the helpful comments and guidance given to me from my thesis committee: Dr. Sujit Banerjee, Dr. Jeff Hsieh, Dr. Art Ragauskas, and Dr. Jeff Empie. I would like to thank the Institute of Paper Science and Technology and all the member companies for their support. Thanks also goes out to my lab colleagues Dr. Myungchul Park, Dr. Jeonghyun Yeom, Dr. Qunhui Sun, Dr. Yulin Zhao, Dr. Zegui Yan, Jihoon, Ying, Zhouhi, Kim, Brett, Delong, Zhengzhi, Hongta. Thanks to my fellow students, Brett, Andy, Cam, Rob, Fran, Jim, Witchit, Shila. I thank Korean students in the department for keeping things fun: Seongho, Yeuchun, Jeongwoo, Ingu, Jaekyu, Jinhoon, Kwanghun, Taehyun, Hyea, Junghyun, and Jongsuk. I want to thank my former advisors Prof. Jungsoo Oh at Dongguk University and Prof. Byungmook Jo at Kwanwon National University for helping me set foot onto the path of the wood and paper science. I cannot possible thank my parents enough. They have supported me all my life and I am truly blessed to have such a wonderful parents. They provided the encouragement to continue my education and gave me the determination to see it through.

Last, but not least, I would like to thank my family for enduring my long hours at school. My wife, Jinhee, and my children, Donhyeok and Youngshin made this possible.

TABLE OF CONTENTS

ACKNOWLEDGEMENTS	IV
LIST OF TABLES	IX
LIST OF FIGURES	X
LIST OF EQUATIONS.....	XIV
NOMENCLATURE.....	XVI
SUMMARY	XX
CHAPTER 1: INTRODUCTION.....	1
CHAPTER 2: LITERATURE REVIEW.....	3
2.1 PAPERMAKING FIBERS	3
2.1.1 Wood fiber types.....	3
2.1.2 Compositions of Wood Fibers	5
2.1.3 Cell Wall Structure of Wood Fibers	10
2.1.4 Effect of fiber structure and operations on paper properties.....	12
2.2 FILLER.....	17
2.2.1 Kaolin clay filler pigments.....	17
2.2.2 Effect of fillers on paper physical properties.....	21
2.2.3 Effect of fillers on paper optical properties	22
2.2.4 Effect of fillers on other properties of paper and papermaking process	27
2.3 FILLER RETENTION	29
2.3.1 Retention mechanism.....	30
2.3.2 Retention aid systems	34
2.4 PROBLEMS OF CONVENTIONAL WET-END SYSTEMS	41

CHAPTER 3: PROBLEM ANALYSIS AND OBJECTIVES	54
3.1 PROBLEM STATEMENT	54
3.2 PROBLEM ANALYSIS	54
3.3 HYPOTHESIS	55
3.4 OBJECTIVES	57
3.4.1 Preparation of coated fillers with bonding materials	57
3.4.2 Determination of the physical and optical properties of filled sheets.....	58
3.4.3 Tensile strength modeling.....	58
 CHAPTER 4: STARCH-BASED CLAY COMPOSITES BY AMMONIUM SULFATE PRECIPITATION METHOD.....	 59
4.1 BACKGROUND - STRUCTURE AND CHARACTERISTICS OF STARCH.....	60
4.2 INTRODUCTION.....	65
4.3 METHOD	68
4.3.1 Material	68
4.3.2 Preparation	69
4.3.3 Characterization of fibrous clay-starch composites	70
4.3.4 Handsheets preparation and determination of paper properties.....	71
4.4 RESULTS AND DISCUSSION	71
4.4.1 Characterization of the clay-starch composites	71
4.4.2 The effects of clay-starch composites on paper strength and optical properties	75
4.4.3 Bonding of clay-starch composites with fiber	80
4.5 CONCLUSIONS.....	84

CHAPTER 5: STARCH-FATTY COMPLEX MODIFIED FILLER FOR PAPERMAKING	85
5.1 BACKGROUND - STARCH-FATTY ACID INCLUSION COMPLEX	86
5.2 INTRODUCTION.....	89
5.3 METHOD	92
5.3.1 Material	92
5.3.2 Preparation	92
5.3.3 Characterization of clay-starch composites by starch-fatty acid complex.....	94
5.3.4 Handsheets preparation and determination of paper properties.....	96
5.4 RESULTS AND DISCUSSION.....	97
5.4.1 Starch-fatty acid complex formation	97
5.4.2 Starch-fatty acid-clay composite formation.....	99
5.4.3 The effects of clay-starch composites on paper strength and optical properties	107
5.4.4 The effects of clay-starch composites on water repellent property of paper .	114
 CHAPTER 6: CLAY-CELLULOSE COMPOSITE BY CELLULOSE DISSOLUTION METHOD.....	120
6.1 BACKGROUND.....	120
6.2 INTRODUCTION.....	124
6.3 METHOD	126

6.3.1 Material	126
6.3.2 Preparation	127
6.3.3 Characterization of fibrous clay-starch composites	128
6.3.4 Handsheets preparation and determination of paper properties.....	128
6.4 RESULTS	129
6.4.1 Characterization of the clay-cellulose composites.....	129
6.4.2 The effects of clay-cellulose composites on paper strength and optical properties.....	134
6.5 CONCLUSION.....	138

**CHAPTER 7: EXPERIMENTAL AND MODELING STUDY OF THE
STRENGTH PROPERTIES OF CLAY-STARCH COMPOSITE FILLED PAPERS**

.....	139
7.1 BACKGROUND - THEORIES OF PAPER STRENGTH	140
7.2 INTRODUCTION.....	148
7.3 EXPERIMENTAL	154
7.3.1 Materials	154
7.3.2 Preparation of clay-starch composites	155
7.3.3 Handsheet preparation and determination of paper physical properties	155
7.3.4 Specific bonding strength measurement	156
7.3.5 Determination of Specific Surface Area for Tensile Strength Modeling	158
7.3.6 Tensile strength modeling.....	159
7.3.7 Stiffness Modeling from Modeled Tensile strength	162
7.4 RESULTS AND DISCUSSION.....	164

7.4.1 Specific bond strength of starch-clay composites with wood fibers and their specific surface area	164
7.4.2 ZDT modeling of starch-clay composite filled handsheets	166
7.4.3 Tensile strength modeling.....	167
7.4.4 Stiffness Modeling.....	172
7.5 CONCLUSIONS.....	175
CHAPTER 8: OVERALL CONCLUSION.....	177
CHAPTER 9: FUTURE WORK.....	179
APPENDIX A: COPYRIGHT PERMISSIONS	181
REFERENCES.....	184

LIST OF TABLES

Table 1: Typical compositions of softwood and hardwood	5
--	---

Table 2: Major hemicellulose components	8
Table 3: Properties of fractionated fiber populations and handsheets made from them .	12
Table 4: General physical properties of typical filler pigments.....	20
Table 5: Scattering coefficient and refractive index of components included in paper....	25
Table 6: Effect of increased filler content during papermaking	28
Table 7: Specific surface area of starch-clay composites and their specific shear bond strength with wood fibers.....	166

LIST OF FIGURES

Figure 1: Cellulose structure.....	6
Figure 2: Fringed micelle model of polymers and scheme of cellulose degradation	7

Figure 3: Galactoglucomannan structure in softwood	8
Figure 4: Glucuronoxylan structure in hardwood	9
Figure 5: Lignin structure	9
Figure 6: Simplified structure of woody cell	11
Figure 7: Cross-section and external surface of well-beaten kraft fiber	15
Figure 8: Different types of clay	18
Figure 9: Mineral structure of kaolin clay	19
Figure 10: Effect of filler particle size on the burst strength of paper	22
Figure 11: Effect of filler particle size on light scattering coefficient of paper	26
Figure 12: Pictorial representation of patch flocculation	31
Figure 13: Effect of PDADMAC on flocculation and reflocculation	32
Figure 14: Pictorial representation of bridging flocculation	33
Figure 15: Effect of CPAM on flocculation and reflocculation	35
Figure 16: Effect of PDADMAC and PAM on flocculation and reflocculation	36
Figure 17: Reflocculation of the dual system related with zeta potential	44
Figure 18: Ionization of carboxyl and tertiary amine group	46
Figure 19: Effect of pH on the charge of various polyelectrolytes	47
Figure 20: Filler preflocculation	55
Figure 21: Coated fillers with bonding material	56
Figure 22: Scheme of bonding between fibers and clay or coated clay	56
Figure 23: Schematic representation of starch granule structure	61
Figure 24: Helix packing and unit cells in A-type (left) and B-type (right) crystalline ...	62
Figure 25: Behavior of amylose in solution and starch crystallinity	63

Figure 26: Preparation of clay-starch composite by salt precipitation method	69
Figure 27: Morphology of clay-starch composite.....	72
Figure 28: Starch swelling power and solubility at different temperatures	74
Figure 29: Tensile strength as a function of filler content.....	75
Figure 30: ZDT (Zero directional tensile) strength as a function of filler content	77
Figure 31: Burst strength as a function of filler content	78
Figure 32: Folding strength as a function of filler content	78
Figure 33: Tensile index vs. ISO Brightness	79
Figure 34: Tensile index vs. Tappi opacity.....	80
Figure 35: SEM pictures of clay-starch composites filled handsheets	81
Figure 36: Model of helical starch chain with iodine molecules	87
Figure 37: Fatty acid inside the helix cavity and conformations	88
Figure 38: Preparation of clay starch composite by starch-fatty acid complexation.....	93
Figure 39: Schematic representation of the FBRM system	94
Figure 40: Change of soluble starch amount with different ratios of palmitic acid	98
Figure 41: X-ray diffractions of starch-palmitic acid complexes	99
Figure 42: Starch solubility and swelling power at different temperatures.....	100
Figure 43: X-ray diffractions of coated clays with different temperatures.....	101
Figure 44: Starch solubility and swelling power at different pH.....	102
Figure 45: X-ray diffractions of coated clays with different pH	103
Figure 46: The change of starch solubility and swelling power at different time	104
Figure 47: X-ray diffractions of coated clays with different time	105
Figure 48: SEM pictures of unmodified clay (above) and clay-starch composites	106

Figure 49: Change of composite size as a function of time at different formation pH...	107
Figure 50: Tensile strengths of the handsheet as a function of filler addition	108
Figure 51: Effect of clay-starch composite on ZDT strength of the handsheets	110
Figure 52: Effect of clay-starch composites on brightness of the handsheets	111
Figure 53: SEM pictures of clay-starch composites filled handsheets	114
Figure 54: Photographs of water drops on the composite filled handsheets.....	117
Figure 55: Wettability (R) of composite filled handsheets.....	118
Figure 56: Hemolytic and heterolytic degradation reactions of NMMO.....	121
Figure 57: Cellulose chain scission as a consequence of hemolytic reactions	121
Figure 58: Heterolytic oxidation of cellulose by NMMO	122
Figure 59: Reactions of propyl gallate as radical trap	123
Figure 60: Process principles in regenerated cellulose technologies.....	125
Figure 61: Schematic structure of the NMMO solvent.....	126
Figure 62: Preparation of coated clay with cellulose.....	128
Figure 63: SEM of untreated TiO ₂	129
Figure 64: SEM of TiO ₂ -cellulose (10 wt. % based on the solid TiO ₂) composite	130
Figure 65: Morphology of clay-cellulose (UKP) composite from SEM	131
Figure 66: Microscopic surface of clay-cellulose (DIP) composite from SEM	132
Figure 67: Microscopic surface of clay-cellulose (BKP) composite from SEM.....	133
Figure 68: Microscopic surface of clay-cellulose (UKP) composite from SEM.....	133
Figure 69: Tensile index as a function of clay or composite dosage	134
Figure 70: Bust index as a function of clay or composite dosage	135
Figure 71: Folding strength as a function of clay or composite dosage	136

Figure 72: Opacity as a function of clay or composite dosage	137
Figure 73: Brightness as a function of clay or composite dosage.....	137
Figure 74: Areas of interest in fiber-fiber bonding.....	145
Figure 75: Predictions from Page equation.....	147
Figure 76: Schematic drawing of sample assembly and the tensile strength test	157
Figure 77: RBA between two fibers in the absence or presence of fillers/ composites .	160
Figure 78: Calculated dimensionless ZDT	165
Figure 79: Calculation of ZDT based on BTM theory	167
Figure 80: Zero span beaking length as a function of filler content in paper	168
Figure 81: Experimental data (points) and modeling results (lines) of tensile strength .	169
Figure 82: Calculated tensile strengths for different specific bond strength	170
Figure 83: Theoretical tensile strength changes for different k and S_c/S_f values	171
Figure 84 : Stiffness modeling for different starch to filler ratios	173
Figure 85: The change of thickness as a function of clay and composite dosage	174
Figure 86: Effect of specific bond strength on stiffness assuming thickness is constant	175

LIST OF EQUATIONS

Equation 1: Specific scattering coefficient	23
---	----

Equation 2: Adsorption coefficient.....	23
Equation 3: Reflectivity	23
Equation 4: Opacity	24
Equation 5: Light scattering coefficient of filled paper	24
Equation 6: The maximum floc size in a suspension.....	39
Equation 7: Reversibility index	40
Equation 8: Formation number	44
Equation 9: Starch solubility in water.....	71
Equation 10: Swelling power.....	71
Equation 11: Washburn Equation.....	115
Equation 12: Young Equation.....	115
Equation 13: The strength of well-bonded paper.....	140
Equation 14: Tensile strength of a random two-dimensional sheet.....	140
Equation 15: Tensile strength of a random two-dimensional sheet.....	141
Equation 16: Specific tensile strength of a random two-dimensional sheet.....	141
Equation 17: Specific tensile strength of a random two-dimensional sheet considering efficiency function	141
Equation 18: Shear lag analysis by fiber failure	142
Equation 19: Shear lag analysis by bond failure.....	142
Equation 20: KBP equation by fiber failure	143
Equation 21: KBP equation by bond failure.....	143
Equation 22: Page Equation.....	143
Equation 23: Page Equation.....	144
Equation 24: Calculation of RBA.....	146

Equation 25: Page equation	149
Equation 26: Simplified Page equation.....	150
Equation 27: Available surface area of filler	151
Equation 28: Available surface area of fiber	151
Equation 29: BDT equation	152
Equation 30: Modified Page equation.....	159
Equation 31: Linear relationship between ZDT and bond strength multiplied by RBA	160
Equation 32: Dimensionless ZDT.....	161
Equation 33: Calculation of ZDT	161
Equation 34: Calculation of tensile strenght.....	161
Equation 35: Bending stiffness	162
Equation 36: Modified form of bending stiffness.....	163
Equation 37: Tensile strength calculation.....	168

NOMENCLATURE

A	=	Size of measuring area
b _C	=	Bonding strength between a filer particle and a wood fiber

b_f	=	Bonding strength between a wood fiber and a wood fiber
BET	=	Brunauer, S., Emmett, P. H., and Teller, E.
BKP	=	Bleached kraft pulp
BDT	=	Beazley, Dennison, and Taylor
CSF	=	Canadian standard freeness (mL)
d	=	Floc size
Da	=	Unit molecular weight, g/mole
DCS	=	Dissolved colloid substance
DI	=	Deionized water
DINP	=	Deinked news paper
DLVO	=	Deryaguin, Landau, Verweg, and Overbeek
DMAc	=	Dimethylacetamide
DMSO	=	Dimethylsulfoxide
DP	=	Degree of polymerization
DSC	=	Differential scanning calorimetry
E	=	Elastic modulus
F	=	Formation number
F	=	Intensity function
f_c	=	Fraction of fibers bearing no load
FBRM	=	Focused beam reflectance measurement
FT-IR	=	Fourier transform infrared spectroscopy
G	=	Applied shear rate
GCC	=	Ground calcium carbonate

h	=	Thickness of paper
HMW	=	High molecular weight
I	=	Momentum of inertia
i	=	Incident light energy
i_A	=	Adsorbed light energy
i_R	=	Reflected light energy
i_T	=	Transmitted light energy
K	=	Adsorption coefficient (cm^2/g)
L	=	Filler loading amount
L	=	Fiber length
l	=	Capillary distance penetrated in time, t
LMW	=	Low molecular weight
MCC	=	Micro crystalline cellulose
ML	=	Middle lamella
n_i	=	Number of fibers
n_f	=	Number of fibers that break at rupture
n_p	=	Number of fibers that pull out intact
NMMO	=	N-methylmorpholine-N-oxide
NMR	=	Nuclear magnetic resonance
od	=	Oven dried sample
ONP	=	Old news paper
PAA	=	Polyacrylic acid
PAM	=	Polyacrylamide

PCC	=	Precipitated calcium carbonate
PDADMAC	=	Polydiallyldimethylammonium chloride
PEI	=	Polyethyleneimine
PEO	=	Polyethyleneoxide
r	=	Capillary radius
r	=	Fiber radius
R	=	Wettability
Ret	=	Retention
S	=	Specific scattering coefficient of sheet (cm^2/g)
S	=	Stiffness
S_0	=	Value corresponding to the unbonded network
S_c	=	Specific surface area of filler
S_f	=	Specific surface area of wood fiber
SEM	=	Scanning electronic microscopy
T	=	Temperature ($^{\circ}\text{C}$)
T	=	Tensile strength
TFA	=	Trifluoroacetic acid
TMP	=	Thermomechanical pulp
TOC	=	Total organic content
UKP	=	Unbleached kraft pulp
V_f	=	Molome fraction of fibers
w	=	Grammage of paper (g/cm^2)
WRV	=	Water retention value (g of water in pulp/g of OD pulp)

XRD	=	X-ray diffractometer
Z	=	Zero-span tensile strength
ZDT	=	Z-direction tensile strength
γ	=	Liquid surface tension
θ	=	Contact angle between the capillary walls and the liquid
η	=	Liquid viscosity.
γ_{SV}	=	Surface tension in the contact surface solid -vapor
γ_{SL}	=	Surface tension in the contact surface solid -liquid
γ_{LV}	=	Surface tension in the contact surface liquid –vapor
σ_p	=	Tensile strength of paper
σ_f	=	Tensile strengths of fiber
ρ_p	=	Paper density
ρ_f	=	Fiber density
τ_b	=	Shear strength of the matrix
δ	=	Strain at failure

SUMMARY

The paper industry utilizes fillers either to reduce the cost or to provide desired functional or end-use properties of paper products. However, there are disadvantages associated with higher filler loadings beyond a certain level, which include reduced paper strengths, increased size demand, abrasion, and dusting. The present study focused on

improving the physical property of filled papers. Based on paper strength theory, two important factors governing paper strength are the strength of individual fibers and the bonding between fibers. If fillers are loaded in the paper, the fiber strength of paper decreases, due to less fiber in the network per unit volume, and bonding strength of paper also decreases because fillers prohibit fiber to fiber bonding. Therefore, the target was to find the possible structuring method of fillers to increase the bond strength between fillers and wood fibers and suggest the mechanism of strength improvement.

Cellulose and starch have hydroxyl groups on the chemical structure. Therefore, the hydrogen bonding between fillers and wood fibers is assumed to be occurred by structuring fillers. To prepare structuring fillers to enhance the bonding with wood fibers, three methods were designed; precipitation with starch, complexation with starch and fatty acid, and regeneration with cellulose. Because

For starch application, we used two different approaches; salt precipitation and fatty acid complexation. The cooked starch can be precipitated by certain salt solutions such as MgSO_4 and $(\text{NH}_4)_2\text{SO}_4$. When clay-starch composites made by the precipitation method were put into the furnish as fillers, dramatic strength improvement was achieved such as 100-200% gains in tensile strength. This is due to the strong bonding between clay fillers and wood fibers, which is determined by Z-directional tensile strength (ZDT) and scanning electronic microscope (SEM). However, this method is hard to be applied in real papermaking system because it takes washing and filtration steps to remove the salt solution.

In order to simplify the preparation method, starch-fatty acid complexation was used to produce an insoluble crystalline structure. The solubility of clay-starch

composites made by this complexation method was very low. The physical properties of handsheets filled with composite fillers were improved significantly. At the same optical property of handsheets, the physical properties filled with clay-starch composite fillers by starch-fatty acid method were higher than those of composites by precipitation method. One of advantages using the starch-fatty acid complex is that it has an inherent water repellent property, sizing effect.

The different structuring method was used to compare the effect of the modification of fillers on the properties of paper sheets. Cellulose as a bonding material was dissolved by N-methylmorpholine-N-oxide (NMMO). The physical properties of the cellulose coated clay handsheets were significantly improved, but optical properties such as brightness and opacity were inferior to the handsheets filled with starch-clay composites due to relatively large particle size.

In order to study the mechanism how bonding material coated fillers improved the physical strength of paper and model the strength of paper filled with composite fillers, BDT theory, which is a modified Page's Equation, was used. After calculating the factors such as surface area and specific bond strength, the model matched well with the experimental results. Using this model, the tensile strength improvement could be predicted in terms of the change of bond strength and composite size.

CHAPTER 1

INTRODUCTION

The process of adding mineral fillers to paper stock prior to the formation of the sheet has been practiced since the 8th century and has become an integral part of the papermaking process today. The paper industry utilizes fillers either to improve process economics or to provide desired functional or end-use properties of paper products. It is estimated that there is a \$2.50/ton of saving for each one percent increase of filler in paper. Most filled papers are produced for the printing and writing sector and 82% of fillers to paper market is consumed in this area. Paper properties normally improved by fillers include opacity, brightness, gloss, smoothness, porosity, and printability. However, there are disadvantages associated with higher filler loading beyond a certain level, which include reduced paper strength, increased size demand, abrasion, and dusting. Even though there has been active research to increase the filler loading without suffering from those disadvantages, no satisfactory results have been reported. Therefore, the overall objective of this thesis was to better understand the strength loss mechanism when fillers are associated and to suggest an effective way to recover the strength without impairing any other properties.

The following thesis starts with a literature review and related relevant topics satisfying the overall objective of this thesis are covered in Chapter 2. Review includes basic fiber and filler properties and characteristics of how fibers and fillers affect the physical and optical properties of the paper. The conventional wet-end problems related

with polyelectrolytes for filler retention and dry-strength aids are also briefly discussed. Specific focus was given to improve paper properties using modified fillers.

Chapter 3 provides an analysis of the problem and outlines of the objectives of this research, respectively. This thesis also analyzes the available literature to provide a background for the issues associated with each chapter. Chapter 4 discusses basic starch theory and suggests a starch precipitation method to prepare clay-starch composite as papermaking filler to increase bonding between fillers and fibers. The solubility of composites was measured to evaluate the wet-end applicability. The physical and optical properties of paper were measured and the bonding structure was determined by SEM. However, the preparation methods need filtration and washing steps to remove the salt solution. Chapter 5 introduces a simplified method to prepare the clay-starch composite, which is the starch-fatty acid complexation method. The optimum amount of fatty acid was determined by the solubility and XRD. The solubility of composites in terms of pH and temperature was measured. The physical and optical properties of paper were measured and compared with conventional wet-end addition method. The distribution and bonding structure was determined by SEM. The sizing effect by fatty acid was also found and discussed in this chapter. Chapter 6 discusses cellulose dissolution techniques and suggests the different bonding structuring fillers which are clay-cellulose composites, and then discusses the effects of using modified clay on paper properties. Chapter 7 provides previous theoretical tensile strength modeling and suggests a way to apply it to composite filler filled paper. The mechanism why the paper strength can be improved by the composite fillers is discussed. Chapter 8 and 9 provides the overall conclusions to this study and the future work.

CHAPTER 2

LITERATURE REVIEW

2.1 Papermaking fibers

Paper has traditionally been defined as a matted or felted sheet of fibers formed on a fine screen from a water suspension [1]. Wood fibers are the main component of paper. The papermaking process is based on the ability of the fibers to form bonds such as hydrogen bonds with other fibers. The properties of final papers are highly affected by the properties of wood fibers. Therefore, it is very important to know fiber properties to deeply understand the paper properties.

2.1.1 Wood fiber types

Wood fibers vary in their shape according to the principal functions, which are (a) to perform the function of liquid transport, (b) to provide the necessary mechanical strength to the tree, and (c) to act as a storage of reserve food supplies [2]. Two basic groups of fibers are those from softwood (gymnosperms) species, such as pines, firs, and cedars, and hardwood (angiosperms) species, such as maples, oaks, poplars, and elms.

Softwood fibers

Softwoods consist of 90%-95% tracheids and 5-10% of ray cells [3]. The thick-wall latewood tracheids provide strength, while the spacious early wood tracheids predominantly conduct water and minerals with the tree. The storage and the transport of assimilates arranged take place within the parenchyma cells, which in softwoods are

predominantly arranged in radially running rays [3]. The most important morphological characteristics of softwood fibers are fiber length (3-7mm), which contributes to their tendency to flocculate when suspended in water, fiber width or diameter (20-50 μ m), and fiber wall thickness (3-7 μ m) [4]. In evolving from earlywood to latewood the cell diameter become smaller while the cell walls become thicker.

Hardwood fibers

In contrast to the tracheid as the main cell in softwoods, hardwoods have a greater variety of cell types. The hardwood consists of 36-70 % fibers (libriform fibers and fiber tracheids, mechanical function), 20-55 % vessel elements (conducting), 6-20 % ray cells (storing), with approximately 2 % parenchyma cells (secreting) [3]. In addition, hardwoods, compared to softwoods, have fibers that are shorter (1-2mm) and narrower (10-40 μ m) and rays that are more variable in width [4].

The morphology of fibers plays an important role in forming the network structure of the sheet. Softwood fibers, in addition to contributing to the strength of the sheet, establish an entangled mat through with the furnish drains due to the long fiber length. Hardwood fibers tend to flow toward and fill the void spaces in this mat, which results in the smoother surface of the sheet [5]. Therefore, hardwood pulps are generally used for somewhat different product applications, for example printing papers, than softwood pulps. In addition, the higher amount of parenchyma cells in hardwoods compared to softwood pulps is largely responsible for the generally higher fines content of hardwood pulps.

2.1.2 Compositions of Wood Fibers

Wood fibers are composed of three major components, cellulose, hemicelluloses and lignin. These compositions change with different wood species, wood age, location, and wood morphology. The typical compositions of softwood and hardwood are shown in Table 1.

Table 1: Typical compositions of softwood and hardwood [6]

Wood Species	Compositions of woods			
	Cellulose	Hemicellulose	Lignin	Extractives
Softwood	42 ± 2%	27 ± 2%	28 ± 3%	3 ± 2%
Hardwood	45 ± 2%	30 ± 5%	20 ± 4%	5 ± 3%

Cellulose

Wood fibers exhibit a number of properties that fulfill the requirements of papermaking. The major advantages of the cellulose fibers include high tensile strength, conformability or flexibility, resistance to plastic deformation, water insolubility, hydrophilicity, inherent bonding ability, and chemical stability due to their chemical and physical characteristics.

Cellulose is the main polysaccharide in the cell wall. It is homopolysaccharide composed of β -D-glucofuranose units which are linked together by (1-4)-glycosidic bonds [7]. The chemical formula for cellulose is $(C_6H_{10}O_5)_n$, where n is the number of repeating sugar units. The cellulose unit structure is shown in Figure 1 [7].

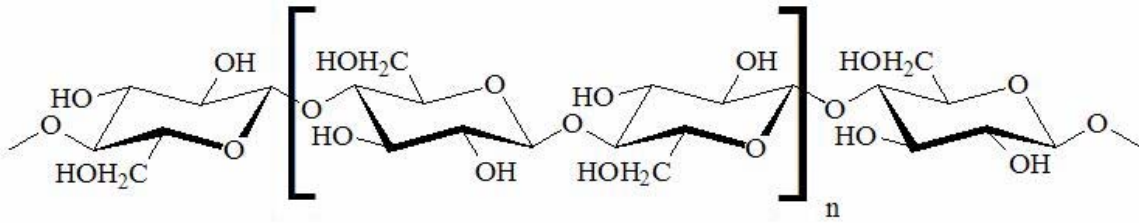


Figure 1: Cellulose structure

The degree of polymerization (DP) of native wood cellulose is on the order of 10,000 and lower than that of cotton cellulose (about 15,000). These DP values correspond to molecular masses of 1.6 and 2.4 million Da and to molecular length of 5.2 and 7.7 μm , respectively. In technical processes, such as chemical pulping or bleaching, the DP of cellulose can decrease by 500-2000 [2].

Cellulose is the main strength-bearing component in wood (and in pulp) and the least accessible, due to its high degree of crystallinity. Cellulose in wood fibers, as with many other polymers, has a two-phase morphology containing both amorphous and crystalline regions. The model most frequently used is the fringed micelle structure in which individual chains pass through several crystalline and non-crystalline regions as Figure 2 (left) shows.

Since the solvent or reagents can more easily access amorphous regions, cellulose degradation is more likely there. When cellulose is hydrolyzed by 1 N sulfuric acid to hydrocellulose, it is attacked randomly only in the amorphous regions. All the amorphous chains are not necessarily of the same length and the newly-formed reducing end groups are randomly located at different distances from the crystalline-amorphous transition region. When the hydrocellulose is subjected to alkaline degradation, the propagation

reaction proceeds and glucose units are peeled off by the alkali as show in Figure 2 (right). Decreasing the molecular weight of cellulose below a certain value will cause deterioration in strength [8].

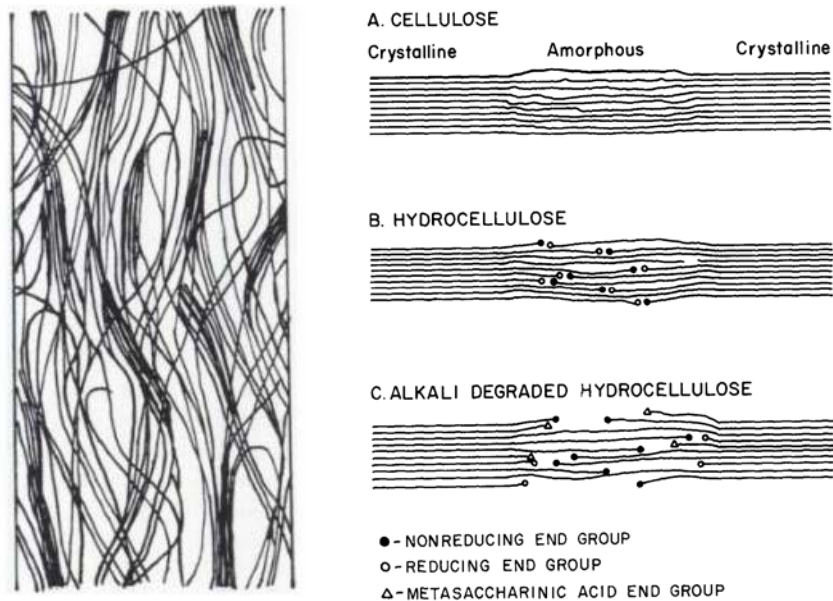


Figure 2: Fringed micelle model of the two-phase structure of polymers [9] and schematic representation of cellulose degradation [10]

Hemicellulose

In contrast to cellulose, hemicelluloses are linearly branched heteropolysaccharides composed of a variety of different sugars such as xylose, galactose, mannose and arabinose and have lower molecular weights, usually containing fewer than 400 sugar units [4].

Softwood hemicelluloses are composed mainly of galactoglucomannan (10-15%) as shown in Figure 3, while hardwoods are predominately glucuronoxylans (15-30%) as shown in Figure 4. Table 2 lists the major hemicelluloses for softwoods and hardwoods.

Table 2: Major hemicellulose components [7]

Hemicellulose type	Occurrence	Amount (% of wood)	DP
Galactoglucomannan	Softwood	10-15	100
Arabinoglucuronoxylan	Softwood	7-10	100
Glucuronoxylan	Hardwood	15-30	200
Glucomannan	Hardwood	2-5	200

In both hardwoods and softwoods, glucuronoxylan with naturally occurring carboxyl groups can be found. The carboxyl groups on glucuronoxylan groups are the principal source of negative fiber surface charge which can benefit fiber swelling and improve the relative bonded area between fibers during paper formation [11]. Hemicelluloses promote internal lubrication, leading to improved flexibility.

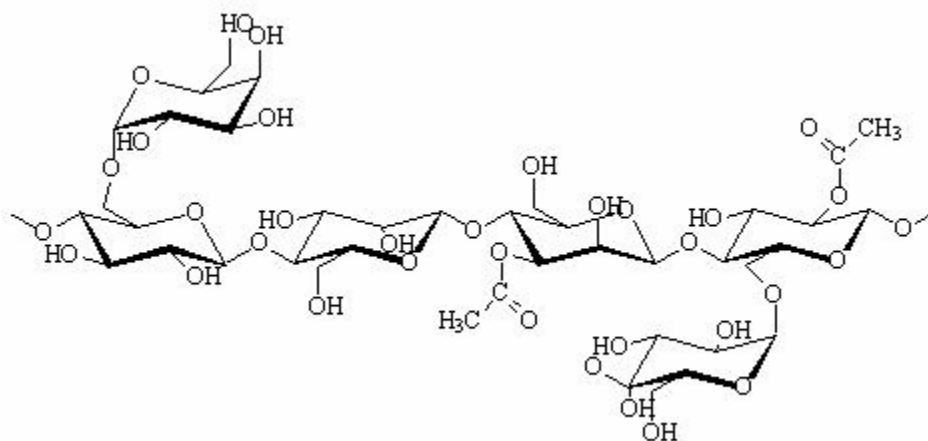


Figure 3: Galactoglucomannan structure in softwood [7]

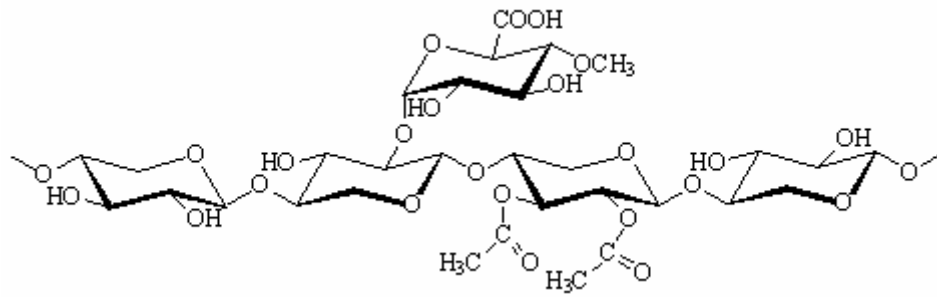


Figure 4: Glucuronoxylan structure in hardwood [7]

Lignin

Lignin is the third component of the wood fiber wall. The structure of lignin is very complicated. Chemically, lignin is amorphous polymer built from phenyl propane units linked together by different precursors; coniferyl, sinapyl, and *p*-coumaryl alcohol, as shown in Figure 5. It plays a major role in holding fibers together in wood. Lignin has a high molecular network structure which contains inter-unit ether (C-O-C) and carbon-carbon (C-C) linkages. Among all linkages, the β -O-4 linkage dominates; 50% in softwoods and 60% in hardwoods [12].

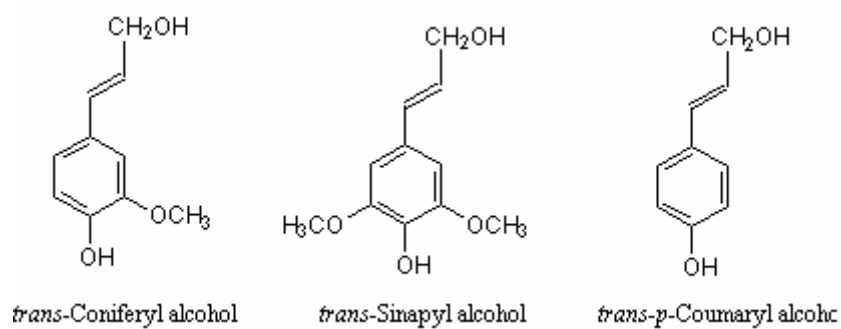


Figure 5: Lignin structure [3]

Chemical bonds between lignin and hemicellulose, so called “lignin-carbohydrate complex (LCC)” have been a subject of intensive studies. These linkages can be either of ester or ether linkage to a 4-O-methylglucuronic acid group present in xylan or through an ether linkage to an arabinose or mannose unit present in arabinoxylan and glucomannan, respectively [7].

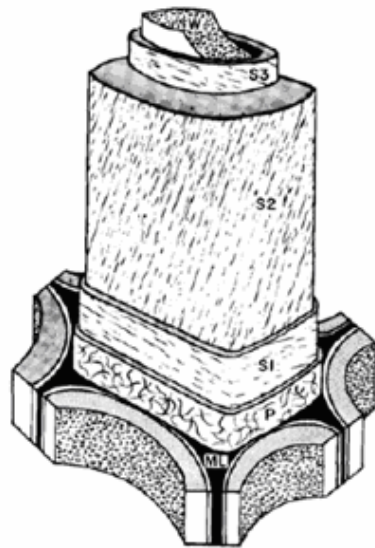
Residual lignin in papermaking fibers after pulping and bleaching adversely influences their ability to participate in interfiber bonds, provides an inhibiting influence on the swelling of fibers in water, and contributes to the formation of a bulky, rapidly draining mat on the paper machine. The free phenolic groups in the structure contributes to the negative fiber surface charge when they ionize [4].

2.1.3 Cell Wall Structure of Wood Fibers

A fiber consists of three main layers, the middle lamella (ML), the primary wall (P), and the secondary wall (S). Figure 6 shows the simplified structure of wood fiber cell wall. These layers differ from one another with respect to their structure as well as their chemical composition. The middle lamella is located between the fibers and works as glue to bind the fibers together in wood. The middle lamella consists mainly of lignin and pectic substances and gives structural support to and imposes swelling restrictions on the fiber [13]. Recent studies with transmission electron microscopy have revealed that the middle lamella has a fine irregular network [14]. The very thin primary wall (P) has a similar composition, and usually these two outer layers are considered together as the compound middle lamella (ML+P) [7]. There are three sub-layers in the secondary wall,

a thin outer layer (S1), a thick middle layer (S2), and a thin inner layer (S3) towards the lumen (L).

The S2 layer of the cell is the largest part of the cell wall, and it is therefore suggested to have the greatest impact on the chemical and physical properties of the fiber. The fibrils in each layer are built up of cellulose microfibrils in which the cellulose chain axis is arranged in parallel to the axis of the microfibril, thus giving a high reinforcing effect in its length direction [13]. The outer S1 layer contains 3-4 lamellae where microfibrils form either a Z helix or S helix and the microfibril angle of the crossed fibrillar network varies between 50 and 70° [7]. In the middle S2 layer, the angle of fibrils is usually between 0 and 30° to the fiber axis. In the inner S3 layer, the fibrils are arranged at a larger angle to the fiber axis in both S helices and Z helices (50-90°) [7].



Layer	Thickness	Angle
S3	~1µm	50°~90°
S2	1.5µm	0°~30°
S1	0.2-0.3µm	50°~70°
P	0.1-0.2µm	irregular
ML	0.2-1.0µm	

Figure 6: Simplified structure of woody cell and the average layer thickness and microfibril angle, showing the middle lamella (ML), the primary wall (P), the outer (S1), middle (S2), and inner (S3) layers of the secondary wall, and the warty layer (W) [15]

2.1.4 Effect of fiber structure and operations on paper properties

Fiber length

The properties of paper are dependent on the structural characteristics of the various fibers that compose the sheet. Fiber length is one of the most important characteristics of papermaking fibers. A long fiber can have more bonds with other fibers and therefore be more strongly held in the network than a short fiber. The tensile strength of a wet web increases rapidly with fiber length. Table 3 shows that tensile strength, rupture strain, and fracture toughness of dry paper often also improve with increasing fiber length, but the tensile stiffness is not sensitive to fiber length. Paper sheets with higher softwood content typically have superior strength than paper with higher hardwood content. Sheets with high hardwood content often have superior tactile feel, as in smoothness and softness, compared with softwood sheets. Thus, liner board, sack paper, and newsprint tend to have high softwood content; whereas fine writing paper and tissue often contain a larger percentage of hardwood fibers.

Table 3: Properties of fractionated fiber populations and handsheets made from them [16]

Mean Fiber Length, mm	Apparent Density, kg/m ³	Tensile Stiffness Index, kNm/g	Tensile Strength Index, Nm/g	Rupture Strain, %	Total Work to Fracture, Jm/kg	Work to Maximum Load, Jm/kg	Fracture Energy, Jm/kg
0.8	560	4.5	39	3.4	13	8	6
1.4	560	5.4	54	4.2	21	14	9
2.2	520	5.5	63	4.4	26	16	13
3.1	500	5.0	60	4.1	30	14	19

Fibril angle

The elastic modulus of fibers also increases with decreasing fibril angle [17]. Page and EI Hosseiny plotted both tensile strength [18] and elastic modulus [17] as a function of fibril angle and showed that both decreased as the angle between the fibrils and the fibers axis increased.

Cell wall thickness

Conformable fibers can bend and match the shape of each other to give a dense and well bonded network. The thin walled fibers from springwood or earlywood fibers with large lumens collapse readily into ribbons during the sheet formation. The thick walled fibers from the summerwood or latewood resist collapse and do not contribute to interfiber bonding to the same extent. Within species, the thin-walled earlywood tracheids are relatively flexible, while the latewood tracheids, having as much as 60 to 90% of their volume in cell wall material, are less conformable [8]. While thin walled fibers can be considered ten times more flexible than thick walled fibers, 55 % of thick walled fibers collapse completely while only 24 % of thin walled fibers fully collapse during sheet formation. The collapse of fibers also increases the area of fiber – fiber bonds.

Pulping

The main purpose of pulping is to release fibers from the wood. In other words, pulping separates fibers that are bonded together through the middle lamella. Wood fiber can be separated either by mechanical methods, chemical methods or a combination of

both. Chemical pulping is a process in which the lignin in the secondary wall is also removed in addition to the lignin in the lamella. The high cellulose yield in the pulping process leads to successively increasing cellulose content up to a high level in bleaching pulp. Cellulose is the most important strength-bearing component in pulp fibers. The zero-span tensile strength of different pulp fibers has been shown to be strongly correlated with cellulose content [19]. In general, paper made of bleached kraft pulp has a 2-3 times higher tensile strength than a mechanical sheet. The lignin content is approximately 30% in mechanical pulps and almost zero in bleached kraft pulps. The low lignin content gives the kraft pulp fibers higher wet fiber flexibility, collapsibility, and swelling than mechanical pulp fibers. The fraction of long, intact fibers can be less than 20% by weight in groundwood mechanical pulps and nearly 40% in TMP. In chemical pulps, the long fiber fraction may be as high as 90%.

The pore size distribution in mechanical pulp fibers is dominated by 1 nm pores [20]. In contrast, kraft and bleached kraft fibers have mainly 5-20 nm diameter pores [21]. It has been said that the pore size increase is due to removed lignin and hemicelluloses from cell walls during pulping and bleaching. Fibers become more swollen in water due to the removal of lignin from the cell wall. The significant difference between chemical pulps and mechanical pulps is that mechanical pulps have high yield and keep much more lignin in the fibers.

The pulping method also affects the specific strength of fiber to fiber bonds. Average values for shear bond stress at maximum load was 0.41kg/mm^2 for holocellulose, 41% higher than that for the thermomechanical fiber bond, 0.29kg/mm^2 [22]. The kraft pulps were also reported to have a higher bonding strength than the sulfite pulps [23].

Beating

Chemical pulp is usually beaten to optimize its contribution to the mechanical properties. The beating of chemical pulp loosens the structure of the fiber wall, internal fibrillation, and surface, external fibrillation. It can also break fragments from the fiber wall. Internal fibrillation corresponds to a partial delamination of the fiber wall as Figure 7 (left) shows. The delamination increases the swelling degree, flexibility, and conformability of the wet fiber wall. This improves the inter-fiber bonding and strength properties in paper at the expense of the optical properties. External fibrillation as Figure 7 (right) shows enhances sheet consolidation in the papermaking process and enforces bonding between fibers.

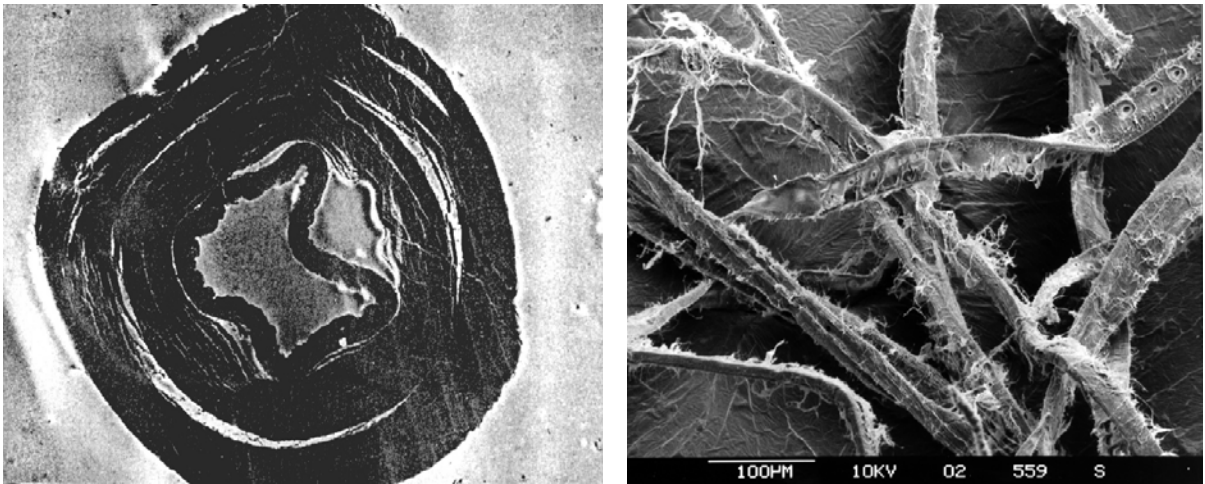


Figure 7: Cross-section (left) [24] and external surface (right) of well-beaten kraft fiber [25]

Tear strength always decreases with refining due to the strength attrition of individual fibers; other strength parameters such as burst, tensile, folding endurance increases due to improved fiber-to-fiber bonding [26]. It has been generally accepted that beating increased the bonded surface area of the fibers. The effect of beating on the specific bond

strength has been intensively studied, but the results were somewhat contradictory; decrease of bond strength as beating increases [27, 28], a small maximum in the bond strength as beating progresses [29], and continuous increase of bond strength as beating is advanced [30]. Mayhoo *et al.* [31] have reported that the bond strength between individual fibers changes very little due to beating. The discrepancy of results is thought that the various methods for measuring the bond strength differ in how the effect of paper structure is affecting the obtained value for the bond strength.

2.2 Filler

Papermakers have been introducing filler pigments into paper through the wet end of the machine as a common practice for many years. Almost all printing and writing grades of paper and paperboard contain fillers today. Although the original reason for the use of filler was a question of economy, i.e. the expensive fiber material could be saved, it was soon established that fillers also improved the properties of the paper in many respects.

Better printability as a result of the improvement in surface smoothness, the greater opacity, and the higher whiteness of the paper are obtained. A better dimensional stability, a better “feel” and better appearance are other advantage.

Recently, papermakers have begun to focus more on the specific property improvement that can be gained from the use of a wider variety of filler pigments. This trend has been particularly accelerated by the large scale conversion from acid to alkaline papermaking.

2.2.1 Kaolin clay filler pigments

The white clay most commonly used in the paper industry today is called kaolin clay, which is composed of the mineral kaolinite. Kaolinite is one of the most widely occurring minerals used as (1) a pigment to improve the appearance and functionality of paper and paint, (2) a functional filler for rubber and plastic, (3) a ceramic raw material, and (4) a component for refractory, brick, and fiber glass products [32]. The most prominent world kaolin mining districts are in North America (primarily Georgia), Brazil

(northern), the United Kingdom (Cornwall-Devon), and Germany (Bavaria and Saxony) [32]. Kaolin deposits can be classified as primary and secondary (or sedimentary) kaolin depending on the origination of the deposit. Primary kaolin generally describes a kaolin ore altered from an igneous or metamorphic rock that was kaolinized in situ by hydrothermal or weathering processes. Secondary (or sedimentary) kaolin is a kaolin ore formed through sedimentary depositional processes [32].

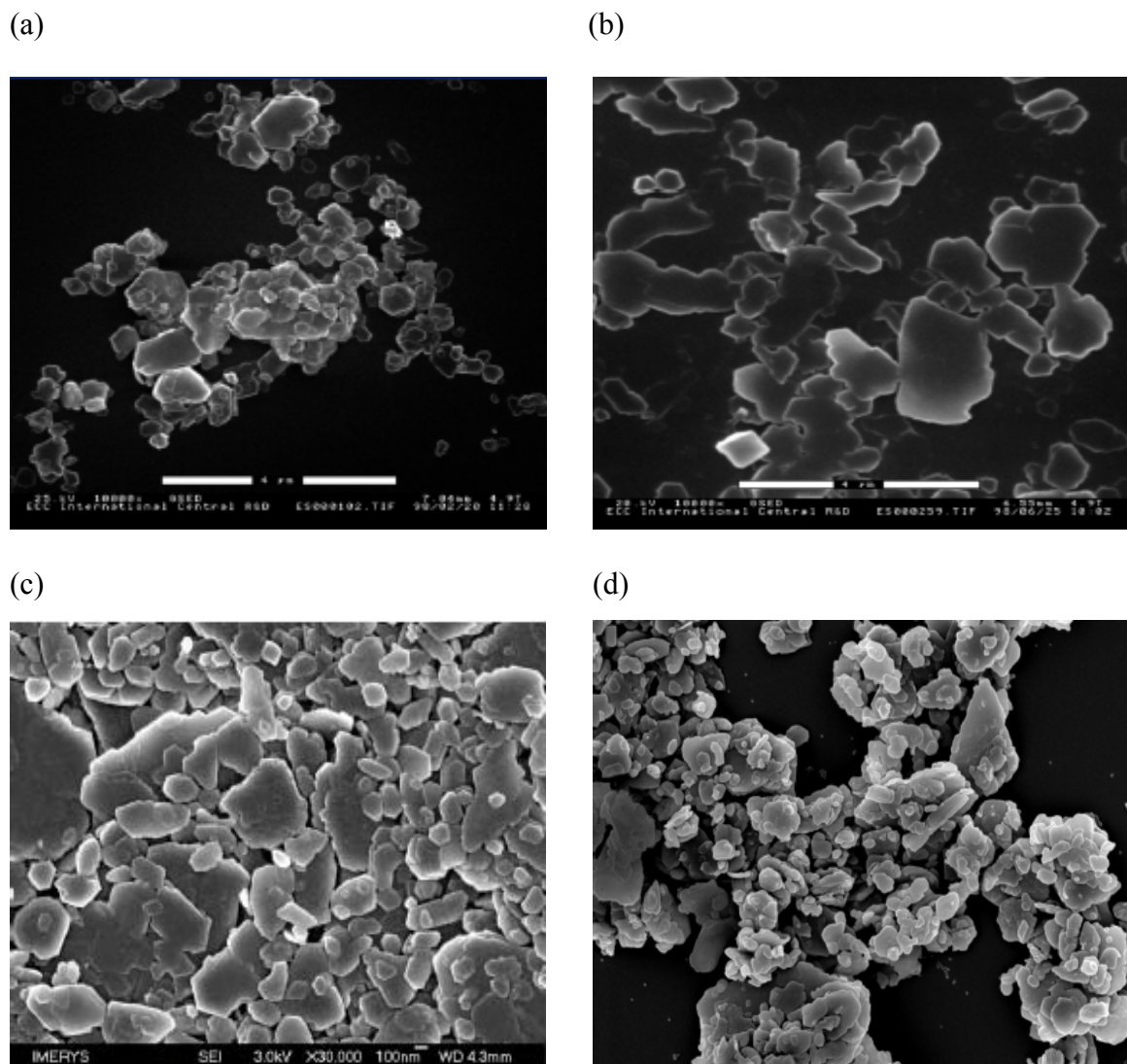


Figure 8: Different types of clay. Georgia hydrous kaolin (a), UK hydrous platy kaolin (b), Blocky kaolin (c), calcined kaolin (d) by courtesy of EMERYS

The European clay is of the primary type, while the North American is of the secondary type [33]. North American kaolin are typically less platy and finer and tends to have higher brightness than English and Brazilian kaolin [34, 33]. Figure 8 shows different kinds of kaolin clay.

The principal mineral in clay is kaolinite, structurally a hexagonal, platelet-type hydrous aluminum silicate. American kaolinite has a typical chemical composition of 38% Al_2O_3 , 46% SiO_2 , 13.5% H_2O , and 1.5% of TiO_2 and the empirical formula $\text{Al}_2\text{O}_3 \cdot 2\text{SiO}_2 \cdot 2\text{H}_2\text{O}$. Kaolinite has a two-layered structure, with one tetrahedral silica layer and one octahedral aluminum layer, linked by oxygen atoms as shown in Figure 9.

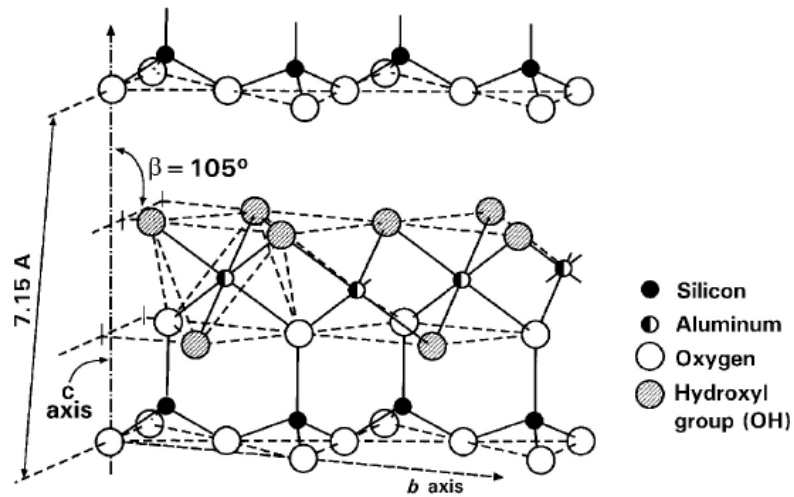


Figure 9: Mineral structure of kaolin clay [33]

Depending upon how they are processed, filler clays can be categorized a hydrous, delaminated, calcined, and/ or structured. The term hydrous clay generally refers to processed kaolin product that contains kaolin minerals with their structural water or hydroxide component. Calcined kaolin refers to thermally processed kaolin exposed to

temperatures higher than 450 °C to form metakaolin, or to temperatures higher than 1,000°C to form high temperature minerals such as mullite, spinel, and cristobalite [32]. The term delamination or structured kaolin refers to mechanically or chemically processed kaolin, which differ by brightness levels, shape factors, and particle size distributions. Average shape factors, plate diameter:plate thickness, can vary between 10:1 and 80:1 depending on the process [34].

Table 4: General physical properties of typical filler pigments [33]

	Clay	Talc	GCC	PCC
Formula	$\text{Al}_4\text{Si}_4\text{O}_{10}(\text{OH})_8$	$\text{Mg}_3\text{Si}_4\text{O}_{10}(\text{OH})_2$	CaCO_3	CaCO_3
Crystal structure	Triclinic, hexagonal platelets	Monoclinic, lamellae	Trigonic, rhombohedra 1	Scalenohehdralr hombohedral aragonite
Density, kg/dm^3	2.7	2.8	2.7	2.7
Refractive index	Hydrous: 1.57 Calcined:1.60	1.57	1.59	1.59
Hardness (Mohs scale)	2-2.5	1-1.5	3	
Brightness,%	Hydrous: 78-90 Calcined: 90-95	85-90	Chalk:80-90 Marble:85-95	>93
Particle size distribution				
Below $10\mu\text{m}$,%	94	84	98	100
< $5\mu\text{m}$, %	75	45	90	100
< $2\mu\text{m}$, %	48	16	40	70
Specific surface area(BET), m^2/g	Hydrous:10-25 Calcined:15-25	9-20	2-12	5-25
ζ -potential, mV	-24(pH 7)	-19(pH 9)	-26(pH 9)	+5(pH 9)
Abrasion(AT 1000), m2/g				
-bronze wire	45	31	24	20
-plastic wire	3	13	27	6
Ignition loss, %				
-600°C	11	5.5	0-2	0
-925°C	12	6.3	42	42
pH	5	9	9	3
Scattering coefficient, cm^2/g	Hydrous:1100-1200 Calcined:2600-3000	-	1400-1700	2200-2700

The surface chemistry of kaolinite affects how the particle interacts with other particles in the papermaking furnish. Because of the silanol groups, the layers have a negative charge and the edges have a positive charge. In a suspension, these charges attract each other, resulting in flocs, which affects flow properties [33]. There are many other different types of fillers for papermaking. Table 4 lists some of the common fillers in use today and compares properties of them.

2.2.2 Effect of fillers on paper physical properties

Generally, paper strength is dependent on the extent to which the fibers are bonded to each other (interfiber bonding), fiber properties such as fiber strength, and the distribution of the fibers within the sheet (formation). Bonding is a result of the formation of hydrogen bonds between the fiber surfaces during drying. The bonds are easily disrupted and their overall strength is dependent on the extent to which the fibers overlap (contact area) and the intrinsic strength per unit area of contact. Fillers reduce paper strength properties by interfering with the interfiber bonding. Furthermore, the strength reduction is due to less fiber in the network per unit volume. Tensile stiffness and tear index are relatively less sensitive, and tensile energy absorption (TEA) is most sensitive to filler loading [35].

The size of the filler particle, the size distribution, and the shape of the filler particles in relation to the fiber network structure are factors that can be of great importance for the properties of the paper. In general, the smaller the pigment particles, the greater their negative effect on strength as shown in Figure 10.

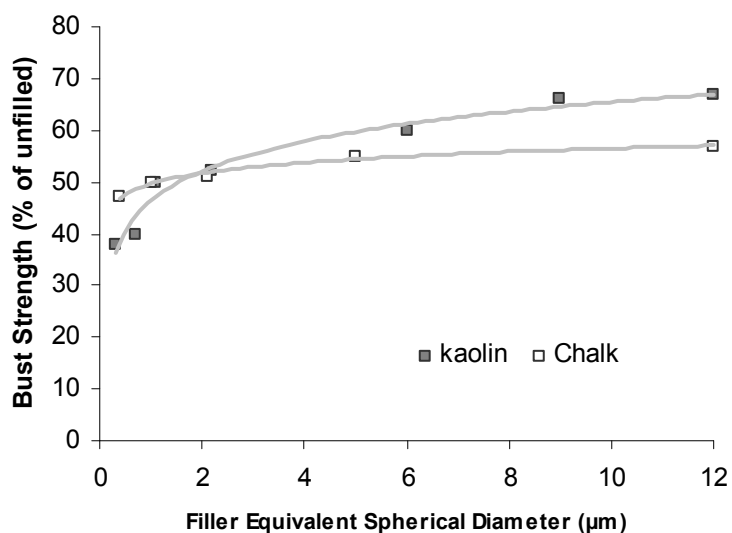


Figure 10: Effect of filler particle size on the burst strength of paper filled with different fillers [36]

For particles greater than 5µm, the relationship is dominated by particle shape and number effects, due to large particles disrupting points of interfiber bonding so that platey kaolin give greater benefit. For particles less than 2µm, surface area becomes more important because the attachment of small filler particles to fibrils prevents collapse and consolidation on drying, and blocky fillers shows better results [36].

2.2.3 Effect of fillers on paper optical properties

Kubelka [37], in his work on non homogeneous layers, developed mathematical equations which may be applied to paper. When incident diffuse light (I_0) strikes paper, it is partially reflected and transmitted. The light transmitted enters the paper where some is absorbed, some reflected, and the remainder is transmitted through the paper. This

mechanism is repeated infinitely. Therefore, the relative scattering coefficient express the relative decrease in light intensity on transmitted light which has its cause in the reflection of light, i.e. the following are obtained;

$$s = \lim_{w \rightarrow 0} \frac{\sum \frac{I_R \div I}{w}}$$

Equation 1: Specific scattering coefficient

where s=specific scattering coefficient(cm²/g), I=incident light energy, I_R=reflected light energy, w=grammage of paper(g/cm²)

$$k = \lim_{w \rightarrow 0} \frac{\sum \frac{I_A \div I}{w}} = \lim_{w \rightarrow 0} \frac{\sum (i - (i_A + i_T)) / i}{w}$$

Equation 2: Adsorption coefficient

where: k=adsorption coefficient(cm²/g), i_A=adsorbed light energy, i_T=transmitted light energy.

The reflectivity is obtained from the equation:

$$R_{\infty} = 1 + \frac{k}{s} - \sqrt{\left(\frac{k^2}{s} + 2\left(\frac{k}{s}\right)\right)}$$

Equation 3: Reflectivity

With the help of the Kubelka-Munk theory, an expression for the opacity can be derived:

$$\frac{R_0}{R_\infty} = \frac{\exp(sw(1/R_\infty - R_\infty)) - 1}{\exp(sw(1/R_\infty - R_\infty)) - R_\infty^2}$$

Equation 4: Opacity

In principle, the opacity of a paper can be increased by increasing s or k . Most of fillers are white, however, and their light scattering ability in the sheet is their most important property. The opacity depends on the number of individual particles in the sheet structure, i.e. on the grammage, on the number of surfaces in the structure and on the differences in refractive index between the particles and the surrounding medium.

Adding fillers to a paper sheet can improve optical properties including opacity and brightness due to the higher light scattering of filler than wood fibers, which has the linear relationship of the following form:

$$S_{\text{sheet}} = S_{\text{unfilled sheet}}(1-L) + LS_{\text{filler}}$$

Equation 5: Light scattering coefficient of filled paper

where S is light scattering coefficient and L is filler loading amount.

In table 5, the refractive index and scattering coefficient are listed for some raw materials used in papermaking. It has been reported [38] that when the montmorillonite which has a very tiny ($<0.1\mu\text{m}$) extremely platy with a hydrophilic surface is used as a filler in the paper, it has little deleterious effect on paper strength. The light scattering coefficient of the paper is, however, not increased, indicating that the filler is in close contact with the fiber and that the bonded area of the fiber remains the same. It is worth noting that even though the refractive index of cellulose which is main material in paper

and that of fillers are very similar as shown in Table 5, fillers can increase the opacity by creating air voids in the structure. Filled papers was reported to have a much higher pore volume than unfilled papers [39], which is an evidence that fillers are playing the role of spacers within a sheet of paper so that fillers cause the increase of optical properties and thickness of paper.

Table 5: Scattering coefficient and refractive index of components included in paper [4]

Material	Scattering Coefficient, cm ² /g	Material	Refractive Index
Filler Clay	1100-1200	Kaolin	1.55
Calcined Clay	2600-3000	CaCO ₃	1.56
Ground CaCO ₃	1400-1700	TiO ₂ (anatase)	2.55
PCC	2200-2700	TiO ₂ (rutiel)	2.7
TiO ₂	4500-6000	Talc	1.57
Bleached Chemical Pulps	220-350	Calcium Sulfate	1.53-1.58
Mechanical Pulps	500-750	Air	1
		Water	1.33
		Cellulose	1.53
		Starch	1.53
		Paraffin	1.43

It is clear from Table 5 that a wide range of light scattering abilities exist in mineral pigment fillers which scatters light to a much greater extent than pulp fibers. There are important factors that influence light scattering and light reflectance in paper as below.

Particle size

Figure 11 shows the sheet light-scattering coefficient contribution of different filler particles. It is clear that as the particle size decreases, light scattering increases.

The two minerals have similar refractive indices. The relationship between filler particle size and light scattering coefficient is clear with a maximum at around $0.7\mu\text{m}$ [36]. It has been reported that the maximum scattering of light is obtained by spherical particles on half the wavelength of light or between $0.2\text{-}0.3\mu\text{m}$ in diameter [40]. For prismatic-PCC and scalenohedral-PCC, the maximum opacity was found to be $0.4\text{-}0.5\mu\text{m}$ and $0.9\text{-}1.5\mu\text{m}$ respectively [41]. During the papermaking process, a variety of retention aids are using to help to retain fillers within the sheet. However, they cause the fillers to agglomerate, which affect negatively on the opacity due to the large agglomerate size and uneven distribution.

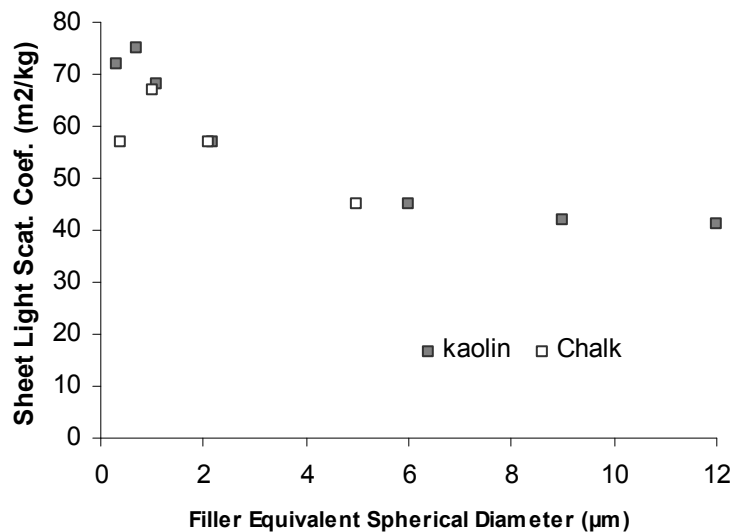


Figure 11: Effect of filler particle size on light scattering coefficient of filled paper [36]

Particle morphology

When fillers are added to a sheet, they can create more surfaces and voids within the sheet, which is as important as the size of individual particle elements. Different morphologies such as aggregated or solid forms cause different behavior in their ability to scatter light and different paper physical properties. Especially, the aggregated type of fillers such as the calcined clay, the acicular (needle-shape aragonite), and the scalenohedral (rosette) PCC shows the much higher light scattering coefficient than the solid type of filler such as clay and GCC due to the larger pore volume of PCC (0.9cc/g) or calcined clay (1.1 cc/g) than clay (0.43 cc/g) and GCC (0.31 cc/g) [42].

2.2.4 Effect of fillers on other properties of paper and papermaking process

The degree to which the use of filler affects paper's apparent density can depend strongly on the particle size and the particle shape. The ability of fillers to contribute to the measured thickness (caliper) of the paper at a given basis weight and filler content depend on the equivalent diameter of the particles. Larger particles are able to open larger inter-fiber spaces within the paper so that the thickness of the paper increases as the particle size increases [43]. Additionally, for a given filler level, the stiffness, sizing, and air permeability increases with increasing the particle size [44].

The volume of paper, per unit mass, increases with increasing content of either PCC or calcined clay, both of which are aggregated fillers and have a lot of internal void space [45]. By contrast, clay and GCC result in decreases bulk, as the filler level increases because they are solid type fillers and have a high packing density [45].

Fillers can also improve print quality by creating smoother surface and allowing more uniform ink absorption. In offset printing, the linting tendency increases with increasing filler content and this often limits the filler content. In gravure, all printability properties are improved with increasing filler content.

It is generally accepted that fillers reduce the degree of sizing at a certain size dosage because of the consumption of the sizing agents which are adsorbed on the filler not on the fibers where they were intended to adsorb. In acid internal sizing, free rosin acid dispersion sizing is more sensitive than sizing with soap rosin.

An increase in filler content has several negative but also several positive effects on the papermaking process. In Table 6, some effects have been compiled.

Table 6: Effect of increased filler content during papermaking

Retention	Decrease
Wire dewatering	Increase
Dry content after the press	Increase
Initial wet strength	Decrease
Rate of drying	Increase
Wire abrasion	Increase

2.3 Filler Retention

Effective filler retention provides an added quality that the papermaker expects or a more cost-effective sheet. It is therefore very important to understand the difference of retention characteristics between the fillers and to choose retention programs and strategy providing maximum benefits of filler application.

Fillers are retained by the mixture of mechanical entrapment of original filler particles or their agglomerates and heteroflocculation with other components of furnish: fines or fibers. If the mechanical entrapment dominates, filler particles are simply trapped in the pores of formed web of paper. In this case retention obviously increases with the particle size of the filler. However, the retention of filler by the mechanical entrapment alone can exhibit some level of two-sidedness in the produced sheets.

Simply adding the filler to the papermaking stock is not sufficient to increase the mineral content of the finished sheet. Since wood fibers and these minerals all have a negative surface charge, there is no mutual attraction between them and the small mineral particles, generally less than five microns will pass through the forming wire and be lost from the sheet.

Even though fibers have a negative surface charge in water, but their lengths are about 3-7mm for softwood fibers and 1-2 mm for hardwood fibers. Therefore, fibers are easily retained on the screen which has around a 70 micron wire opening. However, fillers have a negative charge on their surface in water and their particle sizes are much smaller than wire hole. Therefore, fillers can be attached to fibers, despite negative charges on both through the use of polymers and other retention mechanisms.

Chemical retention systems function through fine particle aggregation and heteroaggregation. The mechanisms which comprise these processes include the adsorption of the additive to the surface of fines and fillers, the neutralization of charge on the surfaces of particles by formation of cationic patches, and the agglomeration of fine particle through electrostatic attraction of oppositely charged particle surfaces or through particle bridging flocculation by high molecular weight cationic additives. Each of these steps is dependent upon the charge density of the polymeric additive used, the conformation of the additive, and the charge density of the particle surfaces. Retention mechanisms are categorized into three mechanisms dependent upon the types of polymers used or the different characteristics of aggregation.

2.3.1 Retention mechanism

Charge neutralization

This mechanism is the simplest in that the addition of an electrolyte salt or very low molecular weight polyelectrolyte compresses the electrical double layer enough that repulsion between particles is diminished and van der Waals attractive forces can induce coagulation whenever two particles collide. Retention aids that abide by this mechanism are typically low molecular weight, high cationic charge compounds. They usually do not extend beyond the electrical double layer but decrease the net charge to zero [46]. These types of retention aids include polyvalent cations (e.g. polyaluminum species), polyethyleneimine, poly-DADMAC, polyamines and polyamideamine epichlorohydrate (PAE) [46].

Patch Model

Patch-flocculation is an electrostatic mechanism that is different from the charge neutralization theory. It based on the formation of cationic sites or “patches” by cationic polyelectrolytes on the anionic fiber or filler surfaces as Figure 12 shows.

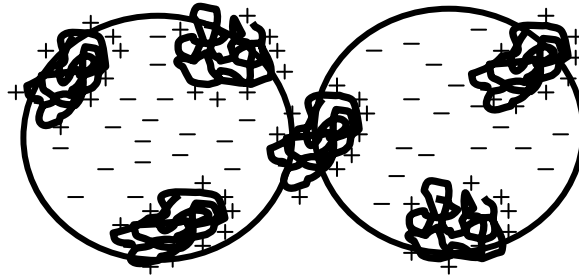


Figure 12: Pictorial representation of patch flocculation [4]

The polymer is absorbed in cationic patches on the negative surface of the particle. Flocculation will then take place by electrostatic forces between the oppositely charged sites on the particles. The degree of attraction depends on the charge density of the polymer and the surface coverage of the polymer. A surface coverage of about 50% or less gives optimum flocculation [47]. In order for the patch model to work, these areas of opposite charge must remain localized and not spread over the entire particle. This means that the patches must be thicker than the electrostatic double layer so they can attract the other particles. If the patch does not protrude beyond the electrostatic double layer, the charge associated with it will only serve to neutralize the opposite charge around it [4].

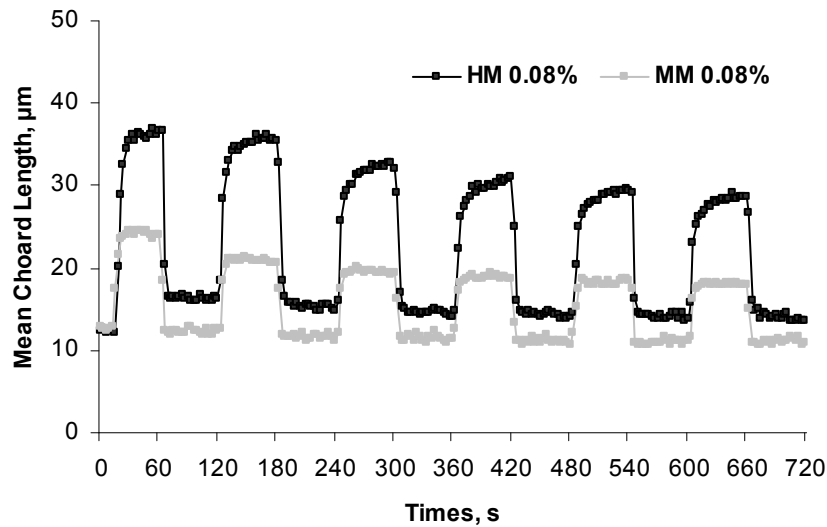


Figure 13: Mean chord length as a function of time after PDADMAC (high and medium molecular weight) was added to the suspension of clay. The shear level was changed by changing the impeller speed between 300 and 900 rpm every 60s [48]

As can be seen from the mechanism, the polymers most suited for patching are in the range of 10^5 to 10^6 Da (Da is the unit molecular weight g/mole), cationic polymers with a high charge density. Polymers with these qualities include modified polyethylene imines (PEI), polyamines and polyamideamine-epichlorhydrin (PAE) [4].

Aggregates by this patch mechanism give good shear stability; at the same time as reflocculation can rapidly take place when the shearing stops as shown in Figure 13. However, the initial flocculation is not significant for both of high and medium molecular weight of PDADMAC, however, the high molecular weight shows the higher initial flocculation.

Bridging

When polyelectrolytes have a high molar mass (typically above 10^6 Da) they are adsorbed on the particle surface forming tails and loops that will interact with other particles, which creates bridges between the particles and therefore flocculation as Figure 14 shows.

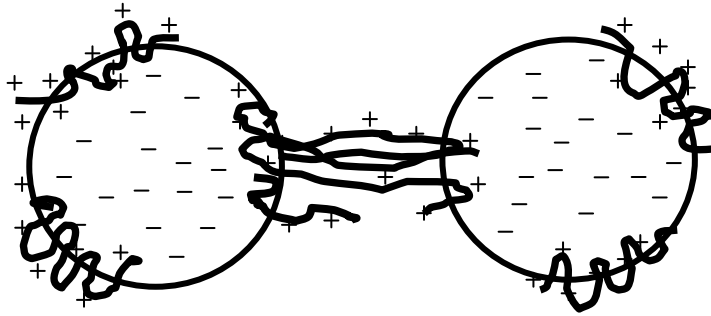


Figure 14: Pictorial representation of bridging flocculation [4]

High molecular weight, cationic or anionic polyacrylamides or nonionic polyethylene oxides (PEO) are often used in flocculation. In the bridging flocculation mechanism, the polymer first adsorbs onto a particle surface in a conformation where loops and tails extend away from the particle surface. These polymer loops attach themselves to another particle surface when an inter-particle collision occurs to form a bridge between the two particles. The loops and tails formed must be at least twice as long as the thickness of the diffuse layers of the particles [49].

Hard flocs made by these polymers are also referred to as “irreversible”, because successive dispersion-reformation cycles cause the floc strength to deteriorate until the aggregates eventually take on the characteristics of a soft floc. The mechanism believed

to produce irreversibility involves, first, separation of bridged particles, either by disruption of the attachment points on a particle surface or breakage of the bridging polymer chains, followed by reformation of the polymer down to the particle surface to form a positive patch. This results in transition from bridging aggregation to patching aggregation.

2.3.2 Retention aid systems

Typically, all chemicals used for retention systems are used based on above three fundamental mechanisms of flocculation. Following polymer retention aid systems have been frequently used for filler retention.

Single component retention aid system

The simplest example of polyacrylamide-induced flocculation is adding a cationic polyacrylamide (CPAM) onto negatively charged fibers, fines, or fillers. When a cationic PAM approaches these particles, it adsorbs on the particles by electrostatic attraction. This action may even help to compress the double layers somewhat by charge neutralization, although this is not a cationic flocculant's main role. Once the particles have closed in on each other, the bridging action can occur. In practice, cationic PAMs, as well as all flocculants, are constrained by the mechanical and chemical dynamics of the paper machine wet end such as shear effect, stock temperature, pH, stock conductivity, and DCS. As shown in Figure 15, the positively charged high molecular weight CPAM showed very high initial flocculation efficiency compared to the low molecular of PDADMAC in patch model. When the shear force was induced, the particle size was

dramatically decreased then could not be recovered. Even though the reflocculation is poor, it needs note that the reflocculation of 20% cationic charge of CPAM has better behavior than that of 10% cationic charge of CPAM [48].

In the case of anionic or nonionic polyacrylamides, since their double layer may be thicker than that of CPAM, a longer anionic molecule may be required, hence a higher molecular weight. Therefore, ultra high molecular weight anionic flocculants are required for good retention (between 4,000,000 and 7,000,000) [50]

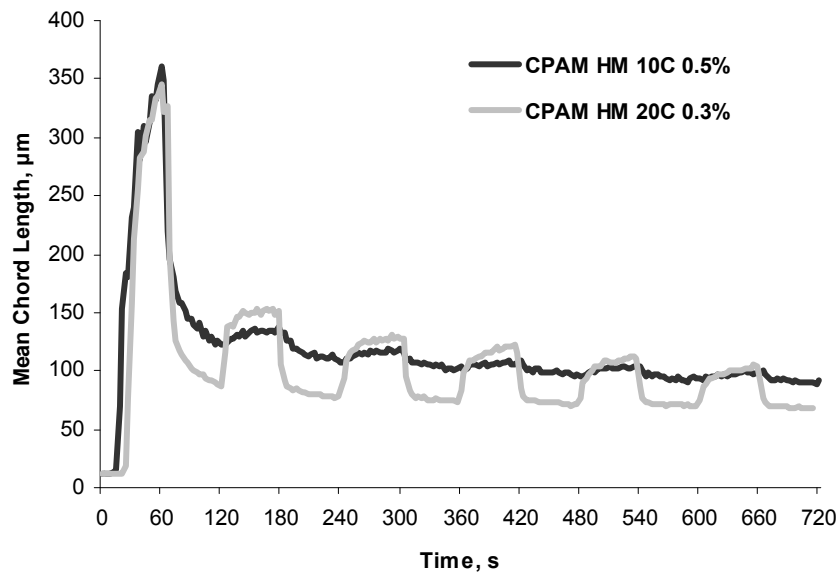


Figure 15: Mean chord length as a function of time after CPAM was added to the suspension of clay. The shear level was changed by changing the impeller speed between 300 and 900 rpm every 60s [48]

Dual component retention aid systems

The negatively charged particles are repelled by electronic repulsion force, which is expressed in DLVO (Derjaguin, Landau, Verwey, and Overbeek) theory. The coagulant partially neutralizes some negative charges and compresses the double layer. The anionic

PAM reacts with the opposite charge on the particles. The commonly known coagulants are alum, polyethyleneimine, PDADMAC, PAC, polyamine, or cationic starch. These cationic polymers are added first to flocculate the anionic fibers and fillers. After a shear stage where the flocs are redispersed, the anionic or cationic PAM is added and new flocs are formed by bridging between the cationic floc fragments [51]. Figure 16 illustrates the dual polymer system where the PDADMAC was first added then anionic charged PAM was added. Initial flocculation size caused by PDADMAC used for charge neutralization was around $30\mu\text{m}$ and then the floc size was sharply increased by the increased amount of APAM. The reflocculation was also very significant compared to the single polymer system.

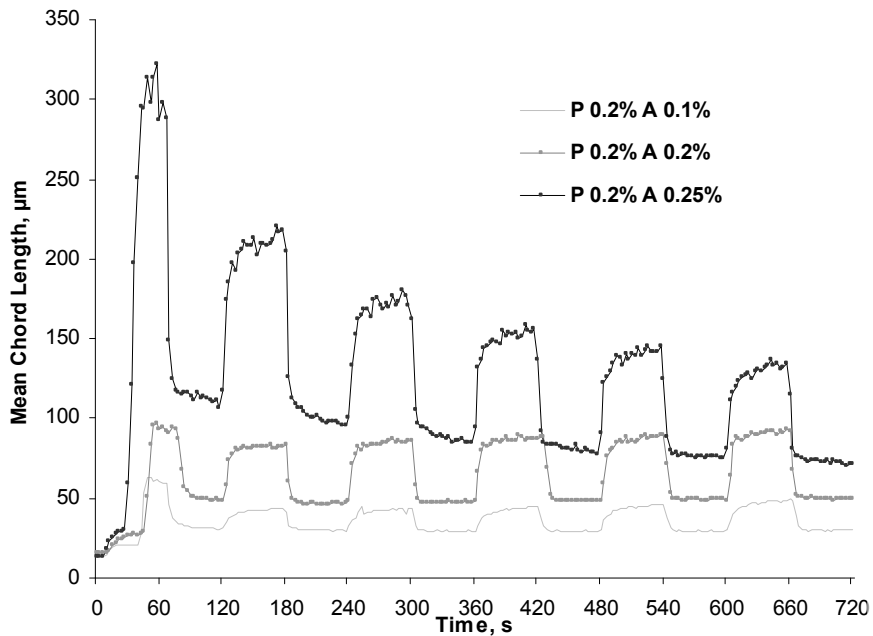


Figure 16: Mean Chord length as a function of time and dosage after PDADMAC and PAM addition to suspension of clay. PDADMAC was added at $t = 10$ seconds under 300rpm speed and then PAM was added at $t=30$ seconds. The shear level was changed by changing the impeller speed between 300 and 900 rpm every 60s [52]

Micoparticle retention system

Charge neutralization creates small coagulated structures which can give good drainage and formation, but poor retention. On the contrary, single or dual polymer systems create large flocs which, when used to produce high retention, can cause drainage and formation difficulties.

To circumvent these difficulties, micoparticle systems allow high first-pass retention without harming, even improving, formation as well as increasing drainage for production increases, and develop energy savings.

The two most widely used micoparticle retention systems are 1) cationic starch and /or cationic PAM with colloidal silica and 2) cationic PAM with hydrated bentonite. The former is the first micoparticle retention aid system made commercially available. The proposed mechanism suggests that the cationic starch or PAM is adsorbed by the fiber fines and generates a floc structure. Usually, cationic starch forms very small cationic flocs and CPAM forms a macrofloc structure in the stock. As stock goes through the last point of shear, the floc structure is broken down and compresses upon itself, a mechanism called peptization. The addition of the colloidal silica reforms a three-dimensional microfloc structure.

The initial step of CPAM/bentonite system involves the creation of a cationic floc with a medium molecular weight PAM before the last point of shear. The shear breaks down the floc, if necessary, which then compresses itself by peptization. At this moment, the flocs would tend to repel each other. The hydrated bentonite is added after the last point of shear and a three-dimensional microfloc structure is created [53-55] .

Network (fishnet) system

In mechanical pulp, high levels of anionic contaminants make it more difficult to neutralize a papermaking wet end with coagulants. In these cases, several retention aid systems which do not require charge neutralization are available to function effectively. The network flocculation [56] is based on hydrogen bonding interactions, typical for systems based on, e.g. phenol formaldehyde resin (PFR) and polyethylene oxide (PEO). The polymer does not have to adsorb onto the surfaces of substrates for entrapment. The transient, unstable networks were believed to trap the fines and fillers by an occlusion process. Another theory centers on the concept of the polymer bridging substrates together. Phenolic resin would adsorb onto the substrate surface which would provide hydrogen-bonding sites for PEO [57]. Recently, the heteroflocculation mechanism of particles with colloidal PEO/PFR complex was issued for PEO/PFR mechanism [58, 59].

Floc break-up and Reflocculation

In modern papermaking, the trends towards higher speed paper machines, the higher turbulence hydraulic headboxes, and the different types of twin-wire formers have increased the need for retention chemicals able to produce shear resistance flocs. Therefore, the flocculation behavior and dynamics of cellulosic fibers and fillers by chemicals are of critical importance in a variety of papermaking processes. For example, the improved drainage and retention by flocculation can be highly advantageous to the papermaker, allowing increased production and process efficiency. However, the chemical flocculation of fibers or fillers can make the paper less uniform. Therefore,

papermakers are continually involved with finding better ways to balance the benefits and penalties of flocculant use.

Tam Doo *et. al.* [60] showed that the unit operations of a typical paper machine system provide a wide range of hydrodynamic shear environments. These unit operations such as pressure screens are very effective for breaking up fiber flocs, including hard flocs caused by retention aids. Generally it is assumed that a steady state is reached at which the rate of floc formation equals the rate of floc destruction. In a sheared suspension, flocculation may initially occur quite rapidly by increased collision frequency, but the flocs eventually reach a limiting size and no further flocculation occurs. This limiting size depends on the applied shear rate and on the strength of the flocs. The traditional method of floc strength characterization correlates the maximum floc size, d_{\max} , in a suspension with the applied shear rate, G , via the expression [61] where C and γ are empirical constants reflecting the average strength of the floc particles.

$$d_{\max} = C \cdot G^{-\gamma}$$

Equation 6: The maximum floc size in a suspension

The polymer bridging process produces stronger flocs than charge neutralization, but in the former case, flocs broken at high shear rates may not easily re-form. This irreversibility may be a result of re-conformation of adsorbed chains during the application of high shear or the scission of covalent bonds within the chain of a polymer [62, 63]. Flocs produced by charge neutralization appear to re-form readily after breakage.

Hedborg and Lindstrom [64] defined a reversibility index based on results from fiber retention experiments at two different stirring speeds, first at 1000 rpm (Ret_{1000}) and after 60s at 500rpm ($Ret_{1000/500}$). The second experiment was carried out at 500rpm (Ret_{500}) as a reference. The reversibility index was defined as below in Equation 7.

$$\text{Reversibility index} = ((Ret_{1000/500} - Ret_{1000}) / (Ret_{500} - Ret_{1000}))$$

Equation 7: Reversibility index

By using this definition it was found that the reversibility of chemical flocculant systems was greatly different in terms of charge density and molecular weight.

Farnwood *et al.*[65] reported that the fibers were found to be reflocculated within about 0.1 seconds in dilute slurry coming from the slice of a paper machine headbox. Such rapid reflocculation is due to the high length-to-width ratio of cellulose fibers and their resulting collisions in a turbulent shear flow regime.

Swerin *et al.*[54] determined the reflocculation of microcrystalline cellulose using Marvern laser diffraction particle size analyzer after adding a wide range of different retention aid systems. Results showed that the degree of reflocculation after high-shear deflocculation was relatively high due to their charge characteristics. For the APAM system the ability of flocs to form again after being dispersed was low.

2.4 Problems of Conventional Wet-End Systems

For many years, the increase in filler content in paper has been driven by the reduction in papermaking cost, improvements in optical properties, paper formation, printability, and the water removal rate during the papermaking. In the early days of papermaking, common retention aids were based on alum, which neutralizes charges on the furnish compounds. Later, single polymers such as polyethyleneimine (PEI) or polyacrylamide (PAM) were introduced with patching or bridging as the dominant mechanism. Dual polymer system with a cationic polymer (PEI, poly-DADMAC, or cationic starch) and an anionic polymer (anionic PAM) was developed also based on both mechanisms. In the early 1980s, micro and nano particle systems were introduced on the market. Recently, systems based on PEO and phenolic resin function according to the network flocculation or at least by hydrogen bond interactions.

Wet-end is the part of the process where the sheet is initially formed and thus a great deal of influence over things such as formation, tensile, tear, and directionality of the sheet is possible. An effective wet-end system is the key to optimum sizing efficiency, good opacity, overall machine runnability and reduced furnish cost through better utilization of fillers or other additives. If the wet end system is not controlled well, there will be many serious problems such as poor runnability, increased deposits, sheet defects, higher additive costs, and higher sewer losses. However, the wet-end system in papermaking is very hard to control, especially when fillers are added, because the factors affecting the wet-end chemistry are varied and complicated, which will be discussed as below;

Charge density

Although dry strength or retention aids such as starch can improve the strength or retention of paper, there are some problems related to high starch addition in conventional wet end papermaking processes because the retention of non charged polymers in a pulp furnish is very poor (less than 40%) [66]. In order to enhance the adsorption of non-charged starch to anionic surfaces of wood fiber, cationic groups needs to be introduced to starch backbones. However, the chemical modification of starch by introducing cationics will significantly increase the cost of papermaking. When anionic trash is presented in the system, the cationic demand increases so that a suitable anionic trash catcher should be added for the high efficiency of cationic charge.

Anionic trash

Although the adsorption of starch or water soluble polymers can be improved by introducing cationic groups, the retention of wood fibers or fillers is still a problem when anionic trash in the wet end furnish is high. The main source of the anionic interfering substances is pulp furnish. Mechanical pulp is rich in hemicellulose derivates and unbleached kraft pulp contains sulfonated lignin byproducts, soaps, and hemicellulose byproducts. Broke form a coating operation tends to contain high levels of polyacrylate dispersants. These anionic substances can form complexes with cationic wet or dry strength aids and retention aids by charge neutralization [67]. Therefore, the effective charge of the cationic additives is reduced due to the complex formation which remains in suspension as colloidal dispersion [68]. Detrimental materials influence the process of machine running by decreased fiber swelling and delayed beating rate. The blocking

effect of anionic trash on beating auxiliaries and strength increasing agents, leads to higher energy costs. In addition there is a loss of retention and dewatering which has consequences on paper quality, i.e. sheet formation.

The adverse effect includes the appearance of dark spots and holes as well as an increase in breaking frequency in the paper. The negative efficiency of cationic additives, like retention aids, starch etc is due to the neutralization reaction of anionic trash with these components. Through this process the cationic chemicals may become ineffective.

Zeta-potential

Addition of a highly cationic material such as alum or polyamine tends to increase drainage or retention up to the point where the electrical potential of the furnish solids approaches zero. If the zeta-potential of the system is not controlled properly, for example overuse of cationic chemicals, the repulsion of particles occurs, which causes the low filler retention, poor runnability, or deposit problem. Brouwer reported that 100% of cationic starch is reached at around 1.5% addition of two types of cationic starch (DS 0.017 and DS 0.047) for bleached pulps, but the adsorption of starches dropped at higher dosage as the zeta potential increased [69]. The zeta potential affects not only the initial flocculation (or aggregation) but also the reflocculation of particles and fibers. As Figure 17 shows, as the zeta potential close to the zero, the reflocculation index increases [48]. Also, severe fluctuations in formation and sheet breaks can be caused by uncontrolled zeta potential .

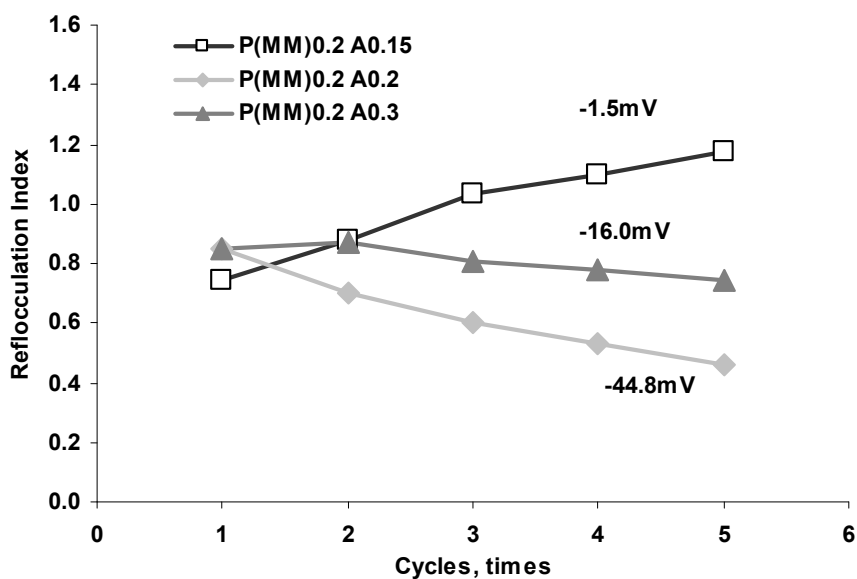


Figure 17: Reflocculation index of the dual polymer system with cationic PDADMAC (medium molecular weight) and anionic PAM and its relationship with zeta potential [48]

Fiber Flocculation

The flocculation of the fiber suspension by polyelectrolytes such as cationic retention aids, or dry-strength agents may also cause poor formation [70]. Formation is a term used to describe the uniformity of fiber distribution in a paper sheet. A scientifically well-defined, dimensionless measure is the formation number F , based on local variation in actual grammage and defined as the coefficient of variation of local grammage W_A

$$F_A = \sigma(W_A) / W'$$

Equation 8: Formation number

where A is the size of measuring area. The formation of a paper sheet is a result of physical and chemical interactions during the forming process.

Small-scale grammage variation of high amplitude can lead to density variation caused by uneven wet-pressing and to a less effective water removal. They may also lead to uneven drying conditions and to corresponding variation in drying stresses. Flocculation may lower the strength of a paper sheet because of uneven stress distribution due to poor formation. Stress is more uniformly distributed in a well-formed sheet [70].

Slime and pitch

If the retention is not well controlled, unretained polyelectrolytes such as cationic starch will accumulate in the whitewater and create pitch, slime, and stickies problems. The concept of slime is not only biological slimes such as bacteria, fungi, and algae, but also biological deposits with inorganic fillers and organic materials such as pitch and fibrils. The most important energy sources for the bacteria or slime are starch and its degradation products [71]. Slime problems usually become apparent first as an increasing frequency of transparent, brittle spots in the paper. These spots consist of fibers stuck together by slime, the grammage of which is twice the normal. Besides spots, slime increases the number of web breaks and breakdowns due to blocked felts, screen, and pipes [71].

pH dependence

Polymers, including starches, containing ionizable groups such as carboxyl or tertiary amine will assume a charge which is pH dependent (Fig 23). The degree of polymer ionization at a given pH can be determined from a simple acid-base titration curve [72].

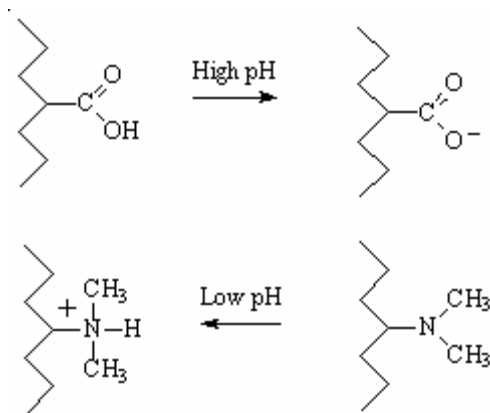


Figure 18: Ionization of carboxyl and tertiary amine group [72]

In water, H^+ ions associate with the amine to give an ammonium salt. The protonated amine has a cationic charge. Alkaline conditions deprotonate the cationic ammonium salt to give the neutral amine salt as shown in Figure 18 [73]. The cationic charge of the additive is significantly reduced, and thereby a special care, in terms of pH, should be taken to maximize the efficiency of the charged polymers in the wet-end as shown in Figure 19 [73].

Addition of charged polymers to a papermaking furnish can have a major effect on fiber charge. Most anionic polymers, including those generally regarded as non-substantive to cellulose, will adsorb on fiber to some finite extent. Cationic polymers will reduce fiber anionicity and at sufficient addition levels reverse the charge to cationic. The change of charge with polymer dose is rarely linear.

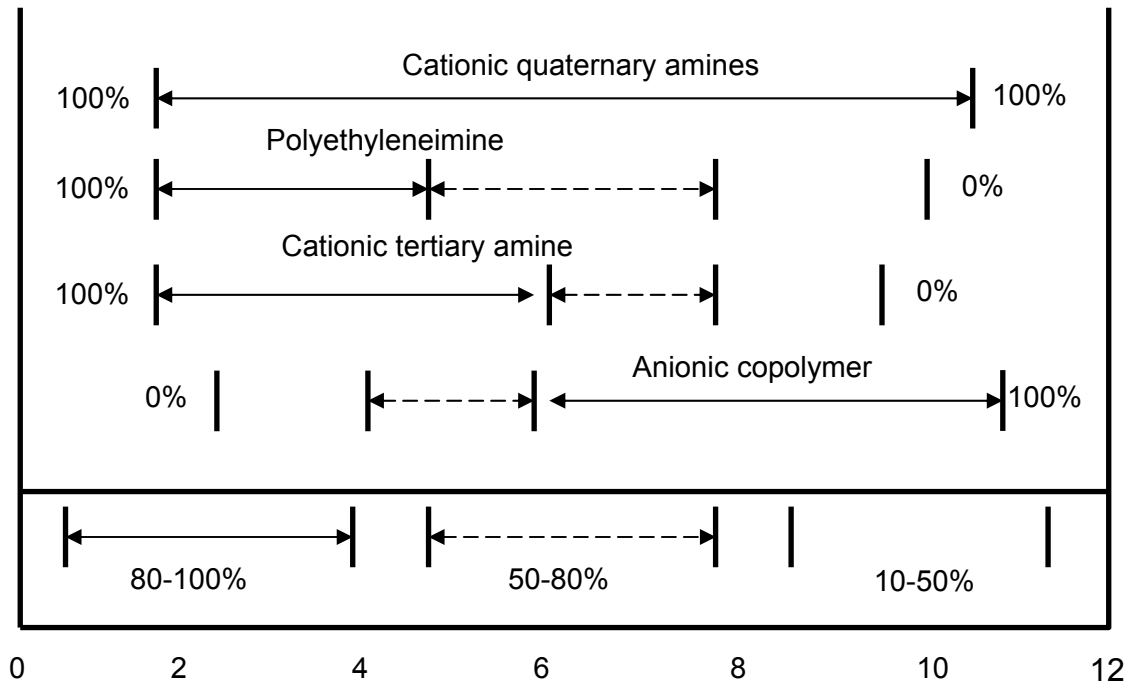


Figure 19: Effect of pH on the charge of various polyelectrolytes (legend: % of functional charge on polyelectrolyte) [73]

Residence time

The time interval between sampling and charge measurement must be kept to a minimum, preferably less than about 3 to 4 minutes. The wet-end chemistry of papermaking systems is rarely at equilibrium, particularly when fiber-polymer interactions are involved. Delay in charge measurements allows certain processes to continue, so that erroneous results may be obtained. Trksak [74] reported that the cationicity of aluminum sulfate (alum) decreases rapidly with time, and was only half the initial level after 5min. The alum solution exhibited no charge after 60min. This effect of time decay of alum affected the CaCO₃ retention. Initial calcium carbonate retention was 63% using 0.5% alum and 1% amphoteric starch, but where the alum was mixed with the

pulp for 60s prior to starch addition, the retention dropped to 56% [74]. The reason for the time decay of cationic polymers can be explained by a three-step mechanism; the initial rapid adsorption of cationic polymer to the fiber surface via loops and tail, the relaxation of the loops and tails on the surface, and diffusion of polymer into the pores of the fiber [75]. Koethe et al. found that the rate of decay is relative to molecular weight, charge density, and degree of turbulence during mixing [76].

2.5 Pretreatment of Filler

As filler loading is increased, the paper strength, bulk, and stiffness are usually decreased. To increase the proportion of filler without sacrificing paper properties, various methods have been explored. The preflocculation method prior to addition to the paper stock has been well studied in the past [77-79]. Marbee and Harvey [80] published the preflocculation of filler materials via the Grain Processing Corporation's filler flocculation technology. They demonstrated that preflocculation could provide a significant increase in sheet filler content without a loss in strength, optical properties, or runnability parameters. From pilot plant trials, they reported flocculation method could provide an approximately 26% increase in first pass ash retention and 13% increase in the tensile strength when same amount of filler was used [81]. Following the addition of the flocculant to the filler stream, the flocculant/filler combination moved through a shear device, which imparted a controlled level of work. By regulating both the flocculant addition on to filler and shear level, they were able to generate a treated filler material which contains a controlled, increased particle size and charge. They used a starch-based product for the preflocculation of filler. And they also added a coagulant agent, polyaluminum chloride, capable of neutralizing anionic trash to the thick stock at the blend chest pump and used additional retention systems consisting of synthetic flocculant, added just prior to the primary screen, and micropolymer, added after the screen. They reported that size degree and burst strength were increased and that both stiffness and opacity did not decrease by this pretreatment [81].

Filler retention can be achieved either by using a retention aid or by modifying the filler particle with a chemical treatment which causes them to flocculate prior to addition to the paper stock [82, 79].

Filler modification with polymers, such as chemically bonded poly(acrylic acid) and poly(vinyl acetate) to fillers was also reported [83]. Gill modified filler surfaces to improve filler-fiber bonding using epichlorohydrin and polyamino-amide or polyamine [82]. Using filler and wood fines composites in handsheet making were reported by Aho *et al.* recently [84].

Hayes [78] compared the four main preflocculated filler systems which were cationic starch/filler, PAA/filler, “Snowfloc” polymer/filler, and amphoteric guar gum/filler. Results showed that the preflocculated filler with PAA had several advantages, including the low cost and the production of stable flocs with good shear resistance.

Gill [85] used the filler consisting of finely divided calcium carbonate that had been surface-treated with 0.1-10 wt.% (based on dry weight of filler) of a cationic polymer containing a dimer. It has been rendered cationic by treatment with a polyamino-amide and/ or a polyamine polymer, both of which have been reacted with an epoxidized halohydrin compound such as epichlorohydrin. The use of this modified filler results in improved opacity and filler retention, better drainage, reduced need for sizing agents, and other benefits.

Novak, Stark and Eichinger [86] showed that pretreatment of filler permitted an increase in filler content in paper without reducing paper strength. This study examined the strength of paper from chemical pulp or TMP to which pretreated clay, calcium carbonate, or amorphous silicon dioxide was added. The fillers were pretreated with

aluminum sulfate, cationic PAM, anionic PAM, and/or cationic starch. Treating the kaolin with either the anionic or cationic PAM or the cationic starch resulted in improved paper strength properties. However, for calcium carbonate or silica, an increase in mechanical properties was achieved only with cationic additives. For all the fillers, better retention was observed with the groundwood.

Park and Shin [87] studied the properties of preflocculated fillers using ground calcium carbonate and talc treated with high molecular weight (HMW) CPAM, low molecular (LMW) CPAM, and cationic starch. The initial floc sizes of HMW CPAM pretreated fillers were larger than those of any other pretreated fillers, and LMW CPAM pretreated fillers were the smallest. Cationic starch pretreated fillers were the weakest and HMW CPAM pretreated fillers were the strongest under shear conditions. The retention of all the pretreated fillers was much higher than untreated fillers in both calcium carbonate and talc. The preflocculation of filler increased tensile index, tear index, burst index, and folding properties, and the strength properties provided by preflocculation were higher when no retention aids were added. In optical properties, HMW CPAM pretreatment gave the poorest opacity, but LMW CPAM and cationic starch pretreatments were good or not significantly different compared to no pretreatment.

To increase the bonding efficiency of CaCO_3 with fibers, Koper *et al.* [88] made the poly(propylene imine) dendrimer which was more highly charged than PEI. They reported that the deposition of dendrimer-coated calcium carbonate particle followed Langmuir kinetics as did uncoated or PEI-coated particles. Measured deposition rate constants were twice as large as observed with PEI on CaCO_3 particles. The deposition efficiency increased with particle size and the detachment rate constants were nearly

constant. From this they concluded that dendrimers were a somewhat better retention aid than PEI.

Vanerek *et al.*[89] reported that untreated calcium carbonate pigments, both precipitated (PCC) and ground (GCC), behave similarly when dispersed in water. Their charge, either positive or negative, depended on the CaCO₃ concentration and the purity of the water. From their experiment with water of different degrees of purity (deionized, distilled, doubly distilled), when the concentration and the total surface area were low, the amount of impurities per particle was much larger, thus these impurities significantly affected the surface charge. However, in neither case was the charge strong enough to prevent aggregation of pigment particles. In the presence of cationic polyelectrolytes, they reported, their behavior depended on the type of adsorbed polymers. Highly charged polyethylenimine (PEI) stabilized both PCC and GCC due to increased electrostatic repulsion which can be explained satisfactorily on the basis of the classical DLVO theory of colloid stability. Polyacrylamide (PAM), on the other hand, flocculated both fillers by a bridging mechanism.

They also showed that introduction of PEI into the suspension promotes deposition driven by electrostatic interaction, provided that PEI concentration is not too large. With an excess of PEI, both the fiber and pigment become positive and repel each other. On the contrary, introduction of cationic PAM causes flocculation of the pigment and its deposition on fibers, regardless of the PAM dosage, indicating that electrostatic interaction was not a dominant effect. They concluded that PAM is more effective as a retention aid due to its flocculation ability and the bridging mechanism alone. However,

this conclusion was not sufficient to account for the observed interaction between pigment particle and fiber at high PAM dosage.

Dunham [90] reported the differences in the chemical nature of the surface of the filler particle had a large impact on the adsorption property of the retention aid. For example, it is well known that polyacrylamide based flocculants adsorb well to the kaolin clay particles and polyethylene oxide (PEO) does not adsorb well onto PCC surfaces. He also reported the value of zeta potential was directly related to the chemistry of filler particle surface or was a result of surface modification. Clays (hydrous, calcined) and calcium carbonates are hydrophilic, while titanium dioxide, talc and sodium aluminosilicate are hydrophobic. Hydrophobic fillers require dispersants to form stable slurries. Dispersants significantly change surface properties and zeta potential of the filler.

Lumen loading method that held filler mainly within the lumens of fibers has been studied for many years [91-93].

Although many approaches have been studied for improving the paper strength at high filler content, except for the preflocculation method, none of these technologies has delivered a practical solution to paper manufacturers.

CHAPTER 3

PROBLEM ANALYSIS AND OBJECTIVES

3.1 Problem statement

The addition of fillers to paper has been driven by the desire to substitute more expensive fibers with less expensive fillers and thereby reduce production costs. Additionally the visual properties of the sheet- the brightness, opacity, and printing characteristics- will be increased. However, the addition of filler reduces the degree of bonding in the sheet, resulting in the decrease of physical properties such as paper strength. Hence, it is necessary to suggest the methods to recover the loss of the strength due to the filler loading without hurting the optical properties and provide a scientific model for the strength prediction.

3.2 Problem analysis

The primary goal of this research is to analyze the mechanism of the strength loss due to the addition of filler in paper and suggest the method to increase the strength of paper based on the analysis.

Hydrogen bonding is a key force in fiber and sheet strength. Paper consists of fibers bonded through a hydrogen bond matrix. However, the filler acts as the debonder between fibers because there is no bonding site on the surface of the filler. The size of the filler particle, the size distribution, and the shape of the filler particles in relation to the fiber network structure are important factors for the properties of the paper. In general,

the smaller the pigment particles, the greater their negative effect on strength. Therefore, as shown from the background in Chapter 2.5, there has been extensive research in the area of the pretreatment of filler in order to improve these factors. The mechanism to increase the strength of paper by the pretreatment of filler has been reported by the reducing the surface area of filler as in Figure 20. However, the cationic polymer such as cationic polyacrylamide (CPAM) or cationic starch for filler preflocculation is easily broken by the high shear force in the system and its charge can be affected by the high charge of other anionic substances. Moreover, the cationic polymers could not cover the whole surface area of the filler because their adsorption is restricted by the cationic demand of the filler surface. Therefore, it is clear that the strength improvement has a limitation by the restricted maximum adsorption of cationic polymers

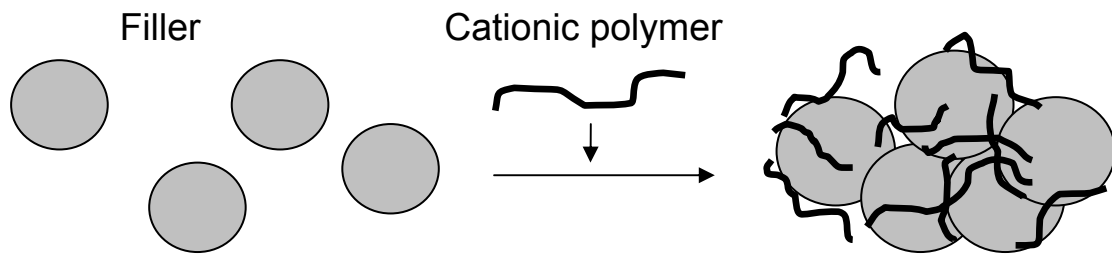


Figure 20: Filler preflocculation

3.3 Hypothesis

1. The background information in Chapter 2 and the above problem analysis suggest that the strong bond strength between fibers and fillers is required to recover the loss of fiber-fiber bond strength by the addition of fillers. It has been well known that cellulose and starch have a good bonding ability with wood fibers. Cellulose and starch

can be dissolved and regenerated or precipitated by appropriate methods such as solvent, charge neutralization, salting out, or complexation and so on. During the regeneration or precipitation, these bonding materials are located (or coated) on the filler surface, which might result in the structure of the core-shell or composite as shown in Figure 21.

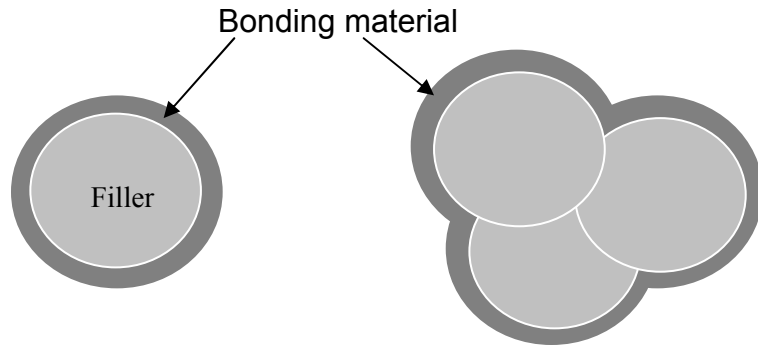


Figure 21: Coated fillers with bonding material

2. From background information, we know that cellulose or starch has a bonding enhancing structure due to three hydroxyl groups in every glucose unit. Therefore, if this bonding material can be evenly coated on the filler surface, the paper strength will be improved by the hydrogen bonding between fibers and fillers as Figure 22 suggests.

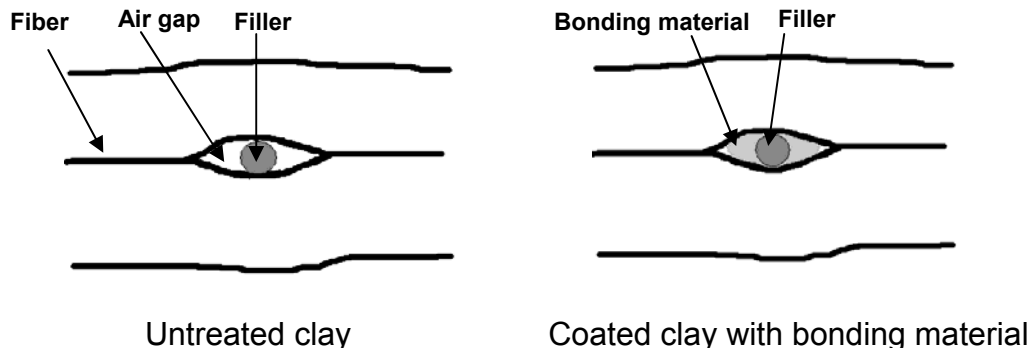


Figure 22: Scheme of bonding between fibers and clay or coated clay

3. Paper strength can be expressed as the sum of the fiber strength and the bond strength. As the mass fraction of fillers or coated filler with bonding materials in paper is increased, the zero span tensile strength reflecting the fiber strength will be decreased, which is measurable. Therefore, the effect of fillers on the bond strength of paper is assumed to be the key to predict the strength of paper. The important factors might be the filler size, mass fraction of filler, and bond strength between fillers and fibers.

3.4 Objectives

In order to prove the above hypothesis, following objectives are provided.

3.4.1 Preparation of coated fillers with bonding materials

The criteria of materials for filler coating are that 1) have a simple coating operation to be fixed on filler, 2) have a good bonding property with wood fiber to improve paper strength, 3) have a strong resistance for pH, temperature, and shear not to be easily dissolved after forming a coating layer on filler.

Fillers coated with bonding materials such as cellulose or starch will be prepared based on the above criteria and their characteristics under different conditions such as temperature or pH need to be determined. The solubility of composites is a very important factor because if the solubility is low, the bonding efficiency with wood fiber will be decreased and operational problems such as slime and pitch will be resulted. This solubility is determined using a total organic carbon (TOC) analyzer. To characterize the composite fillers, other instrument such as XRD will be used. The appearance also plays

an important role for retention. Optical microscopy and SEM will be used for characterizing the appearance and the surface of the composites.

3.4.2 Determination of the physical and optical properties of filled sheets

The effect of fillers coated with bonding materials on the physical properties and optical properties needs to be determined. The aim is to obtain the optimum bonding material ratio to filler or the maximum pulp amount to be able to be replaced without hurting optical properties compared to untreated fillers. Tensile, Z-directional tensile, zero-span tensile, burst, folding, and stiffness will be measured to quantify the physical properties of the sheet. Brightness and opacity will be tested for the optical properties of the sheet.

3.4.3 Tensile strength modeling

The appropriate model of paper strength for filled sheets needs to be derived from the equation which includes characteristics of fillers. The effect of composite size, bonding strength, or mass ratios on the tensile strength will be investigated and used for the modeling of tensile strength.

CHAPTER 4

Starch-Based Clay Composites by Ammonium Sulfate Precipitation Method*

Abstract

Starch-clay composites with different aggregates sizes and starch to clay ratios were prepared by a precipitation method. The aggregates of the composites were used as fillers to improve the paper properties. The experimental results showed that clay-starch composites could increase paper strengths more than 100% compared to untreated clay at 20-30% clay loading. The increase of paper strengths of clay-starch composite filled handsheets was mainly caused by two reasons, i.e. the relatively large aggregate size and improved internal bonding. The optical properties compared at same mechanical strength were also improved. The water solubility of the starch coated on the filler was very low (less than 3%) at 50°C for 30 minutes, which indicates that this material can be used as papermaking fillers. Bonding characteristics were investigated by Scanning Electron Microscope (SEM).

* *This chapter has been modified from the following publication: Yoon, S.Y. and Deng, Y., Clay-Starch Composites and Their Application in Papermaking, Journal of Applied Polymer Science, 100 (2): 1032 (2006)*

4.1 Background - Structure and characteristics of starch

As stated in Chapter 3, the criteria of materials required for filler coating are 1) simple coating operation to be fixed on filler, 2) good bonding property with wood fiber to improve paper strength, 3) shear resistance not to be easily disrupted under high shear conditions, and 4) low solubility at broad range of pH and temperature not to be dissolved in wet-end after forming a coating layer on filler.

One of the promising bonding materials is starch. As shown in the pretreatment part in Chapter 2.5, even though the preflocculation method by the cationic polyelectrolytes such as cationic starch has advantages for filler retention (26% increase) by the reduced surface area of fillers, the improvement of paper strength is not significant (13% increase) [80]. Moreover, because the starch adsorption method such as preflocculation method is basically dependent upon the charge interaction, it is sensitive to zeta potential or pH. Therefore, the different association method of starch and clay is needed to form the structured filler increase the bonding between fillers and fibers. In order to accomplish this task, it is necessary to understand a detailed knowledge of the physical and chemical characteristics of the candidate bonding material, starch.

Starch consists of two main macromolecules, amylose (15-30%) and amylopectin (70-85%). The dense layer in a growth ring consists of about 16 repeats of alternating crystalline (5-6nm) and amorphous (2-5nm) lamellae (semicrystalline layer) as shown in Figure 23 (a) and (b).

Amylose is an essentially linear polymer which consists of (1→4)- α -D-glucose units. The linear amylose molecules can readily align themselves next to each other and form interchain hydrogen bonds through the hydroxyl groups.

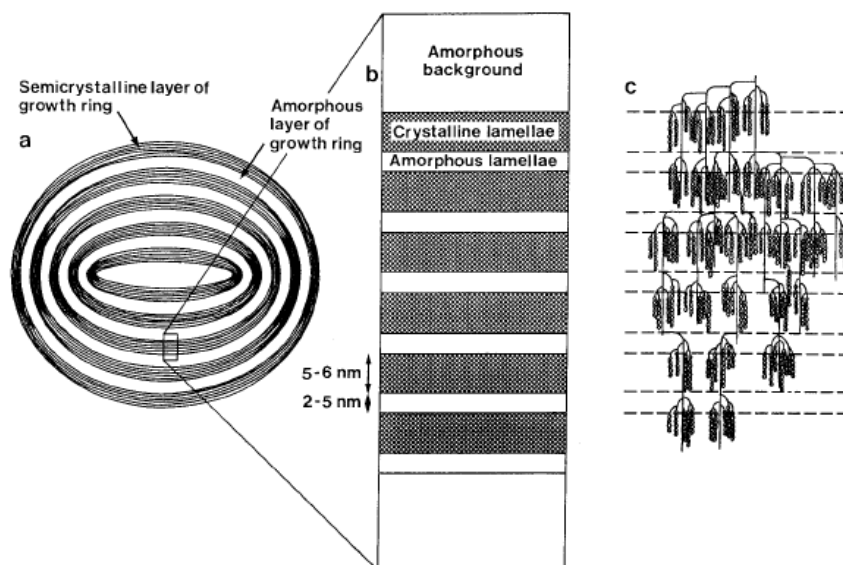


Figure 23: Schematic representation of starch granule structure: (a) a single granule with alternating amorphous and semicrystalline layers, representing growth rings; (b) expanded view of the semicrystalline layer of a growth ring, consisting of alternating crystalline and amorphous lamellae; (c) the cluster structure of amylopectin within the semicrystalline layer of the growth ring [94]

When sufficient interchain hydrogen bonds are formed, the individual amylose molecules are associated to form molecular aggregates with reduced hydration capacity and hence, lower solubility.

Amylopectins have a highly branched structure consisting of short linear amylose chains connected to each other by α -1 \rightarrow 6 linkages. It is generally agreed that these macromolecules are assembled in a cluster structure, in which the crystalline region is made up by amylopectin double helices [95], whereas the amylopectin branch points are in amorphous zones (Figure 23 (c)) [94].

From X-ray diffraction studies of amylose fibers, Wu and Sarko demonstrated that both A- and B-type structures contain ordered arrays of double helices. A model of the starch granule structure is schematically shown in Figure 24.

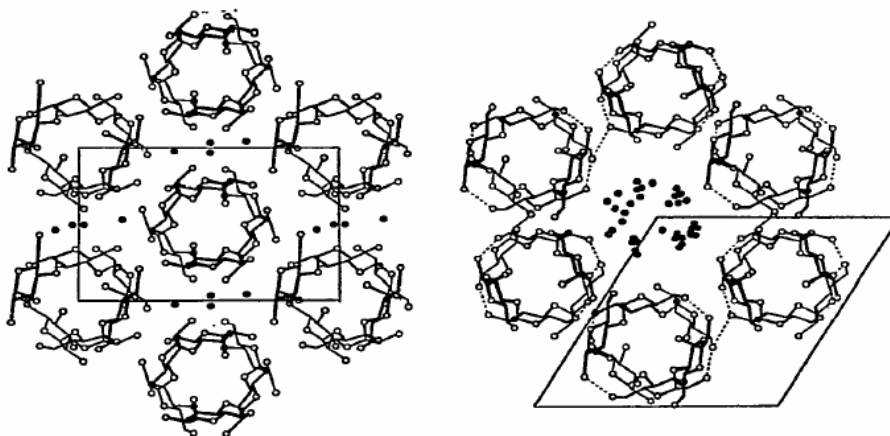


Figure 24: Representation of helix packing and unit cells in A-type (left) and B-type (right) crystalline. Water molecules are indicated in the lower view by dots. Hydrogen bonds are indicated by dashed lines [96, 97]

Because the amylopectin is highly branched, it cannot readily undergo the retrogradation or crystallization phenomenon that amylose so easily does. Hence, in contrast to amylose, isolated amylopectin is easily dispersed in water and does not readily gel. It is also noted that amylopectin does not form strong, unsupported films because the highly branched molecules cannot readily orient themselves in parallel alignment with other amylopectin molecules to form the multitude of associative hydrogen bonds necessary to produce strong films.

In dilute solution (less than 1%), the amylose precipitates. In more concentrated dispersions, the aggregated amylose entraps the aqueous fluid in a network of partially associated amylose molecules, forming a gel as shown in Figure 25 [98].

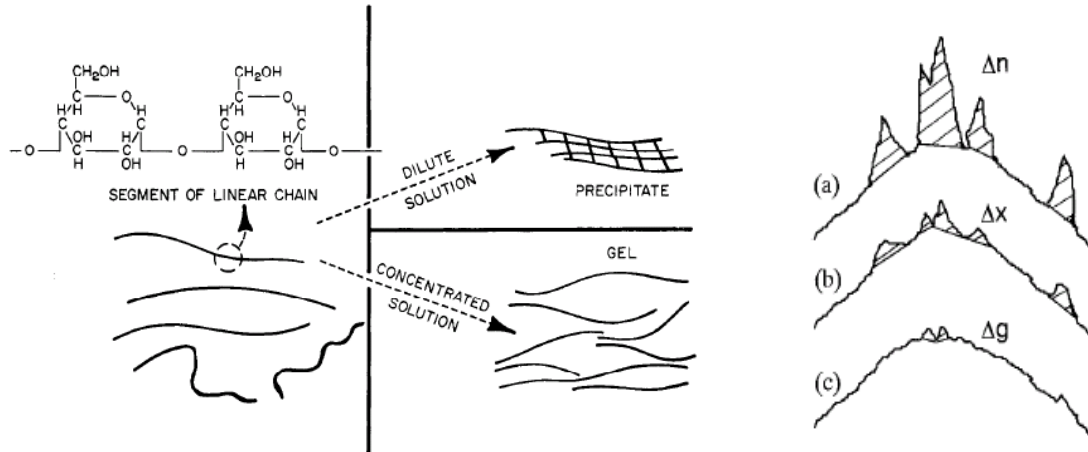


Figure 25: Behavior of amylose in solution (left) [98] and starch crystallinity by X-ray diffractometry (right): (a) native starch; (b) retrograded starch; (c) gelatinized starch [99]

This process of alignment, association, and precipitation is essentially a crystallization process and is known as *retrogradation* (Figure 25 (b)) [99]. The rate of retrogradation depends upon the molecular size and concentration of the amylose, the temperature, and the pH. Because amylose is a linear molecule with a marked tendency to associate, it can form strong, unsupported films similar to those of cellulose.

The starch granule is insoluble in water below about 50°C. However, when the aqueous slurry is heated to temperature (about 55 to 80°C), the intermolecular hydrogen bonds holding the granule together are weakened and the granule undergoes a rapid, irreversible swelling because water enters the gel or amorphous regions of the granule. The granules take up the water, swelling to many times their original volume, rupturing and collapsing as the heating and agitation of the mixture continues, and releasing concurrently some of the starch molecules, particularly amylose, into solution [100]. When the starch granule is heated in water to a temperature above the gelatinization

temperature (cooking process), the water also enters the crystalline regions, which are disrupted.

Insoluble or less soluble starches have been developed for a filling material or ion exchange resin. It can be mainly divided by two categories. One is the precipitation of cooled starch using organic solvents such as ethanol and acetone or saline salts such as MgSO_4 and $(\text{NH}_4)_2\text{SO}_4$. The other is crosslinking method using aldehyde, vinyl sulfone and epichlorohydrin. Among methods, ammonium sulfate salt is an effective “salting out” material for enzymes [101, 102], protein [103, 104], and starch [105]. Generally, it has been known that as the concentration of salts such as Na_2HPO_4 , $\text{Na}_2\text{B}_4\text{O}_7$, $\text{Na}_4\text{P}_2\text{O}_7$, NH_4CNS , and NH_4Cl increases, the crystallization is retarded [106]. Khairy *et. al.* [105] reported that the anion effects follow a lyotropic series which causes retrogradation in the approximate descending order: CNS^- , PO_4^{2-} , CO_3^{3-} , I^- , NO_3^- , Br^- , Cl^- , $\text{C}_2\text{H}_3\text{O}_2^-$, F^- , SO_4^{2-} . Cations also tend to follow the lyotropic series of Ba^{2+} , Sr^{2+} , Ca^{2+} , K^+ , Na^+ , Li^+ . The descending order of ions in the lyotropic series can be explained by the decreasing polarity and decreasing relative intensity of electric charge, due either to increasing ion symmetry or to increasing area of charge distribution as a result of resonance configuration. Therefore, contrary to most salts, the reason why NaF , MgSO_4 , and $(\text{NH}_4)_2\text{SO}_4$ result in increased precipitation of starch as the concentration of them increases is that anions (SO_4^{2-} or F^-) are completely symmetrical and their superficial charge densities are relatively small and they are surrounded only by a narrow shell of immobilized water molecules [107].

4.2 Introduction

Starch is a natural polymer that has been used in many industrial applications. Modified starches have been widely used in papermaking to improve the filler retention and paper strength. However, there are some problems, such as poor starch retention, causing stickies, increasing the difficulty in water treatment, high cost, etc. when starch is over used.

For many years, the increase in filler content in papers has been driven by the reduction in papermaking cost, the improvements in optical properties, paper formation, printability and the water removal rate during the papermaking. However as filler loading is increased, the paper strengths, bulk and stiffness are usually decreased. To increase the proportion of filler without sacrificing paper properties, various methods have been explored. Preflocculation method prior to addition to the paper stock have been well studied in the past [77-79]. From pilot plant trials, Marbee reported flocculation method could provided an approximate 26% increase in first pass ash retention and 13% increase in the tensile strength when same amount of filler was used [81]. Lumen loading method that held filler mainly within the lumens of fibers have been studied for many years [91-93]. Filler modification with polymers, such as chemically bonded polym(acrylic acid) and poly(vinyl acetate) to fillers was also reported [83]. Gill modified filler surface to improve filler-fiber bonding using epichlorohydrin and polyamino-amide or polyamine [82]. Using filler and wood fines composites in handsheet making were reported by Aho *et. al.* recently [84]. Although many approaches have been studied for improving the paper strength at high filler content, except for the

preflocculation method, none of these technologies has delivered a practical solution to paper manufactures.

Traditionally, starch has been used in wet-end papermaking applications because of its relatively low price and its ability to improve paper strength. The mechanism of their contribution to improvements in dry tensile strength has been suggested. It is believed that starch adsorbs to cellulosic fibers during wet end processing and thereby enhances bonding through the formation of hydrogen bonding [108]. Gaspar concluded that improvements in dry strength were due to increase in shear strength per unit bonded area [109]. Although starch can improve the strength of paper, there are some problems related to high starch addition in wet end papermaking process. For example, the retention of neutral starch in a pulp furnish is very poor (less than 40%) [66]. In order to enhance the adsorption of non-charged starch to anionic surfaces of wood fiber, the cationic groups were introduced to starch backbones.

However, many problems may be associated by using cationic starches. For example, the chemical modification of starch by cationics will significantly increase the cost of papermaking. Although the adsorption of starch can be improved by introducing cationics, the retention of starch on wood fibers is still a problem when anionic trash in the wet end furnish is high, such as in ground wood pulps and recycled fibers. It is well known that the adsorption of cationic starch on fibers will reach a saturation condition and further increase of the adsorption amount beyond the saturation point is impossible. Therefore, the amount of starch on wood fibers is limited by its maximum adsorption amount. The positively charged starch may also cause fiber flocculation and over cationic of the system if the amount of starch is high. The flocculation of the fiber

suspension may also cause a poor paper formation [70]. If the retention of the starch cannot be well controlled, unretained starch will accumulate in the whitewater and create pitch, slime and sticky problems.

Recently, a method for modification of precipitated calcium carbonate (PCC) with coated starch gel was reported [110]. The results indicated that the strength of PCC filled sheets can be significantly improved if the filler surface is coated by starch. However, the starch coating process is relatively complicate so a simple coating process is needed.

To maximize the efficiency and reduce the papermaking problems such as pitch or slime using starch coated fillers in papermaking, the solubility of starch after being coated on filler surface should be very low. If starch is insoluble in water and retained perfectly on wire, large amount of starch can be used for improving paper strengths and the accumulation of soluble starch in wet water can be prevented.

Insoluble or less soluble starches have been developed for a filling material or ion exchange resin. It can be mainly divided by two categories. One is the precipitation of cooled starch using organic solvents such as ethanol and acetone or saline salts such as $MgSO_4$ and $(NH_4)_2SO_4$. The other is crosslinking method using aldehyde, vinyl sulfone and epichlorohydrin . It is known that ammonium sulfate salt is an effective “salting out” material for enzymes, protein and starch. Hernandez , et. al. made water- insensitive starch fiber using 10% starch suspension which was extruded from a nozzle into a coagulation bath containing 44% $(NH_4)_2SO_4$ [111].

However, the starch itself after cooking has relatively lower light scattering characteristics than wood fiber. Thus, optical properties such as brightness and opacity will be decreased when a large amount of starch is incorporated into papers.

The shape of filler or filler aggregates also plays a very important role in both filler retention and final properties of paper. Although their high cost makes difficult to apply, various fibrous or needle-like fillers have been developed for improving papermaking process and paper properties [112-114]. For example, fibrous calcium silicate hydrates improved sheet bulk, porosity, and light-scattering properties [111]. These kinds of fibrous or needle-like fillers might also have better retention due to their morphological characteristics.

In this study the different aggregates from clay-starch composites were prepared and their effects on paper properties were investigated. Compared to our previous approaches, relatively larger starch ratio in clay-starch composites was used because of the low solubility of starch prepared in this study. As a result, the paper properties are further improved.

4.3 Method

4.3.1 Material

Dry Branch Kaolin Co., Inc. provided the calcined kaolin clay. Raw corn starch was used for this experiment. Ammonium sulfate was obtained from Aldrich. Bleached hardwood and softwood pulps were each refined in a Valley beater to a freeness of 400 CSF. Equal proportions of the two pulps were mixed, and the mixture was used as the base pulp furnish for the handsheets. Percol-175 (cationic poly acrylamide retention aid) was obtained from Ciba Specialty Chemicals. Crosslinker, Eka AZC 5800LN (Ammonium zirconium carbonate, 30% solution), was procured from Eka Chemical Inc.

4.3.2 Preparation

The 1:1 clay to starch ratio of composites was prepared follows: 5g of clay was added to 3-4% uncooked raw corn starch suspension that contained 5g of dry weight starch. The mixture then was stirred and cooked at 95°C for 30 minutes. The cooked clay-starch mixture was poured into a 40% ammonium sulfate solution and stirred at 500rpm. After 30 seconds of stirring, fibrous starch-clay composites were precipitated out. The resultant composites were collected on filter paper, washed free of salt and recollected. The filtrated ammonium sulfate solution could be reused by adding additional ammonium sulfate salt. Figure 26 shows the brief preparation process.

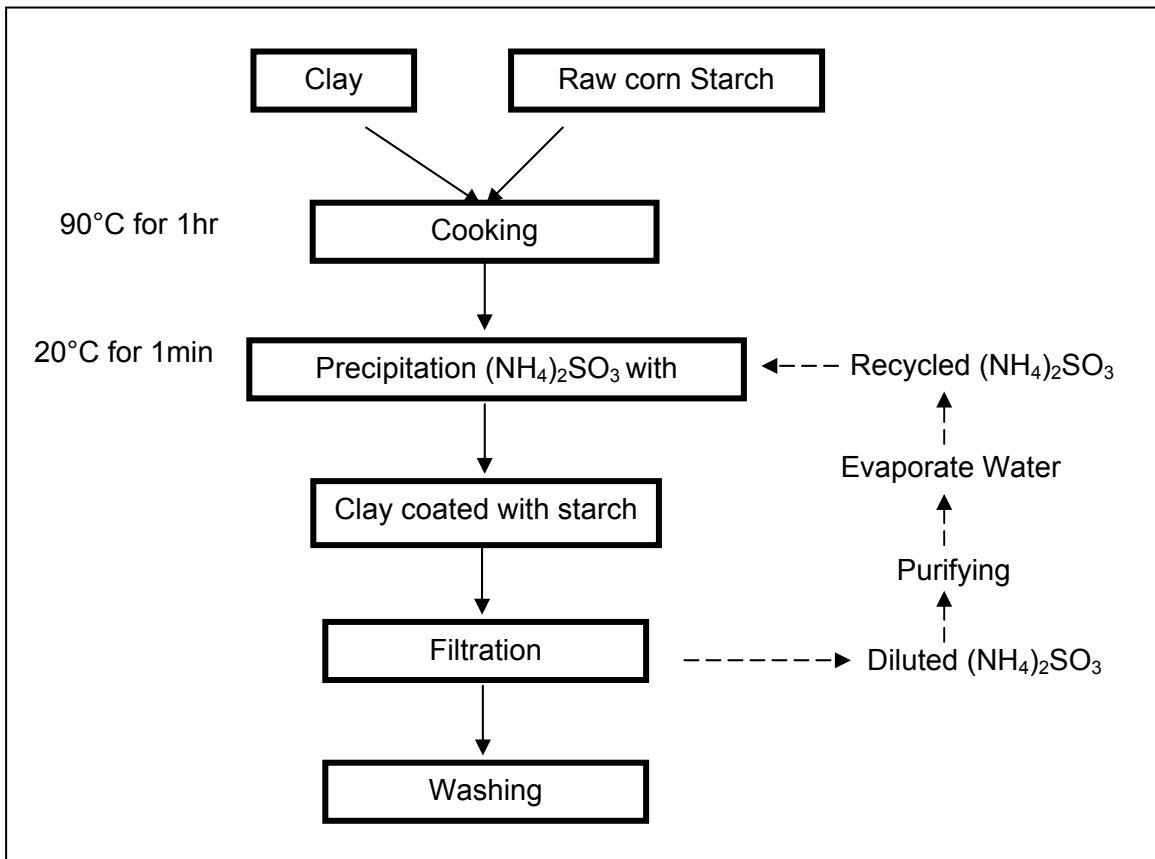


Figure 26: Preparation of clay-starch composite by salt precipitation method

The precipitates of clay-starch composites from ammonium sulfate salt were re-dispersed in water by mechanical stirring before handsheet making. The different solid content ratios of clay and starch composites were prepared at 1:1, 1:0.5, and 1:0.25, respectively. In order to determine the effect of crosslinker on the solubility of starch-clay composites, 3% (based on dry starch weight) crosslinker was added to starch-clay suspension and adjusted to pH 12 after cooking.

4.3.3 Characterization of fibrous clay-starch composites

The morphology of the clay-starch composites was characterized using Leica DMLM optical microscope with digital camera. A Scanning Electron Microscope (SEM) was used for characterizing the detail of the composite aggregates.

Swelling and solubility of starch were measured at different temperatures. Wet clay-starch composite (2g) collected after filtration and washing was agitated in 50g of distilled water for 30 min. The suspension was cooled to 20°C, then was poured into preweighed centrifuge tubes and centrifuged at 3000 rpm for 10minutes. For the measurement of solubility of starch in the clay-starch composites the supernatants were gathered and tested by a measuring total organic content (TOC) using Shimadzu Total Organic Analyzer 5050. Swelling power was obtained from weighing sediments in centrifuge tubes before and after drying using the following Equations:

$$\text{Water solubility (\%)} = \frac{\text{wt. of initial dry starch} - \text{wt. of dry starch not dissolved}}{\text{wt. of initial dry starch}} * 100$$

Equation 9: Starch solubility in water

$$\text{Swelling power} = \frac{\text{wt. of wet starch after centrifuge}}{\text{wt. of starch after drying}}$$

Equation 10: Swelling power

4.3.4 Handsheets preparation and determination of paper properties

Handsheets with a target basis weight of 60g/m² were produced according to TAPPI Test Method T 205 “Forming Handsheets for Physical Tests of Pulp”. Other procedures were same as the cellulose composite filled handsheet making.

Physical properties of the papers were measured according to standard TAPPI methods. The filler content was determined by ashing the paper in a muffle oven according to the standard TAPPI method T211.

4.4 Results and discussion

4.4.1 Characterization of the clay-starch composites

Figure 27 shows optical microscopes and SEM images of clay-starch composites. Kaolin clay from SEM (Figure 27, (a)) shows the plate-like structure and the particle size was less than 3µm. Clay-starch composites (1:1 ratio) from 3 and 4% of starch

concentrations show long fibrous structure from the optical microscope (Figure 27, (b) and (c)).

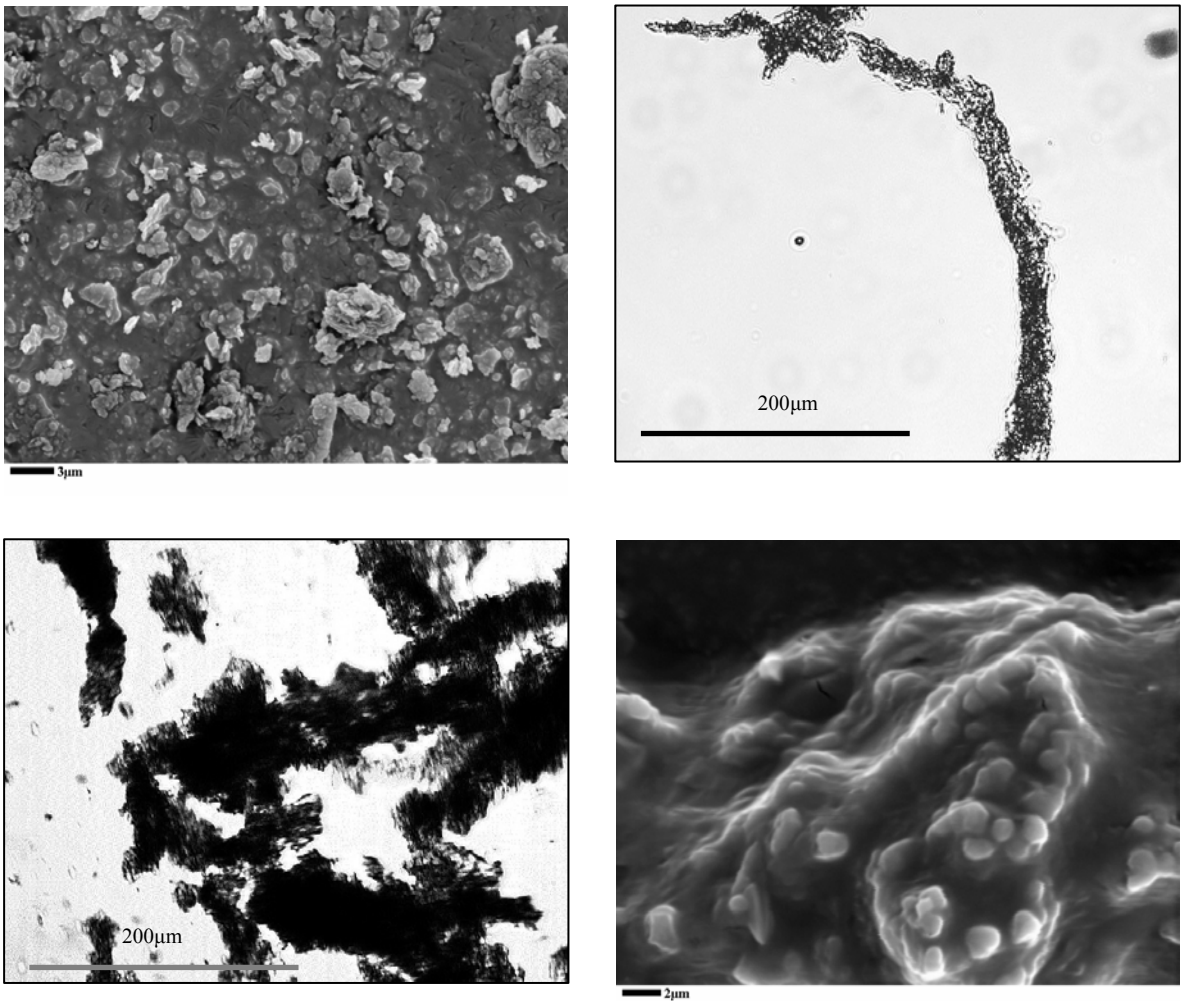


Figure 27: Morphology of clay-starch composite from the optical microscope and SEM. (a): SEM picture of pure clay; (b) and (c): optical microscope picture of the aggregates prepared at clay to starch ratio of 1:1; and (d) SEM picture of clay-starch composite with to starch ratio of 1:1

It was found that the starch concentration in the cooking mixture plays an important role in composite morphology, i.e. large and thick clay-starch aggregates could be obtained when at high starch content solution was used in aggregates preparation. The stirring rate, stirring time and the ammonium sulfate concentration were also important for controlling the aggregate polymorphism. As shearing time or force increased or ammonium sulfate concentration decreased, the size of composite aggregates tended to decrease. At low concentration of ammonium sulfate, the size of composite was very small.

The detail characteristics of the composites were observed by SEM. The surface image of clay-starch composite is shown in Figure 27 (d) and it is shown that clays are distributed well inside composite and perfectly coated by starch. It is expected that this coated starch layer will strongly affect the fiber-fiber bonding, which will be discussed later.

The volume change of coated starch was determined by swelling power. Figure 28 shows the swelling behavior of clay-starch composites in terms of temperatures. It can be seen that as temperature increases, the swelling power increases. At 50°C for 30 minutes, the weight of composite aggregates was about 13 times that of the dried aggregates. Increased volume of composites by swelling might enhance the possibility of hydrogen bonding with wood fibers.

The solubility of coated starch in water in terms of temperature will also be critical issue for application. If starch is dissolved in water, the structure of composite will be disrupted and the clays in composite aggregates will be separated to individual particles. Also, if the starch solubility is high, it will cause many operational problems in

the paper machine and lower physical properties. Therefore, the solubility of precipitated starch in the composites was studied and the results are given in Figure 28.

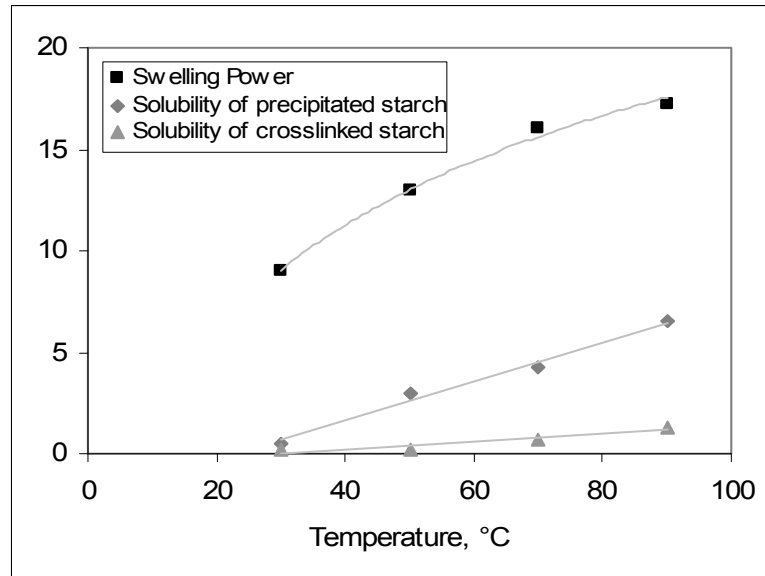


Figure 28: Starch swelling power and solubility at different temperatures

It was found that less than 3% of starch was dissolved in water after the composites were dispersed in water at 50°C for 30 minutes. When the starch was exposed to high temperature, the solubility increased to 5%. However, crosslinked starch could reduce the solubility of starch even at high temperature. Even though the solubility of crosslinked starch increased slightly as temperature increased, the result was only 1.25% at 90°C.

4.4.2 The effects of clay-starch composites on paper strength and optical properties

Figures 29-32 show the effects of the clay-starch composites on paper physical properties. These data indicate that clay-starch composites could significantly improve paper strength properties compared to conventional papermaking filler. As the content of pure clay increased, the tensile strength of the handsheet made from unmodified clay decreased significantly as shown in Figure 29.

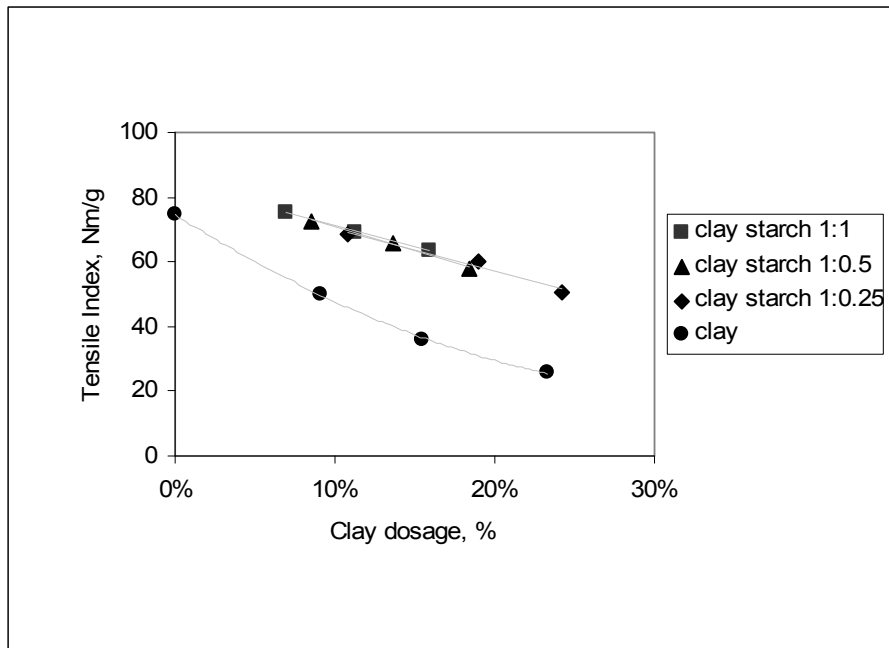


Figure 29: Tensile strength as a function of filler content for pure clay and the clay-starch composites with different clay to starch ratios

It is generally accepted that strength of paper is attributable to the strength and number of inter-fiber bonds. Clay particles in handsheet interfere the fiber bonding, which reduces the strength and number of inter-fiber bonds. Thus, increased clay content

in handsheets caused a greater reduction in tensile strength. It was reported that the starch-coated PCC could improve the tensile strength up to 30% compared to the same amount of pure PCC, which was thought to be that the reduced interfiber bonding by the increasing clay content could be compensated through the improvement of the clay-fiber bonding by the starch coated on filler [110].

As shown in Figure 29 the tensile strengths of the handsheets made from three different clay-starch composites increased about 110% compared to original clay at 20% and 30% clay doses. As shown in the Page equation [30], the tensile strength of paper combines the intrinsic fiber strength, the bonding strength and the contact area. Because the fiber intrinsic strength was the same for all handsheets, the increase in the paper strength should be contributed from the increase of inter-fiber bonding and bonding area. It has been proposed that the internal bond strength such as the Scott Bond Energy, the z-direction strength and peel force in delaminating has the relationship with bonding shear strength [28].

Figure 30 shows the result of z-direction tensile strengths of clay-starch composites filled sheets. For clay-starch composites ratio of 1:1 and 1:0.5, the ZDT increases as composite content increases. However, for the pure clay filled sheets, ZDT decreases as clay content increases. This result means that pure clay interferes fiber-fiber bonding because there is no clay-fiber bonding, however, clay-starch composites can improve clay-fiber bonding due to starch coated on clay surface. Even though ZDT was increased dramatically for clay-starch composites, we saw that the tensile strengths slowly decreased as the composite content increased as shown in Figure 29. This suggests that the strength of this fibrous composite itself is much weaker than that of wood fiber.

However, the bonding strength of this starch coated composite with wood fiber is much stronger than fiber to fiber bonding.

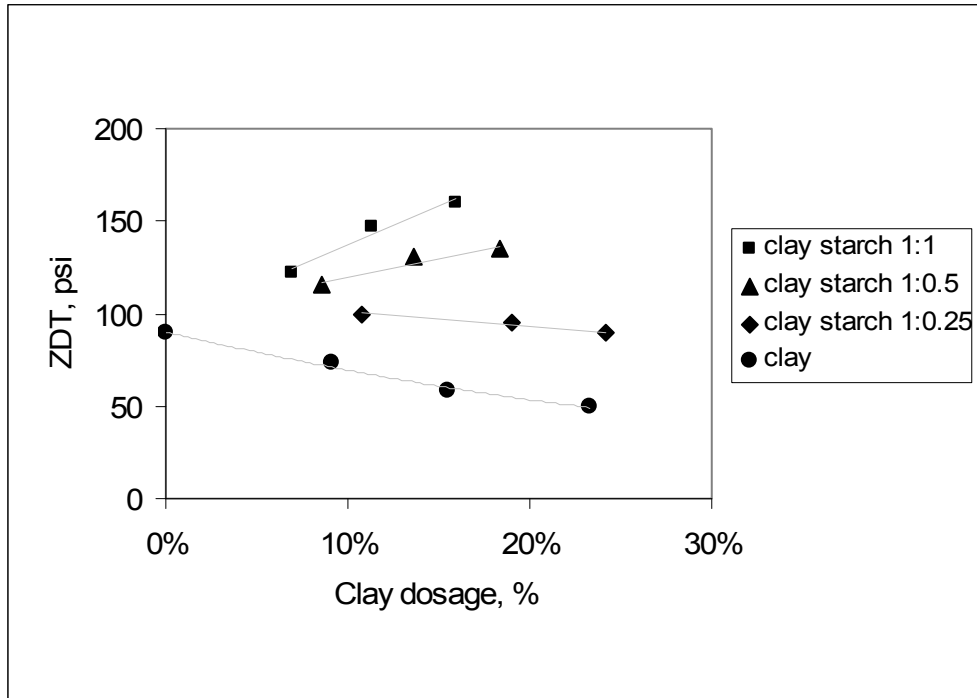


Figure 30: ZDT (Zero directional tensile) strength as a function of filler content for pure clay and the clay-starch composites with different clay to starch ratios

Figure 31 and 32 show the effect of the clay-starch composite on burst index and folding index. The burst strengths of three different ratios of clay-starch composites increased about 100% compared to pure clay at 20% clay addition. The tendency of burst strength using clay-starch composite is almost the same as that of tensile strength as shown in Figure 29. Obviously, the increase of burst strength is due to the improved internal bonding of the sheet by the starch.

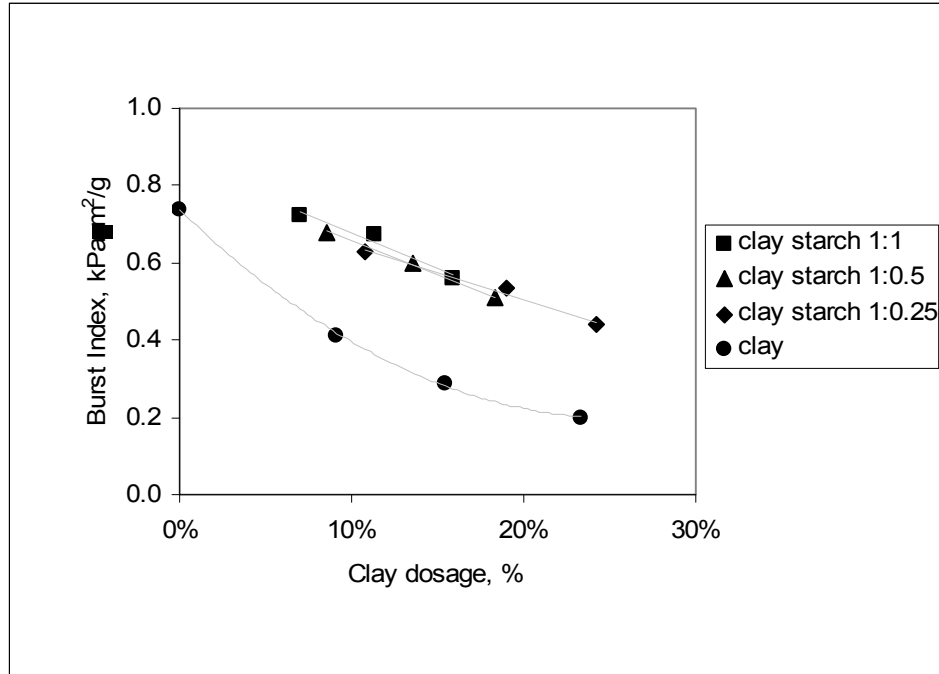


Figure 31: Burst strength as a function of filler content for pure clay and the clay-starch composites with different clay to starch ratios

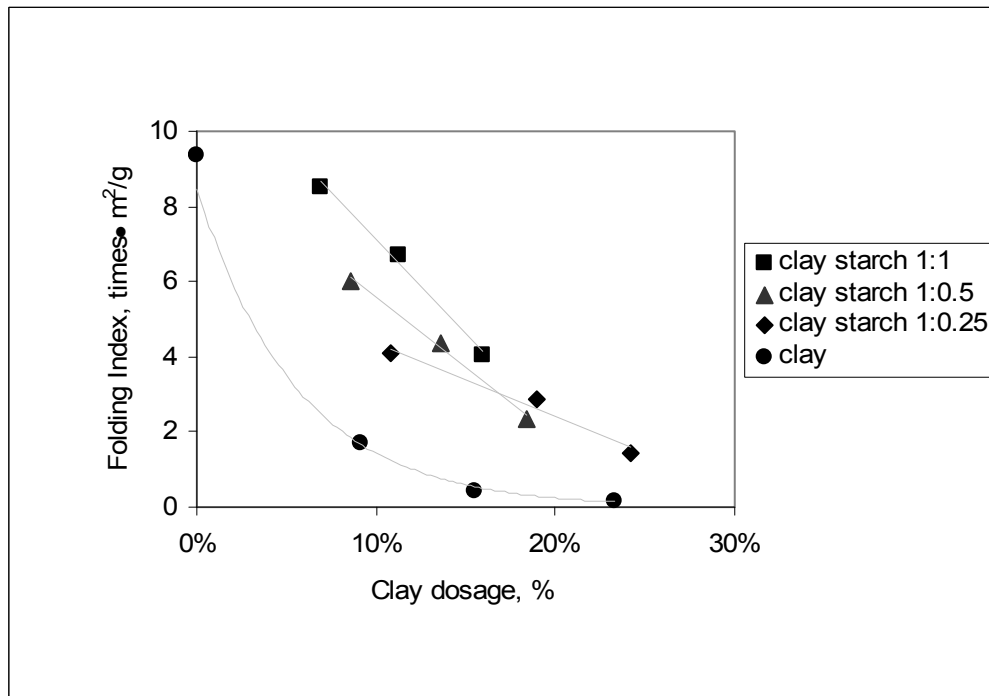


Figure 32: Folding strength as a function of filler content for pure clay and the clay-starch composites with different clay to starch ratios

The similar trend was seen for folding strength of the handsheet. i.e., the pure clay reduced folding strength dramatically but the clay-starch composites had less reduction on the folding strength. It was also found that the folding strength can be significantly improved when the starch ratio in composites was increased.

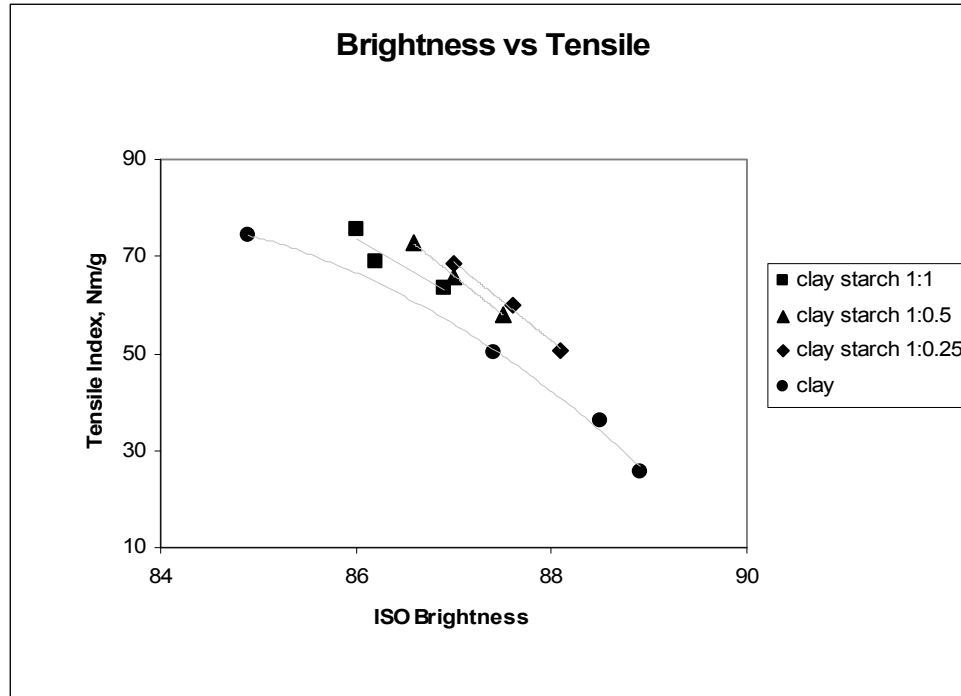


Figure 33: Tensile index vs. ISO brightness as a function of different ratio of clay-starch composites

Figure 33 and 34 compare the brightness and opacity of handsheets made with pure clay and clay-starch composites. Clearly, the increase of the clay-starch content in sheets can improve paper brightness and opacity, although the improvement degree is less than pure clay. The reason of less optical properties of composite than pure clay is thought to be caused by the relatively large particle aggregates as shown in Figure 35 (a)

and (b). The large particle size might positively affects on the filler retention, but reduces the light scattering efficiency. However, the small difference in the optical property improvement between starch-clay composite and pure clay should not be a problem because it can be compensated by adding more composites to the paper without sacrificing if the paper strength. The standard deviation of tested results was very low, which was less than 1.

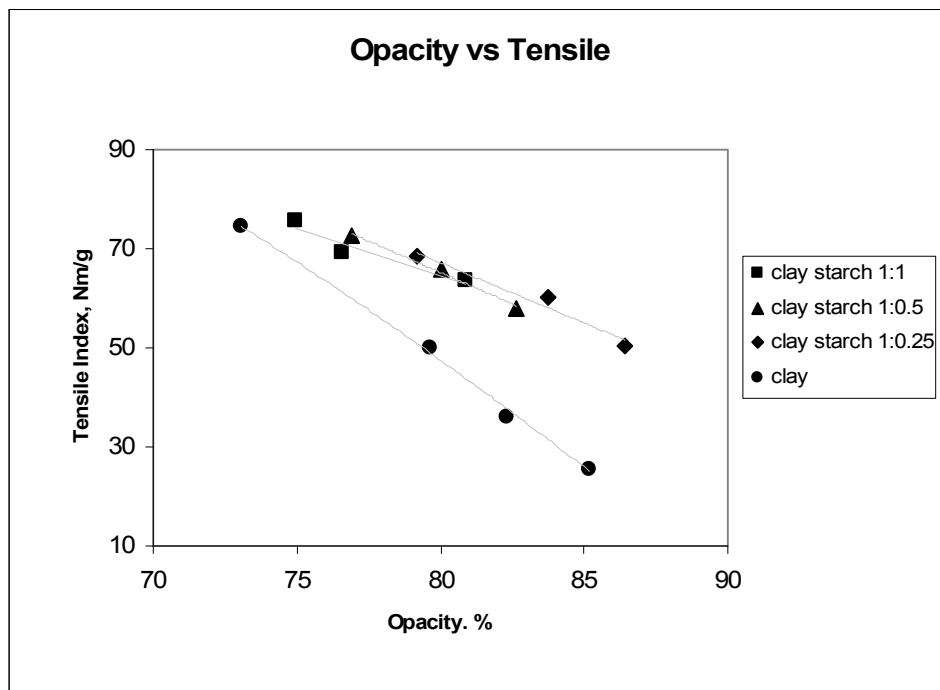


Figure 34: Tensile index vs. Tappi opacity as a function of different ratio of clay-starch composites

4.4.3 Bonding of clay-starch composites with fiber

From ZDT tests, it was determined that internal bonding was improved by adding clay-starch composite comparing to using pure clay. In order to investigate the bonding

between wood fiber and composites, the surface of handsheets filled with clay-starch composites was observed by SEM. Some of the clay-starch composites were stuck on the wood fiber surface and have almost no individual clay particles on fiber surface or between fibers as shown in Figure 50(b). At higher magnification (c) and (d), we could observe the bonding structure between fiber and clay-starch composite in details. The fibrils from the fiber are strongly bounded with the composites so the boundaries of them could not be clearly observed. Appearances of clay-starch composites were also changed during pressing and drying.

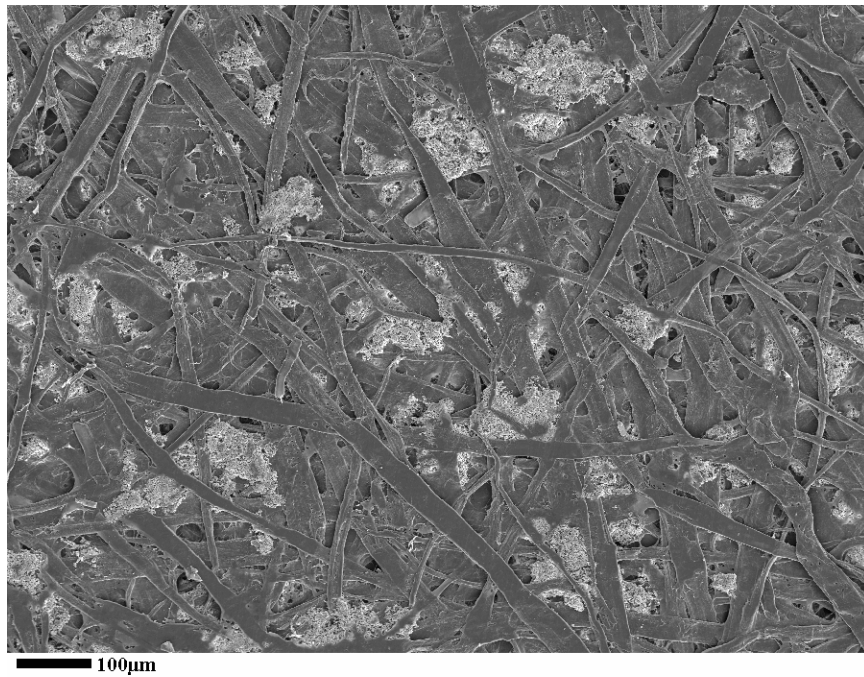
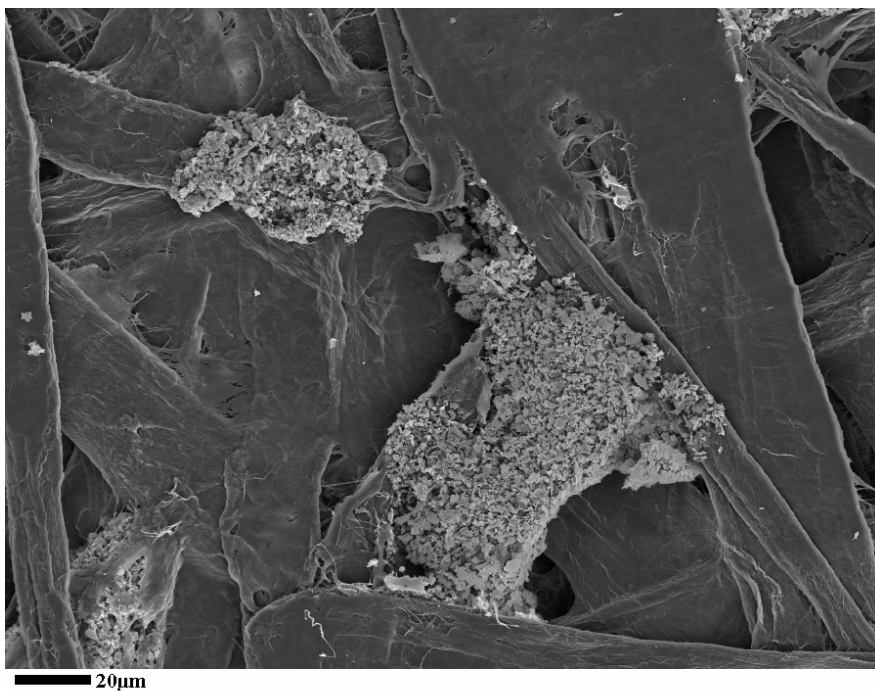


Figure 35: SEM pictures of clay-starch composites filled handsheets (a) clay : starch = 1 : 0.5, 20% in handsheet

(b) clay : starch = 1 : 0.5, 20% in handsheet



(c) clay : starch = 1 : 1, 20% in handsheet

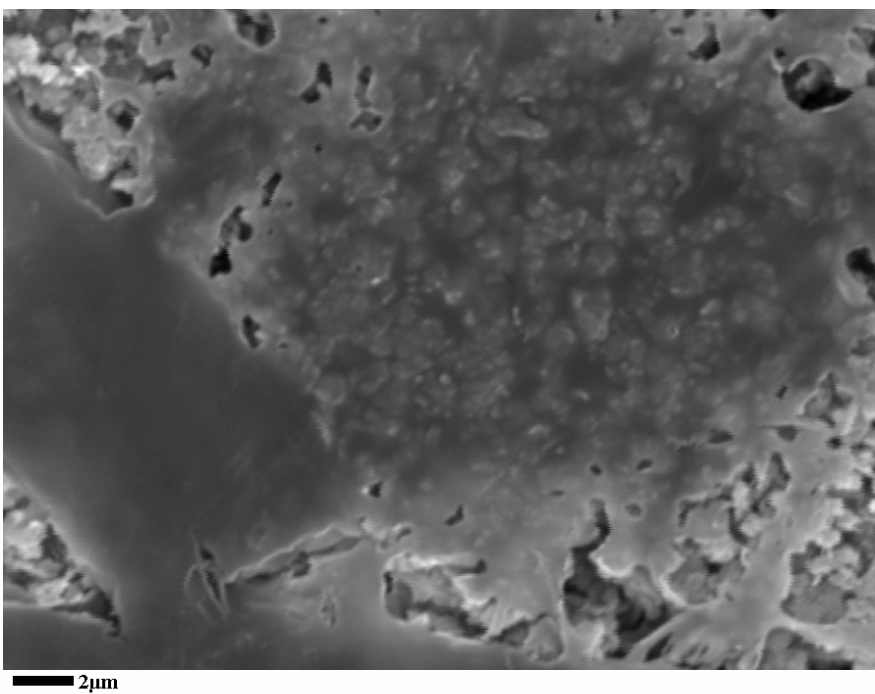
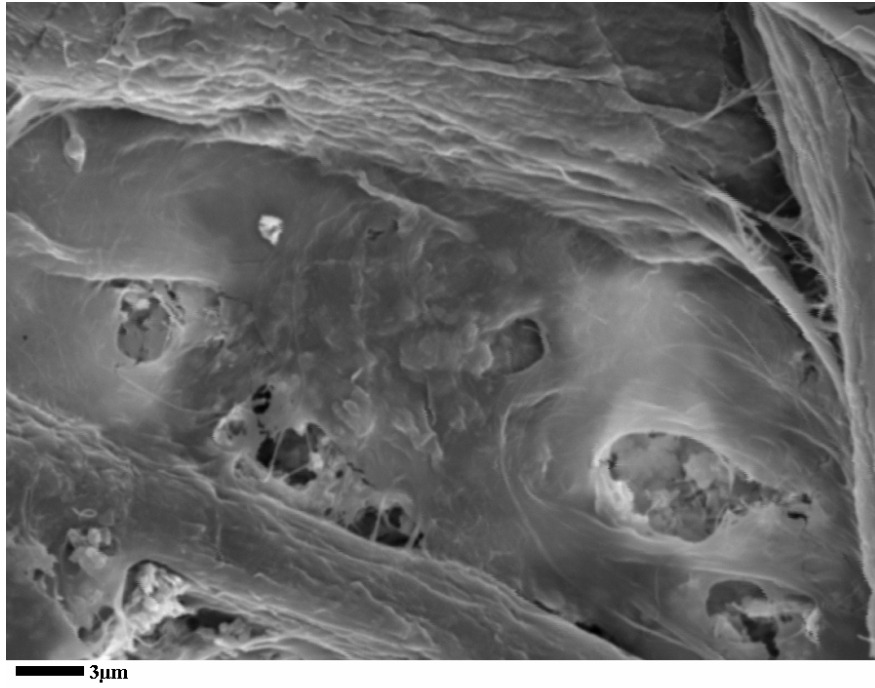


Figure 35: continued.

(d) clay : starch = 1 : 1, 20% in handsheet



(e) clay : starch = 1 : 0.25, 20% in handsheet

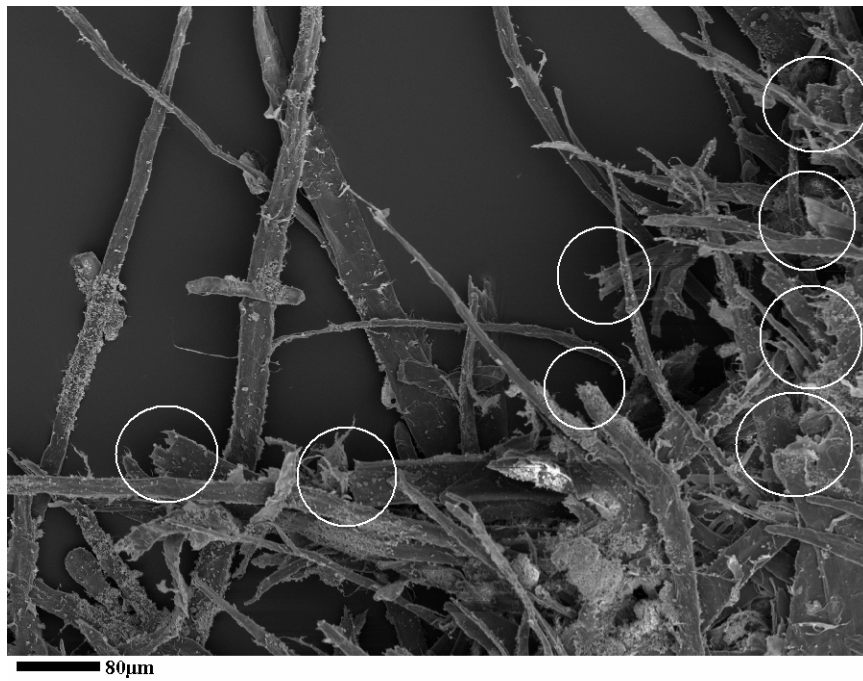


Figure 35: continued.

As can be seen from Figure 35 (c) and (d) the thermo-plasticization makes swollen starch penetrated into fibril network to form a smooth bonding area. Obviously, this will help the bonding of composites with fibrils or fibers.

One of the evidences of strong bonding between fiber and filler can be confirmed by Figure 35 (e). After tensile strength testing, SEM picture was taken for the broken edge part of the sample. It is easily to be seen that many of wood fibers were damaged and cut. This phenomenon only can be seen when strong covalent bonding between wood fibers is formed or wet/dry strength aids make additional strong hydrogen bonding between fibers. Therefore, it can be assume that the bond strength between fibers and composite fillers is high enough to be compatible with the fiber strength.

4.5 CONCLUSIONS

This study provided a method of clay-starch composite preparation. The composite such prepared can be used as papermaking filler with much higher paper strength than untreated clay. The method includes steps of mixing, cooking, precipitation, filtration, and washing. From the physical property measurements, clay-starch composites could increase bonding strength dramatically as shown in ZDT test, thereby tensile, burst, and folding strength were improved up to more than 100% at 20-30% doses compared to untreated pure clay. The optical properties increased as the composite amount in sheets increased. At same opacity and brightness, clay-starch composite filled handsheets have much higher tensile strength than unmodified clay filled sheets. The bonding of clay-starch composites with fibers was confirmed by SEM. This technology could be very attractive for paper grades needing high filler loading and high physical strength.

CHAPTER 5

Starch-Fatty Complex Modified Filler for Papermaking *

Abstract

The clay starch composite method designed in Chapter 4 showed the significant improvement of the physical properties of paper. However, the preparation process is somewhat complicated due to filtration and washing to remove the salt solution. In order to simplify the process and improve filler-fiber bonding in paper without hurting optical properties, starch-filler composites were prepared by a starch-fatty acid complex formation method. These composites were used as a papermaking filler to improve the physical properties of the paper, filler retention, and the sizing effect. The solubility of the starch-fatty acid complex in water at different temperatures was measured. The results indicated that the starch-fatty acid complexes have very low solubility in water below 70°C, which will be acceptable to be applied in paper mill conditions. The clay-starch composite filled handsheets showed that paper strength could increase more than 100~200% compared to untreated clay. It was found that ZDT of the handsheet decreased as the clay content increased when unmodified clay was used, but it increased when the starch-fatty acid composite modified filler was used. It was also found that the presence of fatty acids in the complex increased the water-repellant property of the handsheet, which can be used to aid in sizing during papermaking. Filler distribution and

* This chapter has been modified from the following publication: Yoon, S. Y. and Deng, Y., *Starch-Fatty Complex Modified Filler for Papermaking, Tappi*, 5 (9): 1(2006)

bonding characteristics between the composite and fiber were investigated using Scanning Electron Microscopy (SEM).

5.1 Background - Starch-fatty acid inclusion complex

Due to the problem with the complicated process, filtration and washing, by the salt precipitation method in Chapter 4, a simplified composite preparation method is required. Therefore, the fundamental structure and characteristics of starch were reviewed to find an alternative way to prepare the insoluble starch. The following background study focused on the chemical structure of starch and its association with complexation aids.

The interaction of amylose, the essentially linear component of starch, with various polar and non-polar organic compounds such as iodine, dimethyl sulfoxide (DMSO), alcohols or lipids to give insoluble complexes have been the subject of numerous investigations.

The common X-ray pattern of starch is A or B type, which can be produced from native granules, retrograded starches, or materials prepared by slow evaporation of water [115], on the contrary, the complex with starch formed by a variety of reagents such as iodine, methanol, ethanol, n-propanol, n-butanol, tertiary butyl or amyl alcohol, acetone, and glycerol shows V-type crystalline structure [116]. It was reported that the complex formed by branched-chain alcohols (iso-, secondary, and tertiary butyl and tertiary amyl alcohols) has a larger spacing (up to 20.0 Å) than that by linear alcohols (normal propyl, butyl, and amyl alcohols) [117]. The complex formed by methanol (75%) has the

configuration of a very tight helix about 13.0 Å in diameter, 8.0 Å in repeat period [118], containing six glucose residues per helix turn. These starch-alcohol compounds are structurally similar to the starch-iodine complex (13 Å of spacing), and iodine or organic molecules occupy the helix interior [119-122]. Figure 36 shows that the helical model has a hole through the helix large enough to admit iodine molecules with their long axes coincident with the helix axis.

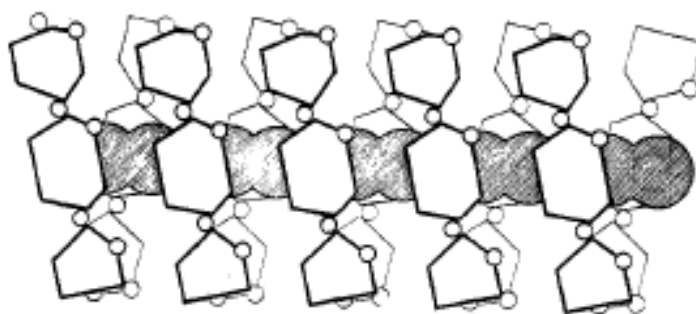


Figure 36: Model of helical starch chain with iodine molecules in the center of the helix [123]

It is well known that the starches as they are obtained ordinary from the plants have a certain amount of fat naturally associated with them. This association forms insoluble products known as “refinery mud” during the manufacture of glucose, or fractionation from corn starch [124]. Therefore, it has been a critical issue to remove this fat from the starch and tried in many different ways such as acids, bases, or solvents [125]. The association mechanism of the fatty acid with starch was initially thought to be an ester linkage [125], mechanical association [126], or adsorption [127]. It was proved later by X-Ray diffraction studies that amylose and the fatty acid forms molecular complexes with helical chain configuration similar to those which amylose forms with

with iodine and the alcohols [119]. Amylose helix has a diameter of 13.0Å (for partial dried sample 13.7 Å) equal to that found for the helix in the amylose-iodine complex. The complexed or guest molecule is thought to occupy the central axis of a helix consisting of 6, 7, or 8 glucosyl residues per turn, with a repeat spacing of 0.8nm and internal cavity is considered to be a hydrophobic tube [128, 119, 129, 130]. Rundle, Schoch and Williams have reported that amylose is precipitated by fatty acids in a microcrystalline condition and the addition of 2, 5, and 10% palmitic acid (calculated on the basis of the dry fraction) to starch reduced the iodine affinity to 12.4, 3.5, and 0%, respectively [131]. Godet et al. suggested the molecular model which presented the six orientations of the aliphatic carbons and the low energy conformations as shown in Figure 37 [132].

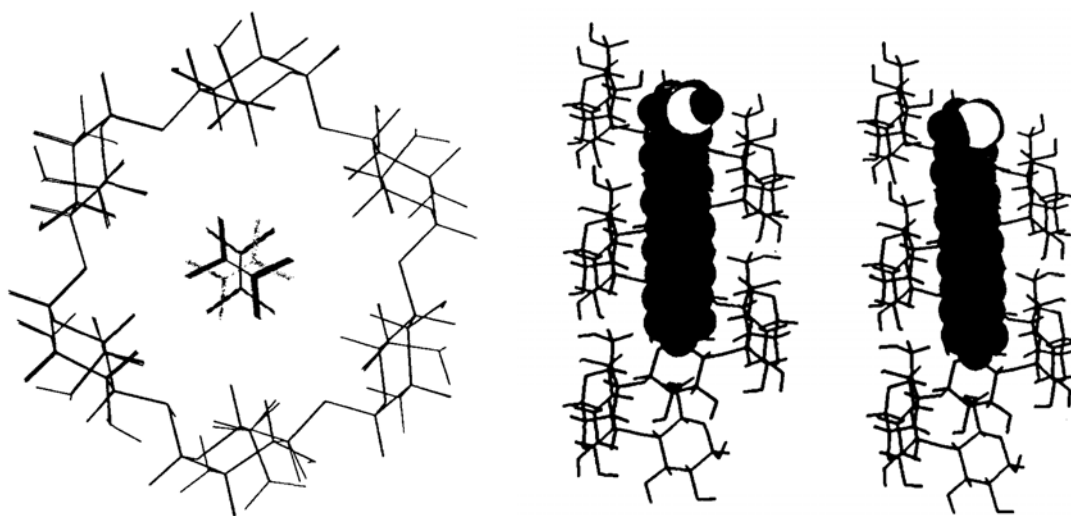


Figure 37 Representation of the six orientations determined for the aliphatic part of the fatty acid inside the helix cavity (left) and the final low energy conformations (right) [132]

The hydrophobic group of complexing agents can lie within the amylose helix and is stabilized by Van der Waal contacts with adjacent C-hydrogens of amylose, while hydrophilic portions of the ligands are outside the helix. Further insertion of the fatty acid

leads to steric conflicts because the steric and electronic repulsions prohibit the polar group from entering the cavity [132]. Recently, the chemical structure and the characteristics of complexes between amylose and different carbon length of fatty acids were studied by DSC [128, 133, 134, 132, 135-137], XRD [138, 134], viscometry [139, 140], NMR [141-143], Raman Spectroscopy [144].

5.2 Introduction

The increase of filler content in paper has been driven by moves to reduce papermaking cost, improvements in optical properties, printability, and the water removal rate during papermaking. However, as filler loading is increased, paper strengths, bulk, and stiffness are usually decreased. To increase the proportion of filler without sacrificing paper properties, various methods such as preflocculation [77, 78, 81, 79], lumen loading [91-93], chemically treated filler with polymer [82, 83] and filler-wood fine composites [84] have been explored. Although many approaches have been studied for improving the paper strength at high filler contents, except for the preflocculation method, none of these technologies has delivered a practical solution to paper manufactures.

Traditionally, starch has been used in wet-end papermaking applications because of its relatively low price and its ability to improve paper strength. The mechanism of the increase in dry tensile strength using starch has been suggested. It is believed that starch adsorbs to wood fibers during wet end processing and thereby enhances bonding through the formation of hydrogen bonds [108]. Gaspar concluded that improvements in dry strength were due to increase in shear strength per unit bonded area [109]. Although

starch can improve the strength of paper, there are some problems related to high starch addition in wet end papermaking process. For example, the retention of raw starch in a pulp furnish is very poor, less than 40% [66]. In order to enhance the adsorption of starch to anionically charged wood fiber surface, the cationic groups are usually introduced to starch's backbones. However, such chemical modification of starch significantly increases the cost of papermaking.

Although the adsorption of starch can be improved by introducing cationic groups, the retention of starch on wood fibers is still a problem when anionic trash in the wet end furnish is high, such as in ground wood pulps and recycled fibers. Furthermore, the saturation adsorption of cationic starch on fibers does not allow papermakers to further increase cationic starch amount beyond the saturation point in the papermaking wet end process. Therefore, the amount of starch on wood fibers is limited by its maximum adsorption amount. The positively charged starch may also cause fiber flocculation or over cationize the system if the amount of starch is too high. The poor formation and slow drainage caused by high starch addition are also practical problems in papermaking [70]. If the retention of starch cannot be well controlled, unretained starch will accumulate in the whitewater and create pitch, slime, and sticky problems.

Recently, we reported a method for modification of precipitated calcium carbonate (PCC) or clay with coated starch [145, 110]. The results indicated that the strength of PCC or clay filled sheets could be significantly improved if the filler surface was coated by starch. In this work, we report an easier and lower cost method for coating starch on filler for paper strength improvement.

To maximize the efficiency and reduce the papermaking problems using starch coated fillers, the starch coating layer should be water-insoluble at papermaking conditions. Insoluble or less soluble starches have been developed for a filling material or ion exchange resin. The precipitation of cooked starch using organic solvents such as alcohol or acetone or saline salts such as MgSO_4 and $(\text{NH}_4)_2\text{SO}_4$ is the most common way. The crosslinking methods using aldehyde, vinyl sulfone, epichlorohyrin can also be used for preparation of water-insoluble starch.

In this study, the precipitation of starch was carried out through the formation of water-insoluble starch-fatty acid complexes in the presence of clay particles. Schoch and Williams reported that amylose could be precipitated by fatty acids in a microcrystalline condition [131]. The mechanism of the complex formation between the starch and fatty acid was thought to be the formation of ester linkages in early days [124] but it is believed now that unbranched polar compounds, *e.g.*, fatty acids and their monoglycerides, form helical inclusion complexes with amylose under suitable conditions [117, 119]. These complexes are considered to be similar to the blue polyiodide complex of amylose whose structure had been originally elucidated by Rundle and Baldwin [123]. The complexed or guest molecule is thought to occupy the central axis of a helix consisting of 6, 7, or 8 glucosyl residues per turn, with a repeat spacing of 0.8 nm and internal cavity is considered to be a hydrophobic tube [128, 130]. The hydrophobic group of complexing agents can lie within the amylose helix and is stabilized by Van der Waal contacts with adjacent C-hydrogens of amylose, while hydrophilic portions of the ligands are outside the helix. Further insertion of the fatty

acid leads to steric conflicts because the steric and electrostatic repulsions prohibit the polar group from entering the cavity [132].

In this study, different aggregates of clay-starch composites by starch-fatty acid complexation were prepared and characterized. The effects of clay-starch composites on paper properties were also investigated. Compared to our previous approaches, relatively larger starch ratio in clay-starch composites was used because of the simple operation process and the low solubility of starch prepared in this study.

5.3 Method

5.3.1 Material

Dry Branch Kaolin Co., Inc. (Dry Branch, GA) provided the calcined kaolin clay. Raw corn starch was used for this experiment. Palmitic acid was obtained from Aldrich. Bleached hardwood and softwood pulps were each refined in a Valley beater to a freeness of 400 CSF. Equal proportions of the two pulps were mixed, and the mixture was used as the base pulp furnish for the handsheets. Cationic polyacrylamide (Percol-175) for filler retention was obtained from Ciba Specialty Chemicals. Cationic starch (STA-LOK 400) for filler retention and dry-strength was procured from Tate & Lyle Ltd (Decatur, IL).

5.3.2 Preparation

Figure 38 show the procedure to form the starch-clay composite by fatty acid complexation method. The composite with clay to starch ratio of 1:1 was prepared as the follows: 5g of clay was added to 3% uncooked raw corn starch suspension that contained 5g of dry weight starch. The mixture then was stirred and cooked at 95°C for 30 minutes.

0.5g of palmitic acid was added to cooked starch-clay suspension and the mixture was then adjusted to pH 11 by 0.01M KOH.

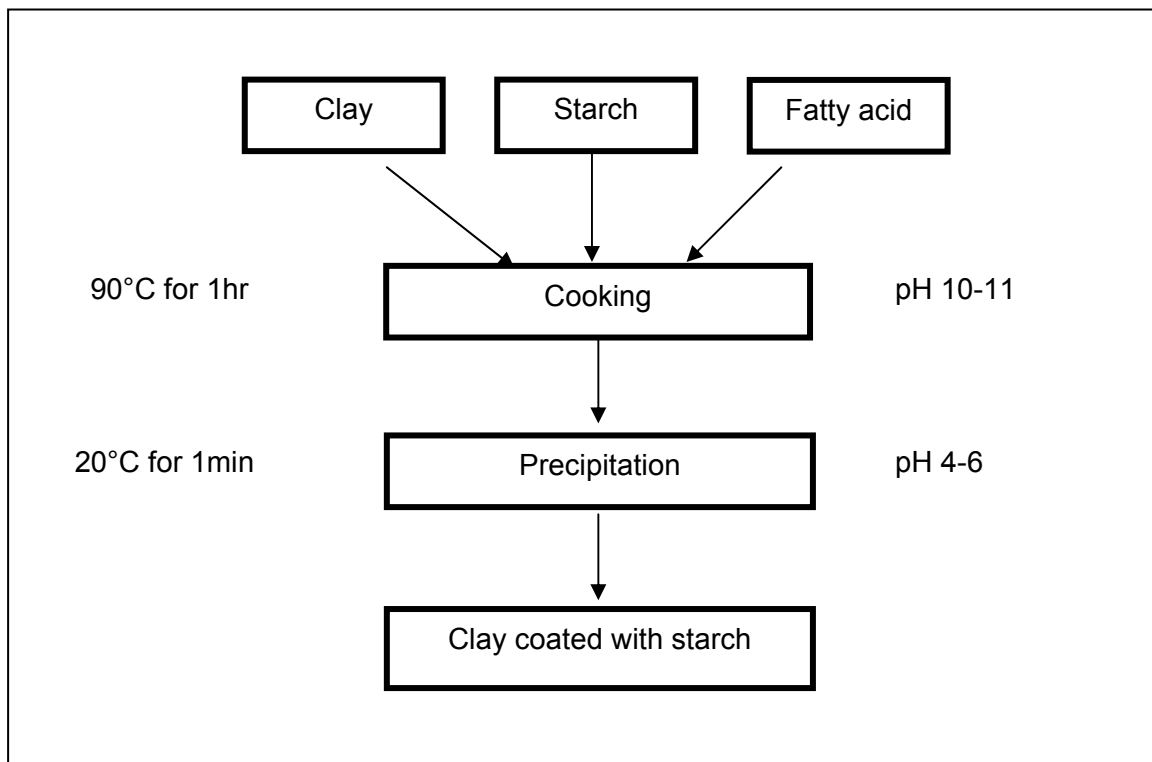


Figure 38: Preparation of clay starch composite by starch-fatty acid complexation method

After stirring for 10 minutes, the cooked clay-starch mixture was poured into 0.01M HCl solution to neutralize it. The complex was then precipitated by adding a few drops of 2M HCl to pH 5 with 200 rpm stirring speed. The resultant composites were directly used for handsheet making. The two different palmitic acid ratios (10% and 30%) based on the solid starch were compared.

5.3.3 Characterization of clay-starch composites by starch-fatty acid complex

The morphology and surface analysis was performed by optical microscope and SEM. Swelling and solubility of starch measured at different temperatures and pH were determined by the previous same TOC method.

In order to characterize the structure of the starch-fatty acid complex, X-ray diffraction was analyzed as follows: Powdered samples (pulverized to pass 150mesh) were equilibrated at 23°C and 45% relative humidity for 2 days prior to analysis. X-ray diffractometer (PW 1800, Philips Co. Ltd., USA) was operated at 40kV, 30mA. Diffractograms were obtained from $10^\circ 2\theta$ to $40^\circ 2\theta$ with a scanning speed of $0.04^\circ/\text{second}$ and scanning step of $0.05^\circ 2\theta$.

The measurement of composite size was performed using a commercially available scanning laser microscope (Lasentec Corporation, Redmond, WA, USA) as shown in Figure 39 [48].

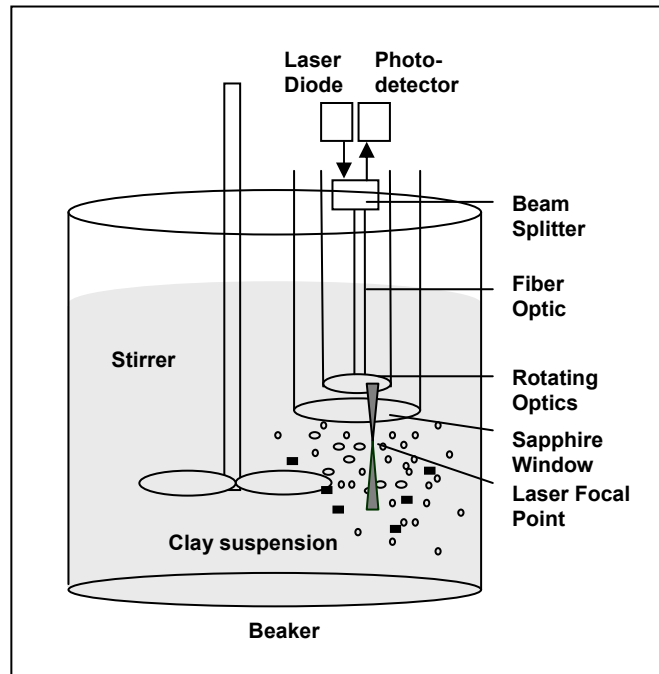


Figure 39: Schematic representation of the FBRM system [48]

The effect of pH and shear force on composite formation was investigated from measuring the composite size using this technique. The real time particle size using the focused beam reflectance measurement (FBRM, Lasentec Corporation, Redmond, WA, USA) was measured to study the effect of pH or shear force on the clay-starch composite size change during the preparation. The detail mechanism and operation method of FBRM is described elsewhere [48].

In this technique, a 780nm diode laser is coupled into the sample of interest via a fiber optic bundle and focused to an elliptical beam waist of about $0.8\mu\text{m} \times 2\mu\text{m}$. The focused beam is then scanned through the solution in a circular motion (rotating lens) at a velocity of 2m/s. When the beam crosses a particle or particle floc, some of the light is reflected back into the probe, and is transmitted via fiber optics to an avalanche photodiode detector. The duration of this backscattered light determined by the detector is proportional to the size of the particle presented in the system. Since the scanning velocity of the laser is known to 2m/s, the time taken for the laser to scan across a particle chord can be converted into a particle chord length. The scanning velocity of the laser is much faster than the particle velocity for all reasonable mixing velocities of the sample, and thus the measurements are not influenced by sample flow velocities.

Thousands of chord length measurements were collected per second, producing a histogram in which the number of the observed counts was sorted in several chord length bins over the range of 0.5-1000 μm . Data from the FBRM histograms were used to calculate the arithmetic mean of the chord length distribution. The details of the instrument and its measurements have been presented elsewhere. The instrument settings

used for this research were: (1) the focal plane of the beam was positioned 20 μ m above the sapphire window/ solution interface; (2) the data acquisition time was 3 seconds per data point; (3) there was no signal averaging between data points; (4) there was no data smoothing/averaging between channels. Although the absolute magnitude of the mean chord length cannot be directly compared to the true average particle size, trends and changes observed in the actual particle size distribution are reflected in changes in the mean chord length.

5.3.4 Handsheets preparation and determination of paper properties

We performed two types of experiments, TAPPI handsheet making using bleached pulp and Dynamic sheet-former method using unbleached pulp.

For TAPPI handsheet making, bleached hardwood and softwood pulps were each refined in a Valley beater to a freeness of 400CSF. Equal proportion of the two pulps was mixed, and the mixture was used as the base pulp furnish for the handsheets.

Handsheets with a target basis weight of 60g/m² were produced according to TAPPI Test Method T 205 “Forming Handsheets for Physical Tests of Pulp”. Other procedures were the same as the previous composite filled handsheet making procedure. For dynamic sheet-former handsheet making, the softwood unbleached kraft pulp, kappa number 105, from Inland Container, Rome, GA. was beaten in a valley beater to C.S.F. 400ml. Formette Dynamique was used to make handsheet with a target basis weight of 150g/ m². The Formette ran at 900m/minute with the pump pressure at 2bar. Once finished, the sheets were removed, pressed at 40psi pressure and dried at 20psi of steam

pressure for 10 minute in a Johnson drum dryer. The sheets were then removed and conditioned before testing.

Physical properties of the papers were measured according to standard TAPPI methods. The filler content was determined by ashing the paper in a muffle oven according to the standard TAPPI method T211.

In order to measure the wettability of handsheets, we used the contact angle analyzer.

The wettability of handsheets (Tappi method T 458) was calculated as follows:

Rate of change of wettability (R) = Change of contact angle / change of time

5.4 RESULTS AND DISCUSSION

5.4.1 Starch-fatty acid complex formation

In order to investigate the complex formation and the coating efficiency of starch-clay composites, the starch and palmitic acid mixture at different ratios without adding clay were first investigated.

The cooked starch and palmitic acid were mixed at pH 11 then neutralizing to pH 5 to form water-insoluble complexes. After separation of the insoluble complex by sedimentation, the amount of the starch left in the supernatant was analyzed by TOC, and the results are shown in Figure 40.

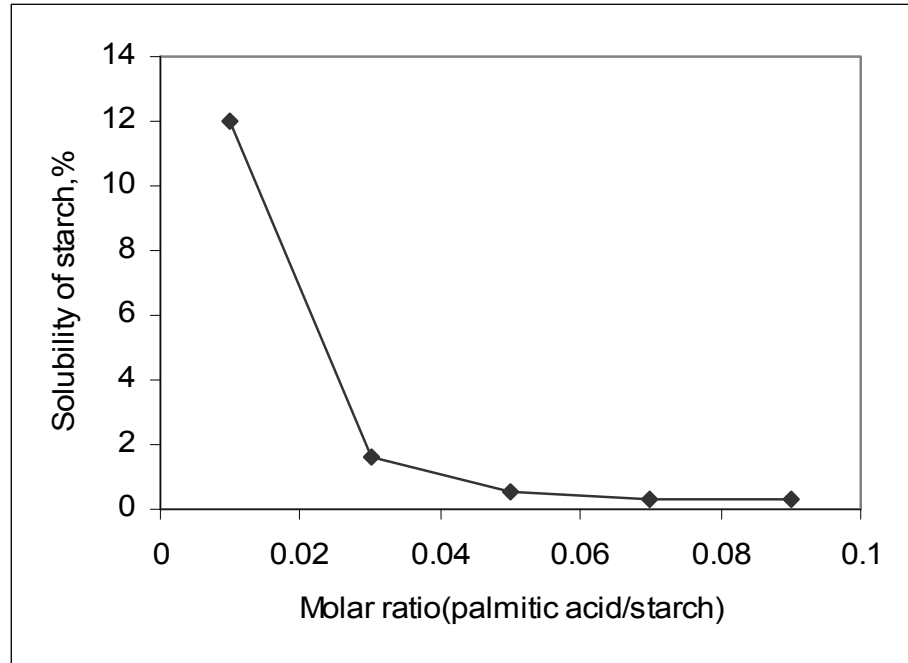


Figure 40: Change of soluble starch amount with different molar ratios of palmitic acid to starch in the complex

It can be seen that the soluble starch amount dramatically decreased as the molar ratio of palmitic acid to starch increased. At molar ratios of greater than 0.07, the soluble starch amount was less than 0.3%, which means almost >99% of starch was precipitated. The effect of the fatty acid ratio on the formation of the complex formation was also investigated using X-ray diffraction. X-ray diffraction scans of starch-fatty acid complexes at different palmitic acid ratios are shown in Figure 41. The spectrum indicated a maximum at $2\theta=19.8^\circ$, which became apparent when the palmitic acid to starch ratio is greater than 0.3. The maximum at $2\theta=19.8^\circ$ presents V-type inclusion complexes of amylose [141]. In contrast with the starch-fatty acid complex, only the amorphous structure without any crystalline peaks was observed for pure cooked starch.

Therefore, the reduction of solubility of starch is believed to be caused by the crystalline structure of starch-fatty acid complex. As the fatty acid ratio increased above 0.3, two peaks at 21.4° and 23.8° were also observed. These peaks reflect the presence of a pure crystalline fatty acid [138].

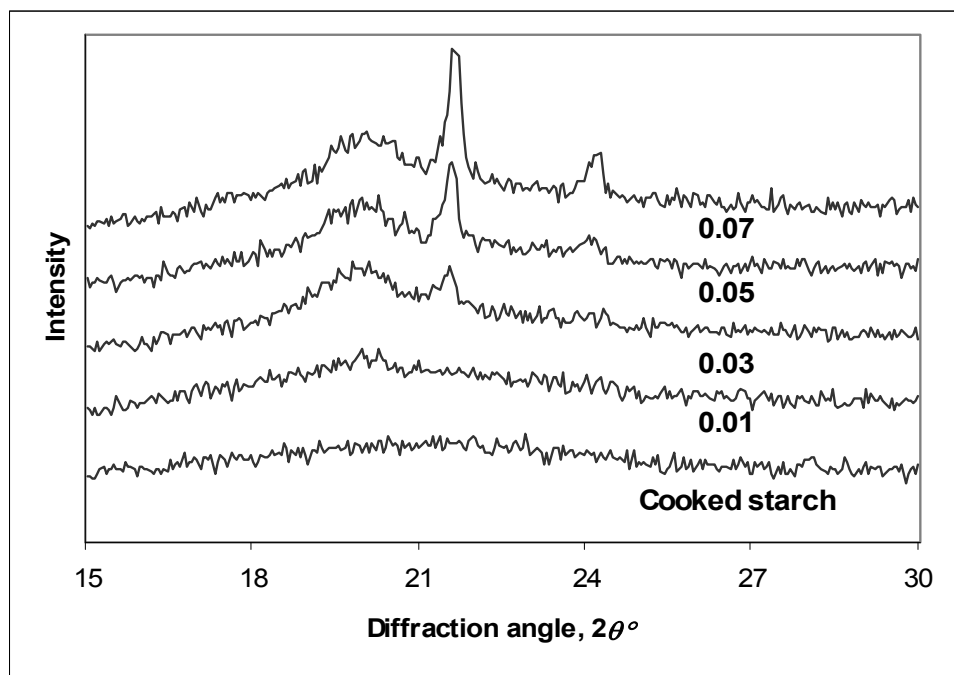


Figure 41: X-ray diffractions of starch-palmitic acid complexes at different ratios of palmitic acid to starch

5.4.2 Starch-fatty acid-clay composite formation

The clay-starch composite was prepared by precipitation of starch-fatty acid complexes on the clay surfaces. In the experiments, required amounts of clay, starch, and palmitic acid were mixed and cooked together at pH 11. The cooked mixture (6.5% total solid concentration) was then poured into 0.01M HCl solution (the same volume as the cooked mixture) to be neutralized while stirring at 200 rpm. As soon as the shear forces were stopped, the white composites were formed quickly within 20 seconds and

precipitated out from the solution. The solubility of this coated starch in water at papermaking conditions will be a critical issue for real application. If the solubility of coated starch in water is high, the structure of composite will be disrupted and the clays in composite aggregates will be separated to individual particles. Furthermore, the high solubility of starch complex will cause many operational problems during papermaking process. Therefore, the solubility of precipitated starch in water at different temperatures was studied and the results are given in Figure 42.

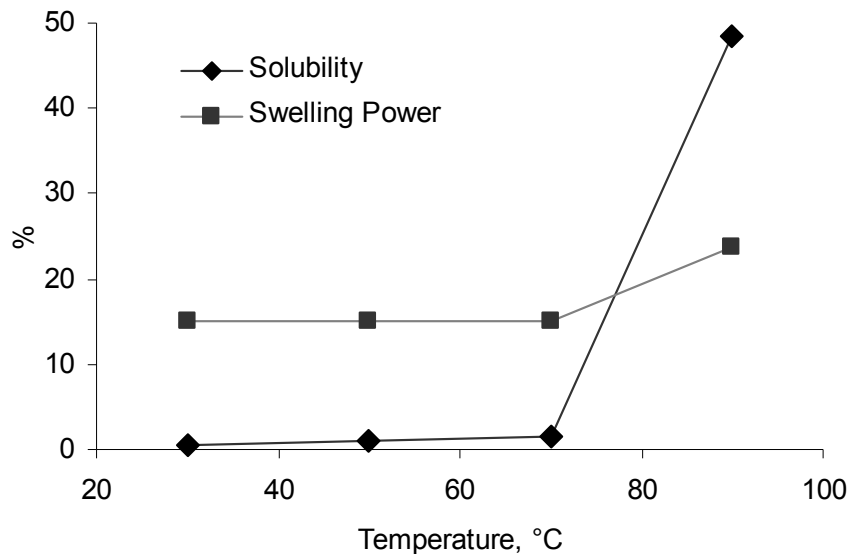


Figure 42: Starch solubility and swelling power at different temperatures

Figure 42 shows the solubility and swelling behavior of clay-starch composites as a function of temperature. The volume change of coated starch was determined by swelling power. Previous reports [145] showed that the swelling power of starch-clay composites without fatty acids increased as the temperature increased. However, the swelling power of starch-fatty acid-clay composites did not change much at all conditions

studied. The low swelling ratio of starch-fatty acid complex relative to pure starch might be caused by the hydrophobicity of the fatty acids.

The measurements indicated that the solubility of the composites below 70 °C was very low. However, the solubility was sharply increased at 70 °C, and almost 50% of starch composite was dissolved at 90 °C. The high solubility of the complex above 70 °C may relate to starch's gelation temperature. It is well known that starch molecules usually undergo a remarkable conformation change at the gelation temperature. Because of this dramatic change, the bonding between starch and fatty acid molecules may be damaged or weakened so they are no longer able to be in the form of complexes. After determining the solubility at each point, the composites were centrifuged and freeze-dried to investigate the change of crystal structures. X-ray diffraction results indicated that the peak intensities for V-type inclusion complex ($2\theta=19.7^\circ$) and the fatty acid crystal ($2\theta=21.4^\circ$ and 23.8°) decreased at the temperature above 70 °C as shown in Figure 43.

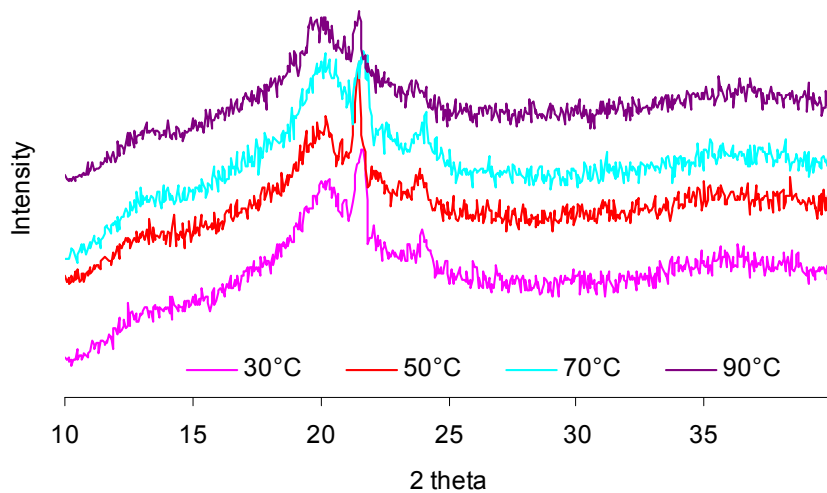


Figure 43: X-ray diffractions of coated clays with starch-palmitic acid complexes exposed at different temperatures for 30 minutes

Another possible reason for the sharp increase in the starch-fatty acid solubility and decrease in crystalline peaks may be that the parts of the fatty acid combined with the starch can be leached out from the helical structure of starch over 70 °C and then the crystalline structures are disrupted.

It is important to determine the effect of pH on the solubility of the composite, because the pH of papermaking conditions can be varied from acid to alkaline depending on the grade, sizing, filler type, and so on. Figure 44 shows the solubility and swelling behavior of clay-starch composites as a function of pH. The results indicated that the solubility of the composites below pH 7 was very low. However, the solubility was sharply increased as pH increased from 7 to 11, and almost 20% of starch composite was dissolved at pH 11, even though the temperature for all measurements was 50 °C for 30 minutes mixing.

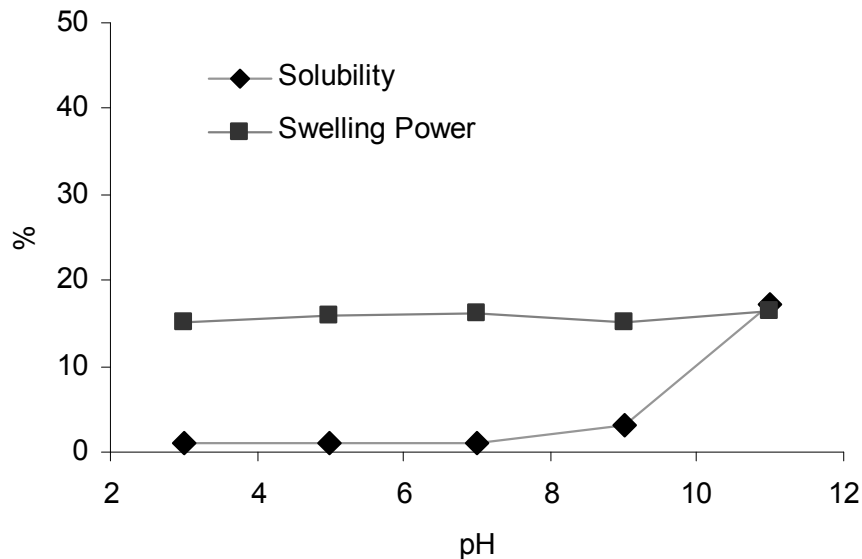


Figure 44: Starch solubility and swelling power at different pH

The relatively high solubility of the complex at alkali condition may relate to starch's swelling and gelation characteristics. Our X-ray diffraction results indicated that the peak intensities for V-type inclusion complex ($2\theta=19.7^\circ$) and the fatty acid crystal ($2\theta=21.4^\circ$ and 23.8°) decreased from pH 7 to 11 as Figure 45 shows.

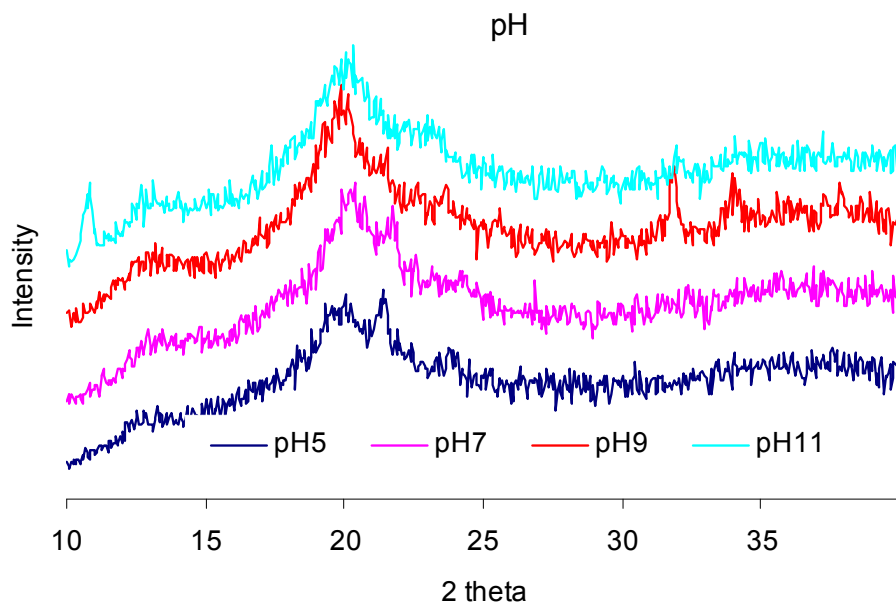


Figure 45: X-ray diffractions of coated clays with starch-palmitic acid complexes at different pH. (temperature: 50 °C, mixing time: 30 minutes)

Jackson *et al.* [146] reported that starch molecules underwent depolymerization, when cooked with NaOH at concentrations as low as 0.001N for 5hr. It was also suggested that increasing amount of NaOH increased the total quantity of solubilized starch fraction; amylopectin was solubilized more readily by NaOH than amylose. Their solubility results showed that the total solubility of starch was increased from 43% to

78% when the alkali concentration was increased from 0 to 0.048*N*. However, the solubility of starch-clay composite was relatively much smaller than unmodified starch, which may relate to the starch-fatty acid complexation. Banks and Greenwood [147] suggested that in caustic alkali at pH 12, amylose undergoes solvent expansion, presumably due to the ionization of the hydroxyl groups. They proposed that adding complexing agents such as butan-1 or potassium chloride to amylose at pH 12 would be to effectively suppress this ionization, and so cause the macromolecular coil to collapse until it attained its unperturbed dimensions.

Figure 46 shows that the effect of time on the solubility of clay-starch composite. During the papermaking process, the filler usually added at the mixing chest, and then travel through machine chest, stuff box, primary fan pump, deculator, secondary fan pump, pressure screen, and headbox [148]. Therefore, it is worth determining the effect of time at certain papermaking condition.

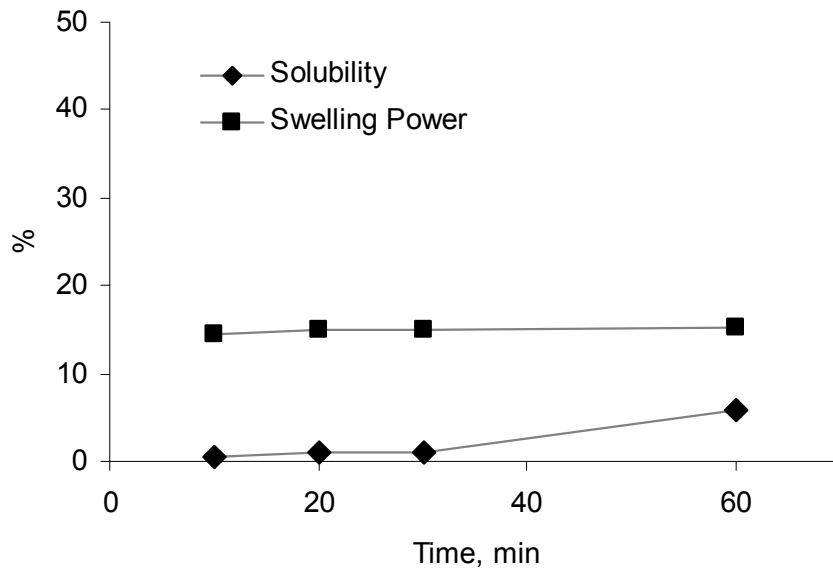


Figure 46: The change of starch solubility and swelling power at different time

As shown in Figure 46, the effect of the time on the solubility at 50 °C and neutral condition (pH 7) was not significant compared with the effect of previous temperature and pH. X-ray diffraction results support this result as shown in Figure 47.

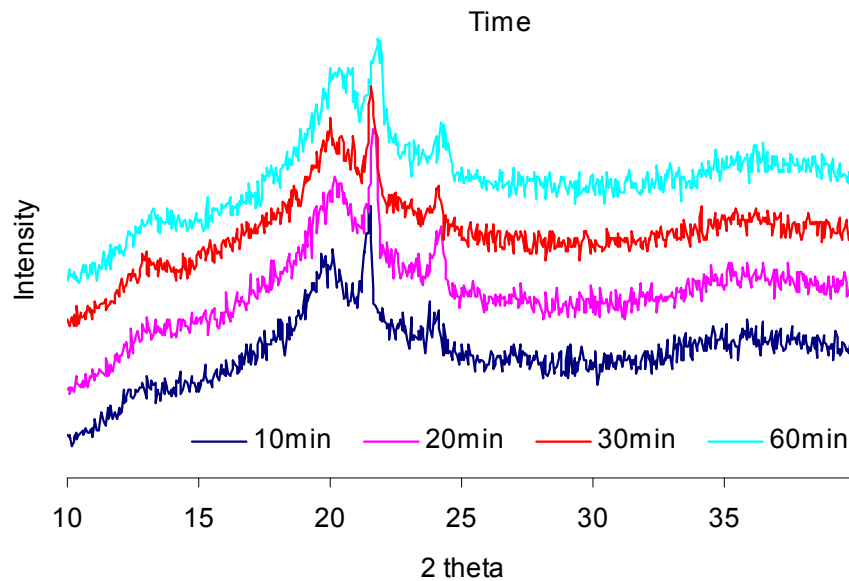
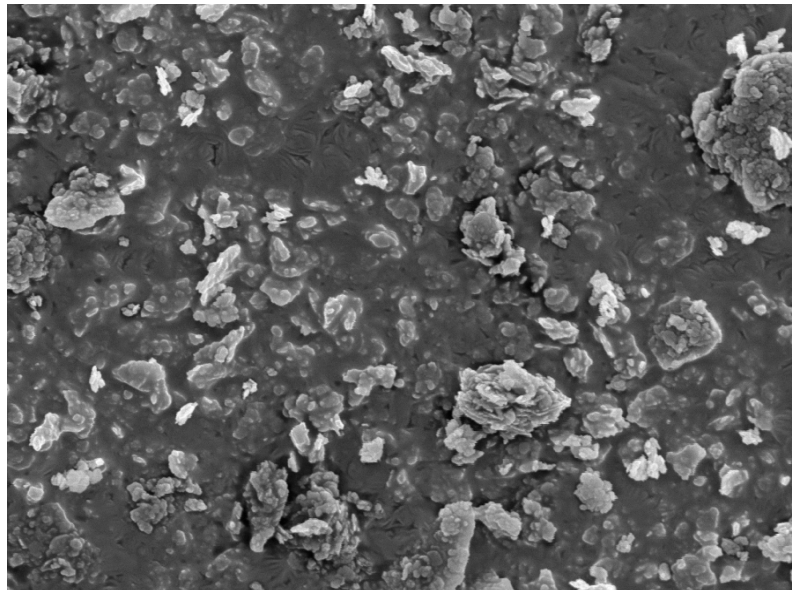


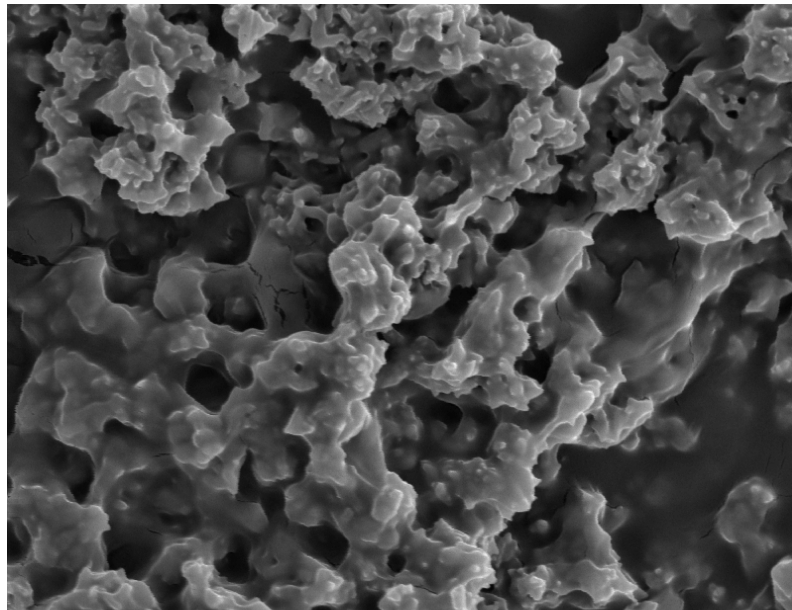
Figure 47: X-ray diffractions of coated clays with starch-palmitic acid complexes at different time (temperature: 50 °C, pH: 7, and shear: 500 rpm)

The peak intensity for V-type inclusion complex ($2\theta=19.7^\circ$) was not changed from 0 to 30 minutes and slightly decreased at 1 hour, which matches well with the solubility data. The peak intensity for the fatty acid crystal ($2\theta=21.4^\circ$ and 23.8°) did not change much even though as the time increased from 0 to 1 hour.

It has been known that the particle size and shape of filler have a direct relationship with the physical properties of paper [149, 150]. Therefore, it is important to investigate the particle morphology for understanding the filled paper properties.



3 μm



5 μm

Figure 48: SEM pictures of unmodified clay (above) and clay-starch composites by starch-palmitic acid complexation method (bottom)

Figure 48 shows SEM images of clay and clay-starch composites. It was found that the starch-fatty acid complex could perfectly coat the clay surface and form aggregates which are much bigger than pure clay. The aggregate size is not only the function of starch and fatty acid concentration, but also a function of the total solid

concentration, stirring rate and time, ratio of starch to clay, pH, etc. For example, as shearing force or pH increased during composite formation, the size of composite aggregates decreased as shown Figure 49.

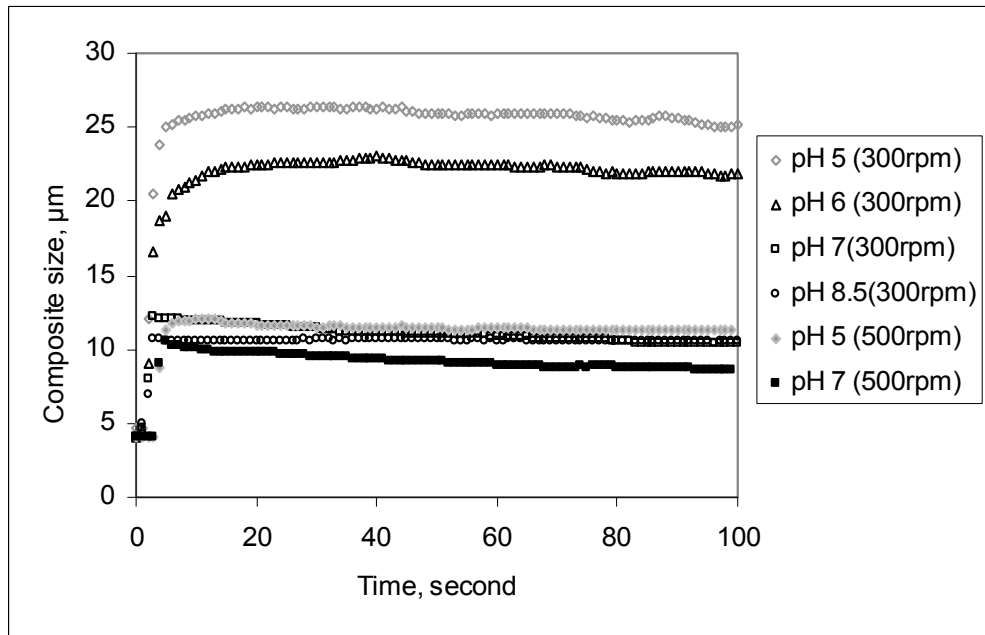


Figure 49: Change of composite size (mean chord length) as a function of time at different composite formation pH

It was found from the real time particle size measurement using FBRM that the mixture of clay with starch and fatty acid could not form aggregates effectively at pH 7 or values of higher.

5.4.3 The effects of clay-starch composites on paper strength and optical properties

Figure 50 shows the effects of clay-starch composites with two different palmitic acid ratios on paper physical properties. This result indicates that starch-fatty acid-clay

composites could significantly improve paper strength properties compared to the pure clay. As the content of unmodified clay increased, the tensile strength of the handsheet made from unmodified clay decreased significantly because the clay particles in the handsheet interferes the fiber bonding, which reduces the number of inter-fiber bonds. As shown in Figure 50, the tensile strengths of the handsheets made from two different clay-starch composites improved about 100~200% compared to the original clay at about 15% clay addition.

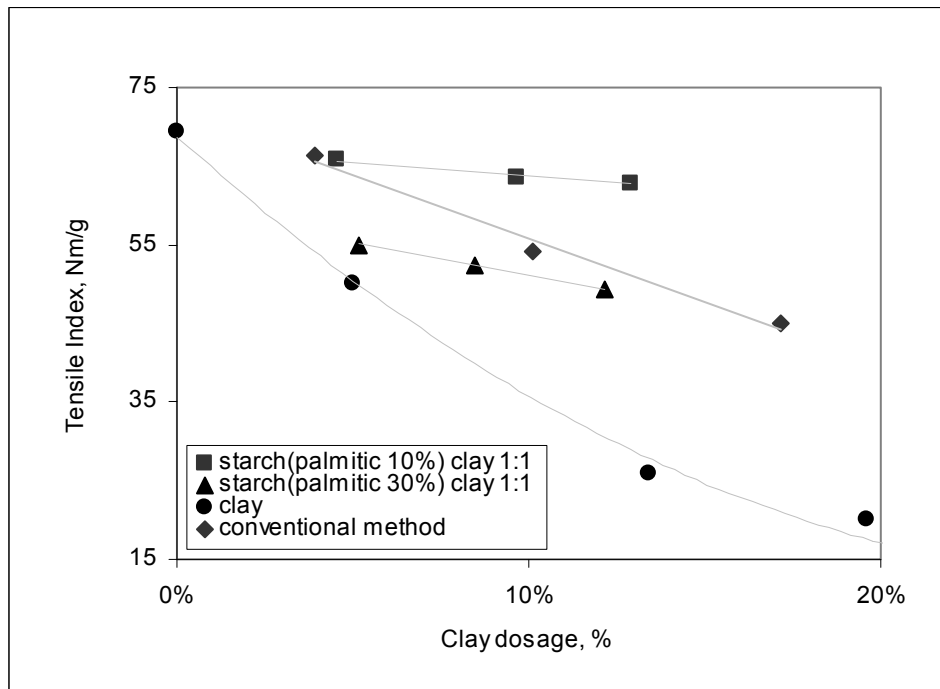


Figure 50: Tensile strengths of the handsheet as a function of filler addition

As the palmitic acid content increased from 10% to 30% based on the starch solid weight, the tensile strength decreased. This result indicated that the increased

hydrophobicity due to fatty acids interfered with hydrogen bond formation between starch and fibers.

To compare the handsheets using clay-starch-fatty acid composites as filler with that using regular filler, the cooked cationic starch (0.1% solution) was used as a wet end additive for unmodified filler. To match the total starch amount in the composite, the same amount of cationic starch with the clay amount in the paper was added. For example, at 10% clay dosage, 10% of cationic starch based on total solid weight of the handsheet was added. It should be noted that this starch amount is much higher than the amount of cationic starch used in most papermaking processes. It is worth noting that when the cationic starch was added at 1~3 wt. %, large fiber flocs were formed. However, when the starch amount went up to 10 wt %, fibers were well redispersed and fiber flocs were not distinguished in the slurry, and the formation of these handsheets was very good. Although the fibers could be well dispersed with very high starch addition, the drainage rate was very slow. In real papermaking condition, this large amount of cationic starch can not be used because of price, slime or pitch problems, charge reversion, etc. The reason for using this high starch content in this study is to compare our approach with an extreme condition. Although the actual starch retention on the paper sheet was not measured, we believe it is much higher than the starch amount retained on paper sheet in a regular papermaking process. The result from this conventional wet-end addition method showed the tensile strength was much better than pure clay filler, but it had a lower tensile strength than the composite method (10% fatty acid). Because the starch was coated on the filler surface in our approach, both the starch retention and water drainage were very high for our approach. Therefore, one of the

significant advantages of this starch-clay composite approach is that very high starch content can be used for paper physical property improvement without starch retention problems.

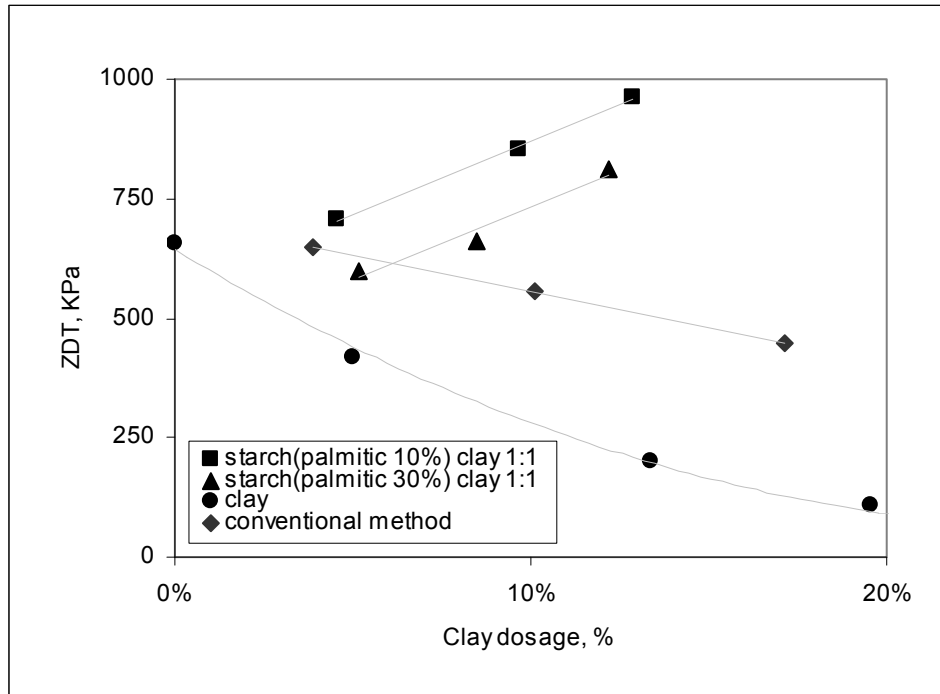


Figure 51: Effect of clay-starch composite on ZDT (Zero directional tensile) strength of the handsheets

Figure 51 shows the results of z-direction tensile strengths of clay-starch composite filled sheets. It is well known that the ZDT usually decreases as the filler content in the paper sheet is increased because filler interferes the fiber-fiber bonding. However, surprisingly, the ZDT increased as the composite content increased in the handsheets made from clay-starch composites with a ratio of clay to starch of 1:1. The result from the conventional wet-end method using cationic starch showed that as the

clay amount increased, the ZDT decreased. Other physical properties such as burst and folding strength were also significantly improved about 200~300 % (not shown here). The main reason for this significant improvement is believed to be an increase in bonding strength between wood fiber and clay-starch composite filler as shown in ZDT test.

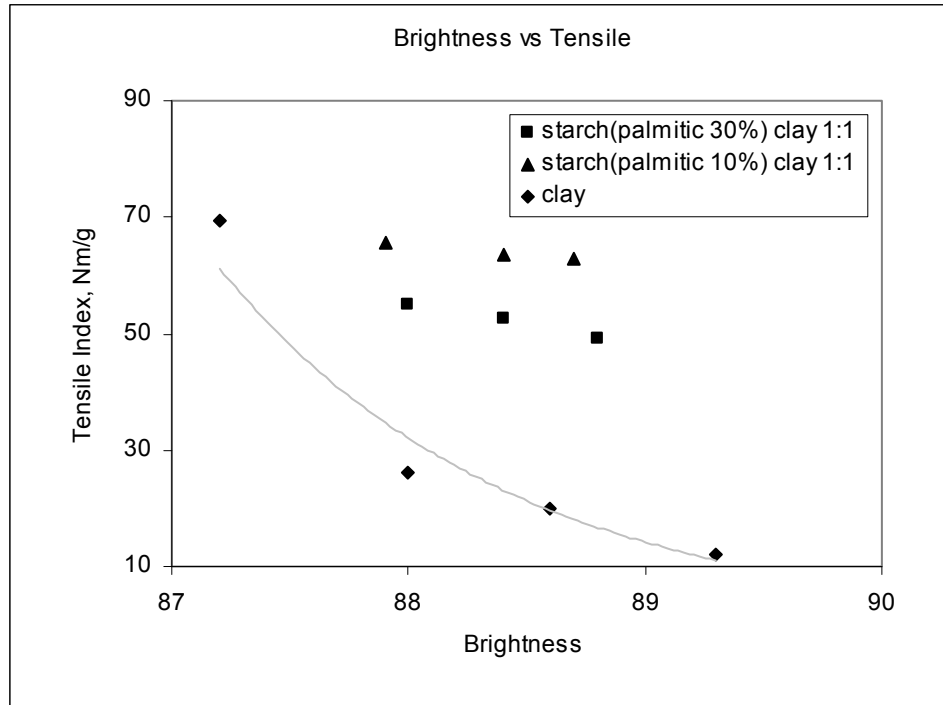


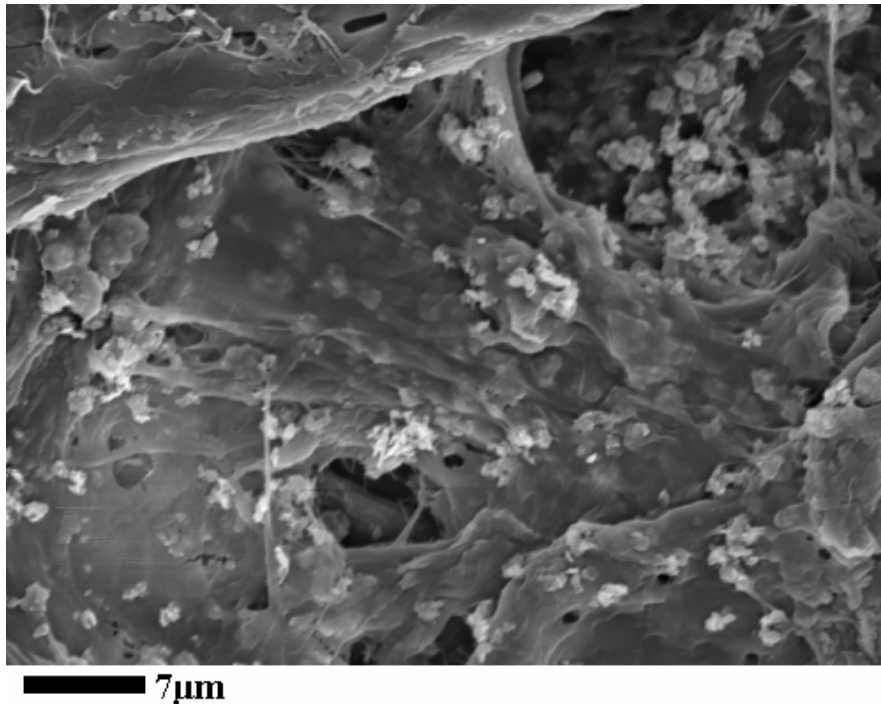
Figure 52: Effect of clay-starch composites on brightness of the handsheets

Figure 52 shows the brightness of the handsheets made with pure clay and clay-starch composites. Clearly, at the same tensile strength, the brightness of handsheets filled with the clay-starch composite was much higher than that of pure clay because much higher filler content was in the handsheet made from composite. It results suggests that, at the same paper tensile strength, the brightness of the paper can be improved by using starch-fatty acid-clay composites. The standard deviation of tested results was very low, which was less than 1.

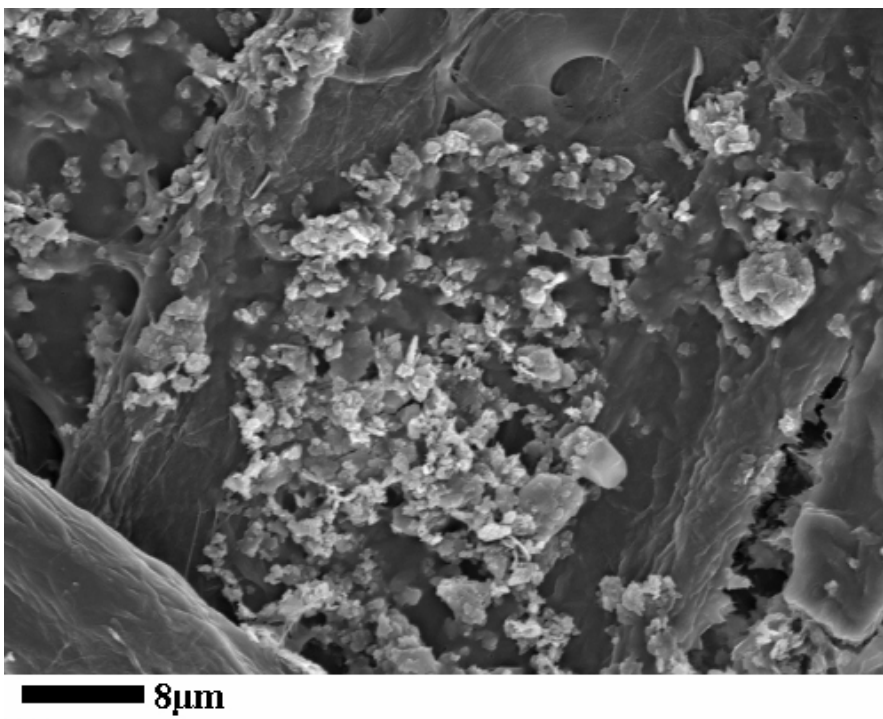
In order to investigate the bonding between the wood fibers and composites and uniformly distribute composites on the paper, the surface of the handsheets filled with composites was observed by SEM as shown in Figure 53. The SEM picture also clearly showed that the thin starch film was spread over both filler particles and fibers. Obviously, this starch film will enhance the bonding strength of the handsheet. It is believed that the starch-film was formed during drying at 105°C.

It is also shown that the clay-starch composites with 10% fatty acid addition were distributed uniformly on the handsheets compared to the clay-starch composites with 30% fatty acid. This agrees well with the brightness results, i.e. the handsheets made from clay-starch composites with 10% fatty acid have higher brightness values than those with 30% fatty acid.

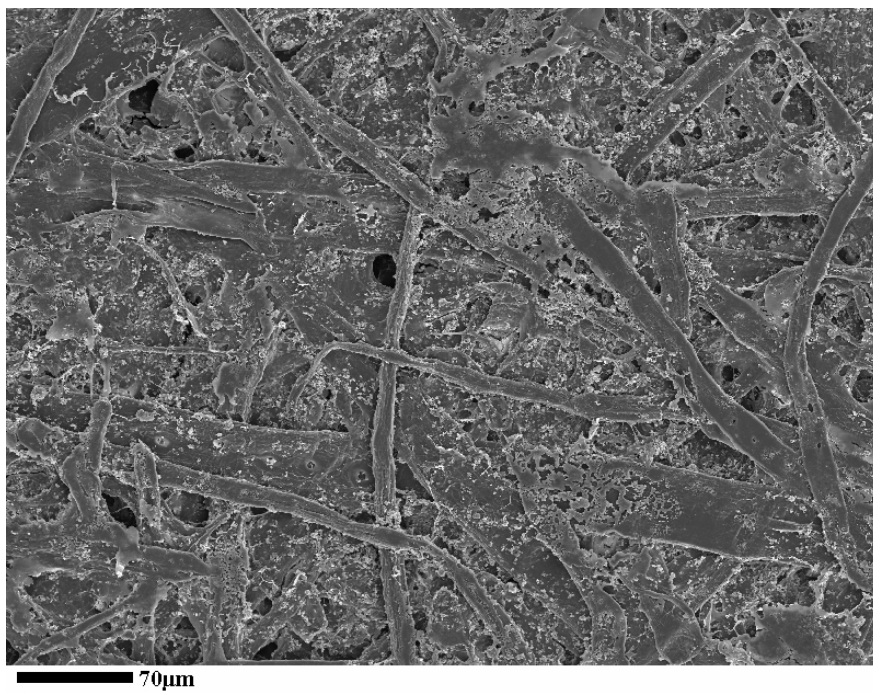
(a)



(b)



(c)



(d)

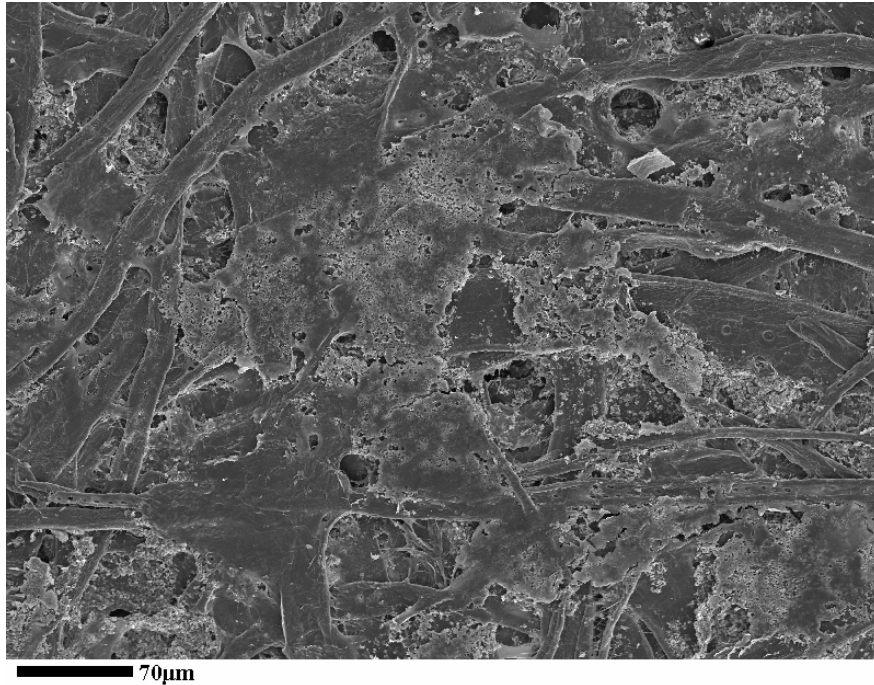


Figure 53: SEM pictures of clay-starch composites filled handsheets. (a) and (c): palmitic acid 10% to starch, (b) and (d): palmitic acid 30% to starch

5.4.4 The effects of clay-starch composites on water repellent property of paper

One of the additional advantages of using clay-starch composites formed by fatty acid is that the fatty acid in the composites can increase the hydrophobicity of the filler, so the water repellent property of the paper sheets increases. The use of hydrophobic agent lead to a considerable reduction in the liquid penetration provided external pressure is not applied.

Since a paper web can be considered to consist of a series of interconnected pores, liquid moves though paper by capillary action through pores, diffusion through pores, diffusion through fiber fraction, evaporation. Washbrun developed the equation to

describe the penetration of liquid into fiber beds or packed powders [151]. In its differential form, the Washburn Equation is the following:

$$\frac{dl}{dt} = \frac{r\gamma \cos \theta}{4\eta l}$$

Equation 11: Washburn Equation

where l = the capillary distance penetrated in time, t ; r = is the capillary radius ; γ = the liquid surface tension ; θ = the contact angle between the capillary walls and the liquid; η = the liquid viscosity. It is assumed that no significant external pressure exists on the penetrating liquid and that the penetrated structure does not change with time. The Washburn Equation suggests that in order to achieve low capillary penetration, it is necessary to have a high contact angle and / or a small radius.

Between the surface tension and the contact angle, the following Young Equation expresses:

$$\cos \theta = (\gamma_{SV} - \gamma_{SL}) / \gamma_{LV}$$

Equation 12: Young Equation

where γ_{SV} = surface tension in the contact surface solid - vapor ; γ_{SL} = surface tension in the contact surface solid - liquid ; γ_{LV} = surface tension in the contact surface liquid - vapor

In order to investigate the effect of clay-starch composite on the liquid penetration through the handsheet, the dynamic contact angle was measured as shown in Figure 54. The images from contact angle measurements showed a much higher initial contact angle ($t = 5s$) of water drop on the handsheet filled with clay-starch composite (10% loading amount) than that with unmodified clay. Even after 60s the contact angle of the handsheet filled with clay- starch composite fillers (10% of fatty acid) showed only a slight decrease. For clay-starch composites complexed by 10% and 30% palmitic acid, the contact angle was decreased from 77.3° ($t=5s$) to 64.1° ($t=60s$) and from 77.1° ($t=5s$) to 66.6° ($t=60s$). However, the contact angle of the handsheet filled with unmodified clay was decreased from 26.4° ($t=5s$) to 0° ($t=60s$).

Palmitic acid is hydrophobic and lower the surface energy (surface tension) of the fiber and filler surfaces (γ_{SV}), thereby reducing the value of the numerator in the Young Equation. As ($\gamma_{SV} - \gamma_{SL}$) decreases, $\cos\theta$ decreases also and the dl/dt term in the Washburn Equation becomes smaller. Thus, water penetration rate will decreased on the handsheet filled with clay-starch composite.

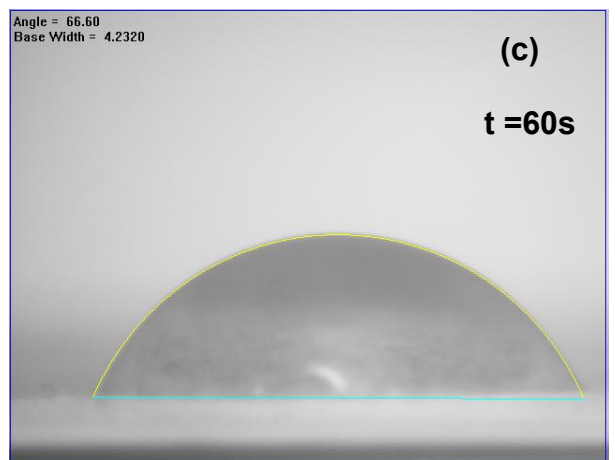
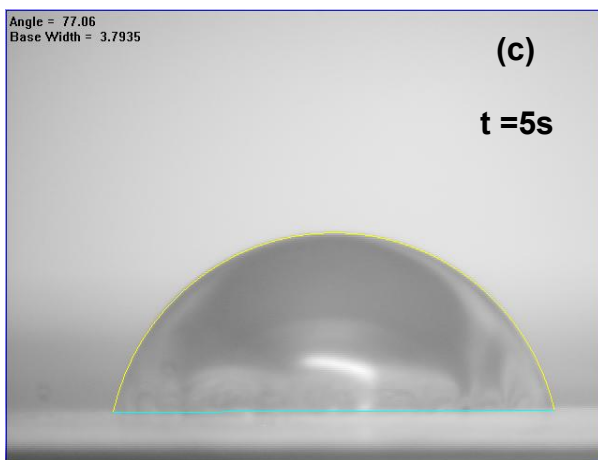
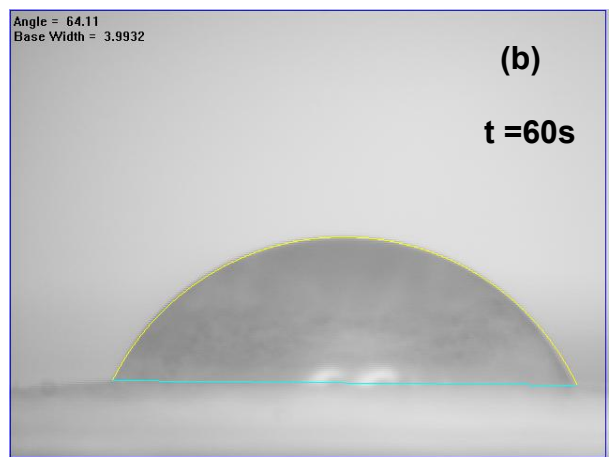
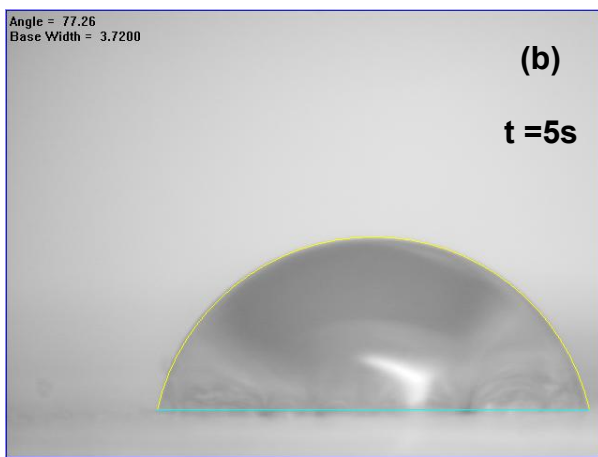
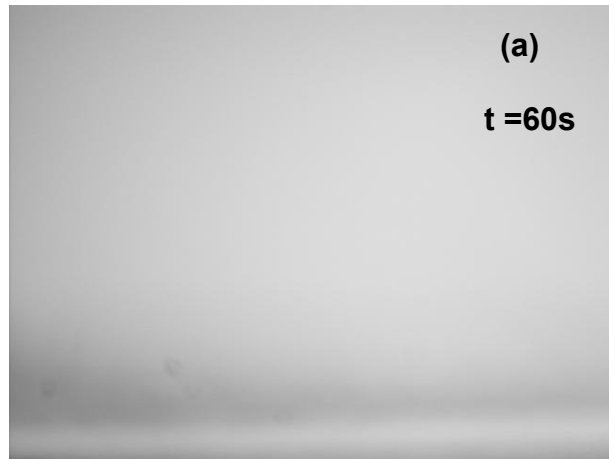
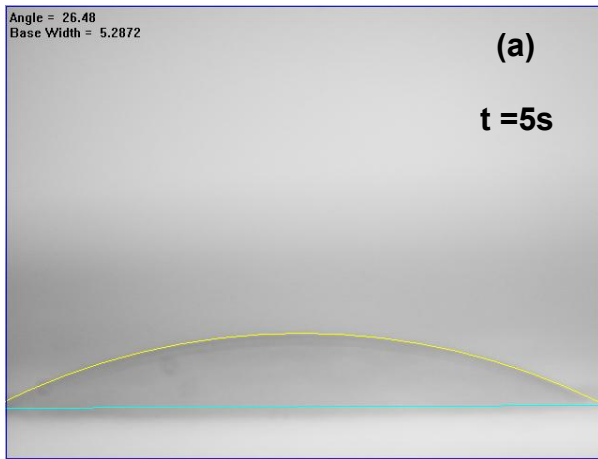


Figure 54: Photographs of water drops on the composite filled handsheets. (left: at 5 seconds, right: at 60 seconds; (a): unfilled handsheet, (b): 10% palmitic acid to starch, (c): 30% palmitic acid to starch)

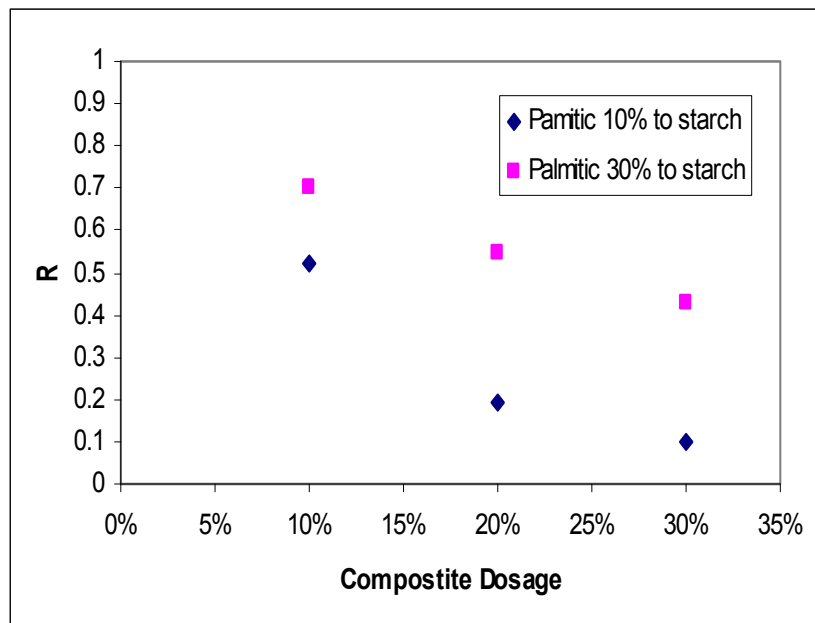


Figure 55: Wettability (R) of composite filled handsheets calculated from contact angle results

However, a water droplet was immediately adsorbed into the handsheet with pure clay. It was also found that as the fatty acid ratio increased and the composite dosage increased, the wettability of the handsheets decreased as shown in Figure 55. Even though the sizing degree of the composite filled paper may not be as high as AKD or ASA sized papers, the improvement in the hydrophobicity of paper sheets using starch-fatty acid-clay composite will significantly reduce the dosage of sizing agent during papermaking.

5. 5 CONCLUSIONS

This study provided a method of clay-starch composite preparation by starch-fatty acid complexation. Thus, the composite prepared can be used as a papermaking filler with much higher paper strength than untreated clay. From the physical property

measurements, clay-starch composites could increase bonding strength dramatically as shown in ZDT tests, thereby the tensile strength was improved up to more than 100~200% at 15% composite addition compared to untreated clay. The optical properties increased as the composite amount in sheets increased. At the same brightness, the clay-starch composite filled handsheets have much higher tensile strength than unmodified clay filled sheets. Additionally, handsheets filled with clay-starch composites improved the water-repellant property due to the hydrophobicity of the fatty acids. The bonding of clay-starch composites with fibers was confirmed by SEM.

It should be noted that our research group has reported several filler modification methods such as $(\text{NH}_4)_2\text{SO}_4$ precipitation method , starch gel coating method , and spray drying method in recent publications. Combining the results reported in these studies, we concluded that the paper strength can be significantly improved by coating starch on filler surfaces. The starch-fatty acid complex method reported in this study has more advantages for paper grades that need high filler loading, high physical strength with certain sizing requirements.

CHAPTER 6

Clay-Cellulose Composite by Cellulose Dissolution Method

6.1 Background

From Chapter 4 and 5, it was found that the starch coated fillers could increase the physical properties of paper. In this chapter, different bonding material, cellulose, was used to improve the paper properties for comparison. Due to the high polarity of the N-O bond, NMMO is a compound with very high hydrophilicity, resulting in extremely high solubility in water, i.e. complete miscibility, a pronounced tendency to form hydrogen bonds, and a very high hygroscopicity. The oxygen of the N-O bond in NMMO is able to form hydrogen bonding with the hydroxyl groups of cellulose. This hydrogen bonding is thought to be the cause for cellulose dissolution [152]. However, during the processes, several chemical processes occur, which cause degradation of cellulose, discoloration of cellulose, decreased product performance, and decomposition of NMMO. Radical reactions have been shown to be a possible cause of NMMO degradation as well as cellulose oxidation [152, 153]. The main radical species are the primary radical and the carbon-centered radicals as shown in Figure 56. This primary radical is a strongly electron-deficient species which will react with electron-rich positions in cellulose. The main result of the action of this radical on cellulose will be the introduction of keto groups into the 2-position of the anhydro glucose repeating units of cellulose, finally leading to chain cleavage by β -elimination and thus, a decreased DP from 472 to 177 during 6h at 105°C (Figure 57) [154]. In addition to radical reactions, there are essentially two main heterolytic degradation processes, *Polonowski*-type reactions

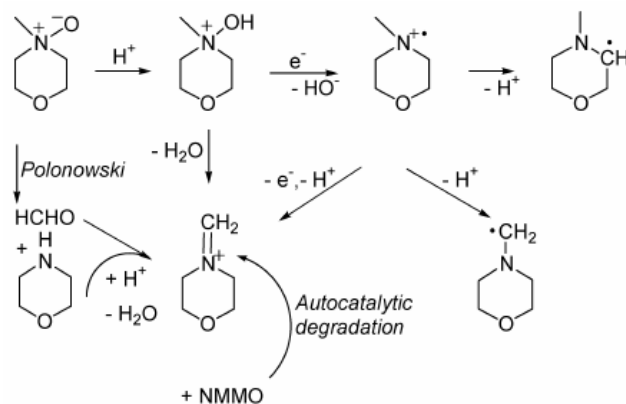


Figure 56: Formation of harmful, reactive intermediates by hemolytic (radical) and heterolytic (ionic) degradation reactions of NMMO [152, 153]

involving HCHO formation [155], and the autocatalytic decomposition of NMMO catalyzed by *Mannich* intermediates, such as N-(methylene)morpholinium [156] as shown in Figure 58. Different types of heterolytic side reactions with cellulose are summarized.

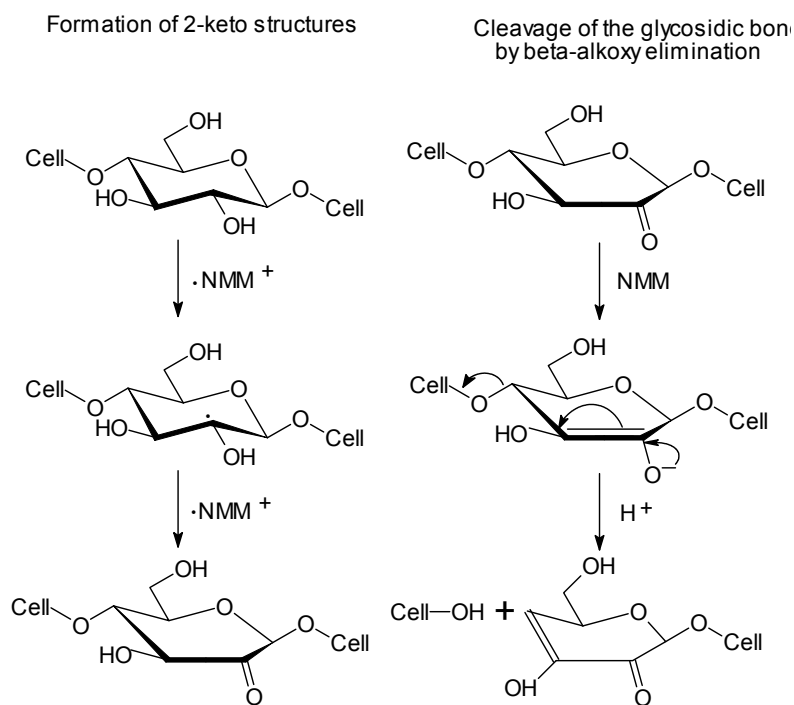


Figure 57: Cellulose chain scission as a consequence of hemolytic reactions [154]

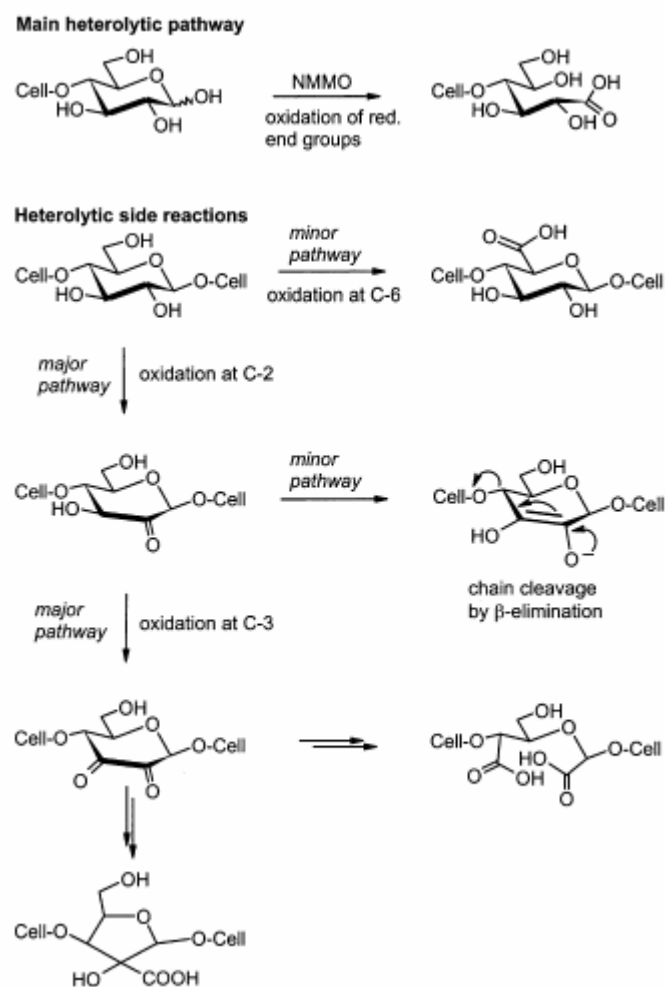


Figure 58: Heterolytic oxidation of cellulose by NMMO: different reaction sites and pathways [156]

To prevent those hemolytic and heterolytic reactions, the research has been focused on the empirical search for new and better stabilizer. After the first patent in 1980, in which propyl gallate was found to act profoundly beneficial as antioxidant in the system, a series of further patents ensued, covering a wide variety of stabilizers coming from synthetic polymer chemistry: phosphonates, bases, sterically hindered phenols, and also mild reductants. Propyl gallate reacts with radical species shown in Figure 59 to give

corresponding phenoxy radical, two of which undergo carbon-carbon coupling to ellagic acid [154]. Ellagic acid is a phenolic antioxidant itself and is oxidatively converted by four radical equivalents into the highly conjugated bis(ortho-quinone), which is the major ‘metabolite’ of the stabilizer in Lyocell solutions [154].

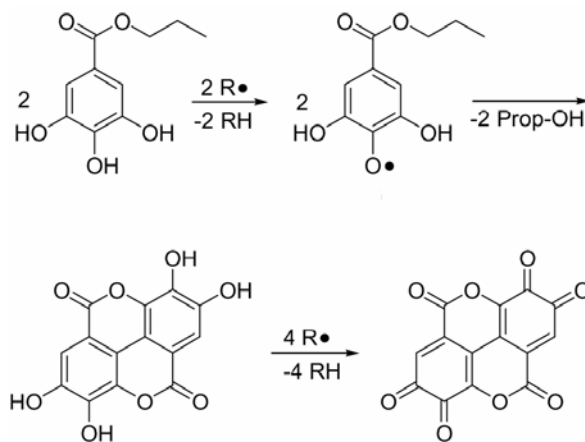


Figure 59: Reactions of propyl gallate as radical trap [154]

6.2 Introduction

Cellulose is a polydispersed linear homopolysaccharide consisting of β -D-glucopyranose moieties linked together by (1 \rightarrow 4)-glycosidic bonds. The degree of polymerization (DP) of native wood cellulose is of the order of 10,000 and lower than that of cotton cellulose (about 15,000). These DP values correspond to molecular masses of 1.6 and 2.4 million Da and to molecular lengths of 5.2 and 7.7 μ m, respectively. In technical process, such as chemical pulping, the DP of cellulose can decrease to 500-2,000. However, chemical processing of cellulose is difficult in general because this natural polymer is not meltable and not soluble in usual solvents due to its strong inter- and intramolecular hydrogen bonded, partially crystalline structure. Thus, the production of cellulose-regenerated material is based largely on the more than 100 years old viscose technology by which fibers (viscose, rayon), films (cellophane) and others are produced via a metastable soluble cellulose derivative (cellulose xanthogenate) (Figure 60, left). This process is technically complex, requires highest-quality dissolving pulp, and leads to problematic environmental loads from the use of CS₂ heavy metal compounds, and resultant by-products.

The cuprammonium process is another classical route for producing regenerated cellulose, but also faces environmental burdens. Researchers have developed several direct dissolution systems (Figure 60, right) for cellulose such as N-methylmorpholine-N-oxide (NMMO)/H₂O, trifluoroacetic acid (TFA)/1,2-dichloroethane, LiCl/dimethylacetamide (DMAc) solution [157], ammonia/ammonium thiocyanate [158], calcium and sodium thiocyanate [159, 160] dimethylsulfoxide/paraformaldehyde [161],

and so forth. The most appropriate solvent for cellulose from among these solvents is NMMO.

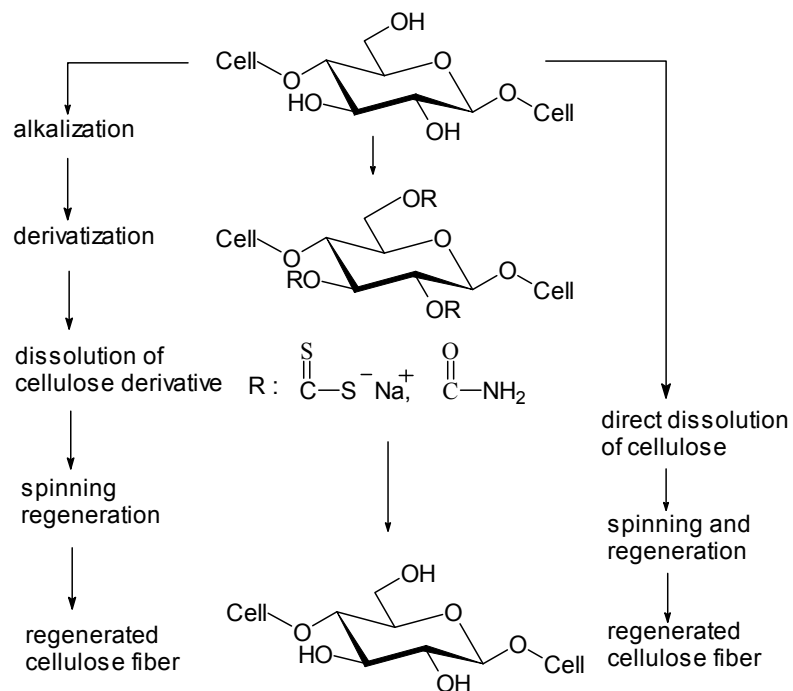


Figure 60: Process principles in regenerated cellulose technologies: left, derivate methods; right, direct methods

The ecological safety of this compound and its high activity of interaction with cellulose stimulated extensive investigations into the process of cellulose dissolution in NMMO (The chemical structure of NMMO is displayed in Figure 61). The cellulose-dissolving potential of the amine oxide family was first realized in 1939 [162]. But not until 20 years later, Johnson patented a solvent system on the basis of cyclic amine oxides, particularly NMMO as a solvent size for strengthening paper by partially dissolving the cellulose fibers [163].

Lyocell production is entirely physical process which does not cause chemical changes in pulp or solvent. Since the 1980s, cellulose fibers manufactured by direct dissolution named as the lyocell fibers have been commercialized and intensive researches for various applications have been done. The cost of NMMO is offset by the greater than 99% recovery and reuse, causing the production cost of lyocell fibers to be similar to that of producing viscous rayon fibers.

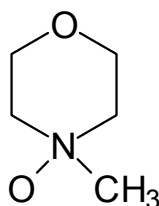


Figure 61: Schematic structure of the NMMO (N-methylmorpholine N-oxide) solvent

In this study, we tried to dissolve cheap cellulose materials by NMMO method to coat the filler surface. We assume that if the surface of clay is coated by cellulose, the bonding between fillers and wood fibers will be increase, which will result in improved physical properties.

6.3 Method

6.3.1 Material

Dry Branch Kaolin Co., Inc. provided the calcined kaolin clay. TiO_2 was purchased from Sigma. The cellulose sources studied here included bleached kraft softwood pulp (BKP), unbleached kraft softwood pulp (UKP), and deinked news paper (DNP). N-methylmorpholine-N-oxide (NMMO) containing 50 wt % water (melting

point: 72 °C) was supplied by Aldrich. Bleached hardwood and softwood pulps were each refined in a Valley beater to a freeness of 400 CSF. Equal proportions of the two pulps were mixed, and the mixture was used as the base pulp furnish for the handsheets. Percol-175 (cationic poly acrylamide retention aid) was obtained from Ciba Specialty Chemicals.

6.3.2 Preparation

The cellulose sources studied here included bleached kraft softwood pulp (BKP), unbleached kraft softwood pulp (UKP), and deinked news paper (DINP). Aqueous NMMO from Aldrich has a water content of 50 wt.-%. Before clay-cellulose composites were experimented for a filler material for papermaking, the preliminary study was done using TiO₂. After confirming the possibility of forming the composite, clay was used for a composite filler material. Clay and cellulose materials (10% or 5% to clay solid weight) were added into 50 wt.-% NMMO solution and mixed well in rotary evaporator at 70°C.

The cellulose concentration was set to 4% to 10 wt.-% NMMO solution. Under continuous mixing and vacuum, the surplus water in NMMO solution was distilled off until the monohydrate form was obtained. Then the mixing and dissolving of cellulose were carried out at 100°C. After cellulose was completely dissolved, the dope was poured into the deionized water then immediately induced high shear force using a high speed dispersing machine, ULTRA TURRAX T18(IKA, Wilmington, NC). The fibrous composites were prepared after 30 seconds under high shear force. The preparation procedure to form the clay-cellulose composite is briefly shown in Figure 62.

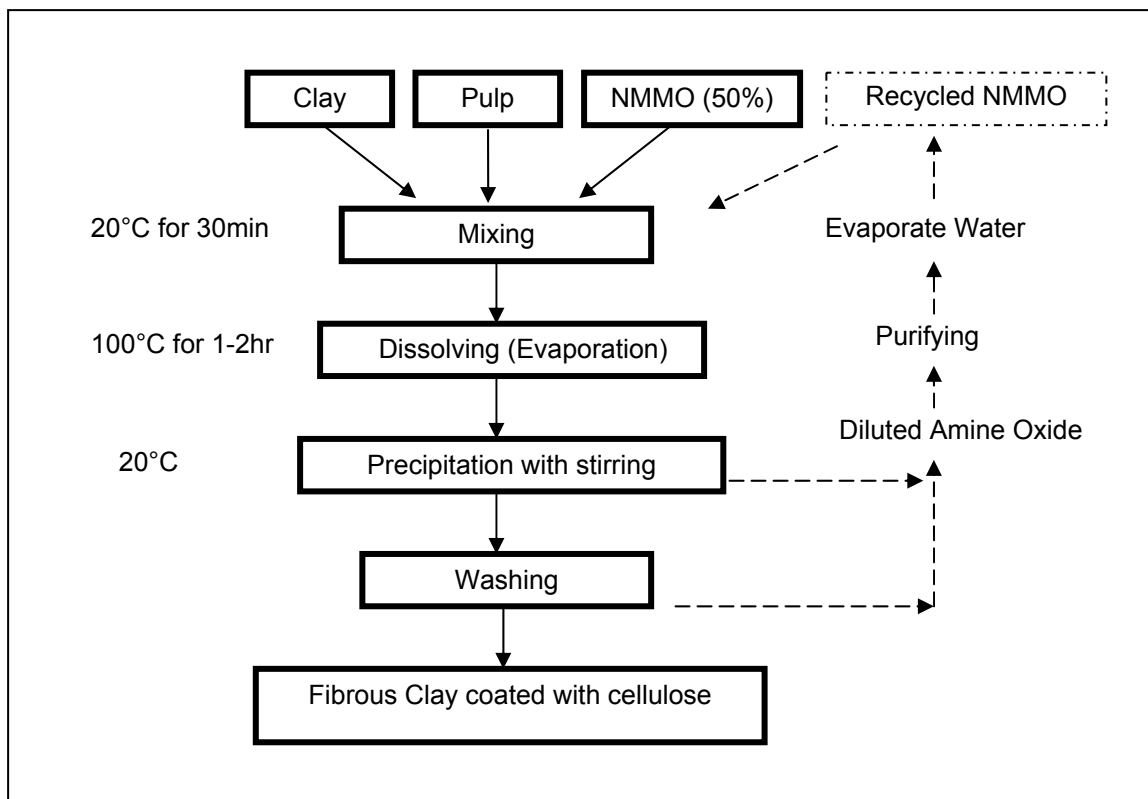


Figure 62: Preparation of coated clay with cellulose

6.3.3 Characterization of fibrous clay-starch composites

The morphology and surface characteristics of the clay-cellulose composites were characterized using Scanning Electron Microscopy (SEM).

6.3.4 Handsheets preparation and determination of paper properties

The pulp was diluted to 0.5 wt% and various amounts of composite aggregates were added during handsheet preparation. After the addition of composites, the slurry was stirred for 20s at 700rpm without adding any retention aids. Handsheets with a target basis weight of 60g/m² were produced according to TAPPI Test Method T 205 “Forming

Handsheets for Physical Tests of Pulp”. For comparison, the control handsheets were prepared using pure clay and Percol-175 was added at 0.05-0.1wt% based on solid fiber for clay retention. After twice wet pressing, all handsheets were dried at 105°C for 7 minutes on the dryer (Emerson Speed Dryer, Model 130). The filler content was determined by ashing the paper in a muffle oven according to the standard TAPPI method T211.

6.4 Results

6.4.1 Characterization of the clay-cellulose composites

Before starting the experiment, TiO_2 was used for preliminary study to confirm the possibility to form a composite. TiO_2 has very small particle size (~100 nm) and narrow particle size distribution, thus the composite formation was thought to be relatively easy to be identified. Figure 63 shows the SEM pictures of untreated TiO_2 .

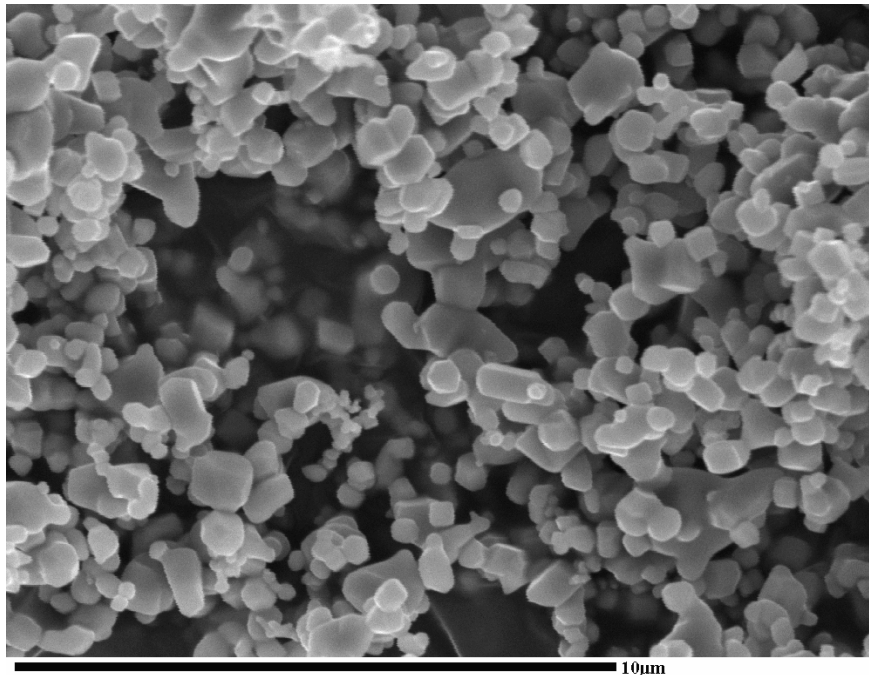


Figure 63: SEM of untreated TiO_2

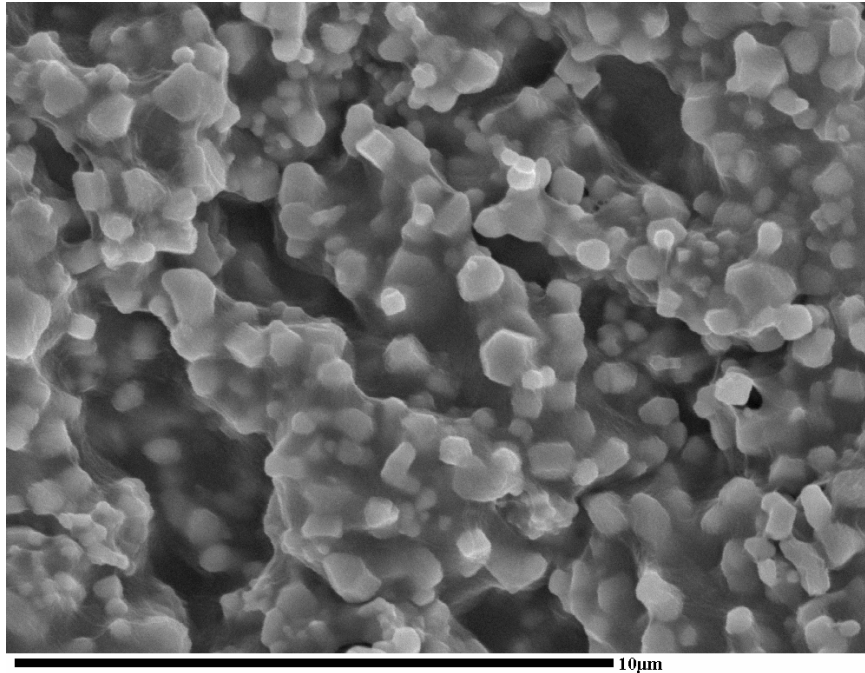


Figure 64: SEM of TiO₂-cellulose (10 wt. % based on the solid TiO₂) composite

It is well known that TiO₂ has the highest refractive index of any white pigment and, consequently, has the greatest specific opacifying power, which is an important asset in view of the continuing pressure to reduce paper basis weights, while retaining optical properties. Figure 64 shows the SEM picture of TiO₂-cellulose composite. Even though only 10 wt. % of cellulose based on solid TiO₂ was used, the dissolved cellulose was evenly coated on the TiO₂ surfaces. From the SEM pictures, we convinced the cellulose could be used for filler coating material to increase the bonding between the fiber and filler. TiO₂ has been used for a paper coating material however it is rare to add TiO₂ in wet-end system because of the high cost of TiO₂.

In this research, clay was used instead of TiO₂ and the same cellulose dissolution method was used. Figure 65 shows the morphology of clay-cellulose composites from

SEM. UKP-clay composites are shown to be a fiber type which is around 1-2mm in length and 100-150 μ m in width. However, the morphology of composites is highly depend upon the ratio of clay and cellulose, the shear speed, the type of cellulose (degree of polymerization and lignin content), and the concentration of cellulose in NMMO. DIP-clay composites, some of them were fiber type but most of them were an irregular relatively small aggregate type, which might be caused by the low DP of DIP pulp. Among the composites prepared from BKP, UKP, and DIP, the composite shape and surface structure of BKP and UKP were similar, but those of DIP were a little bit different.

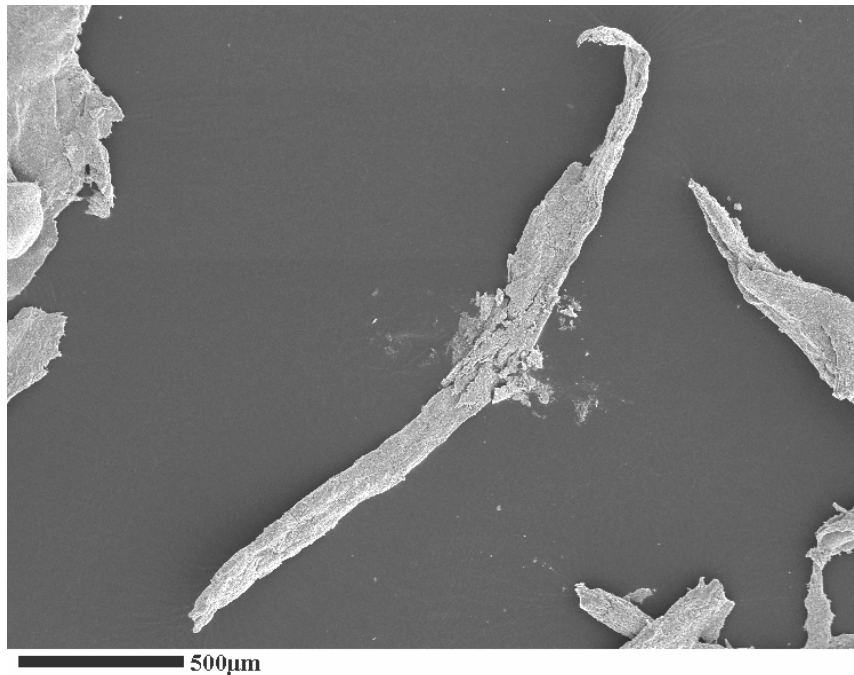


Figure 65: Morphology of clay-cellulose (UKP) composite from SEM

From higher magnification SEM pictures, the surface of clay was shown to be coated by cellulose as shown in Figure 66-68. The micro-structure of clay-cellulose composites was porous because the cellulose ratio was small (10%) so that they could not have a perfectly smooth surface. The porous structure of composite can affect positively on the optical properties because the additional void makes light scatter more, however the spacer often can negatively affect on the physical properties due to the additional reduction of the fiber-fiber bond. From the microscopic observation, cellulose covers the clay surface so that the clear appearance or boundary of clay could not be seen.

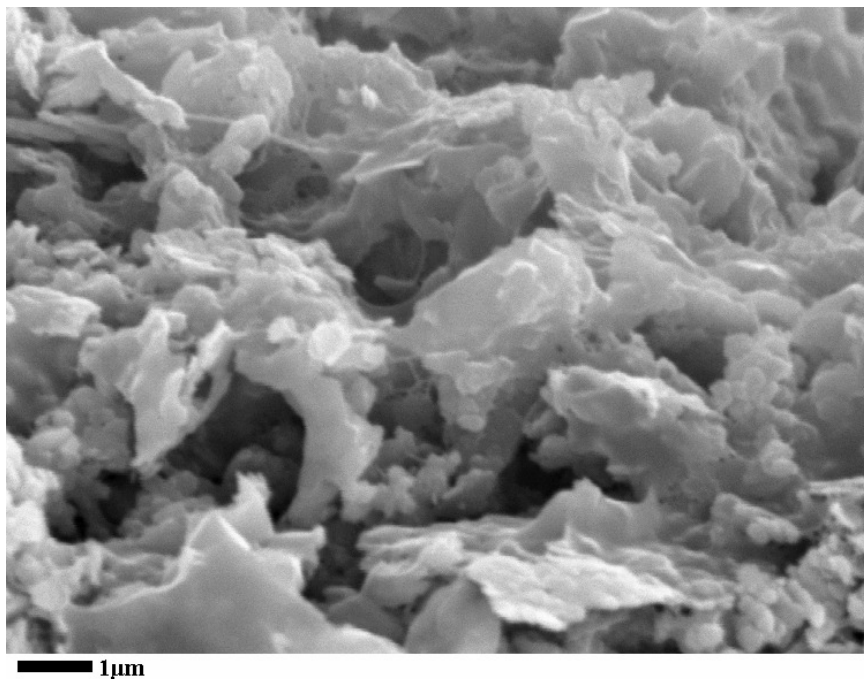


Figure 66: Microscopic surface structure of clay-cellulose (DIP) composite from SEM

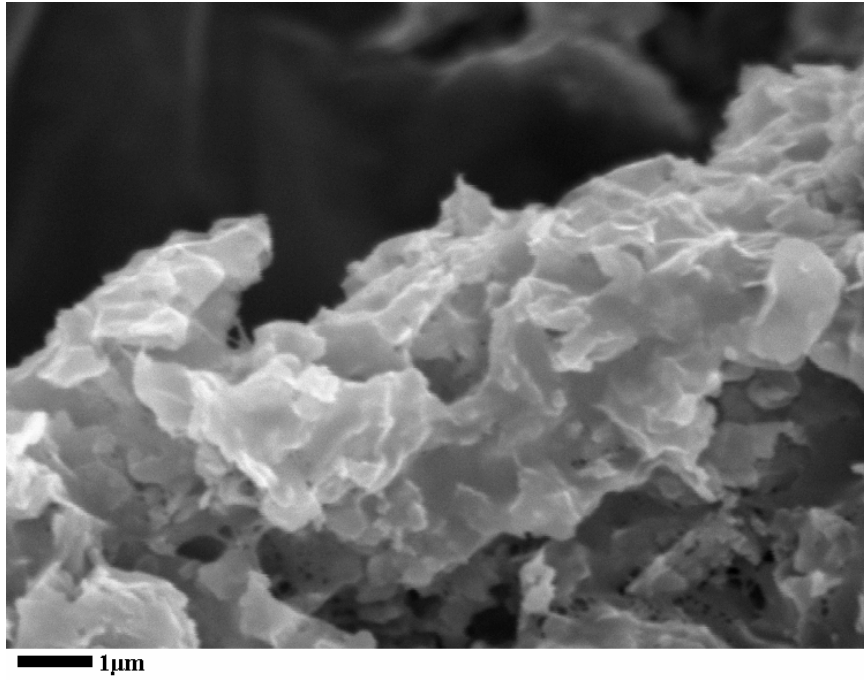


Figure 67: Microscopic surface structure of clay-cellulose (BKP) composite from SEM

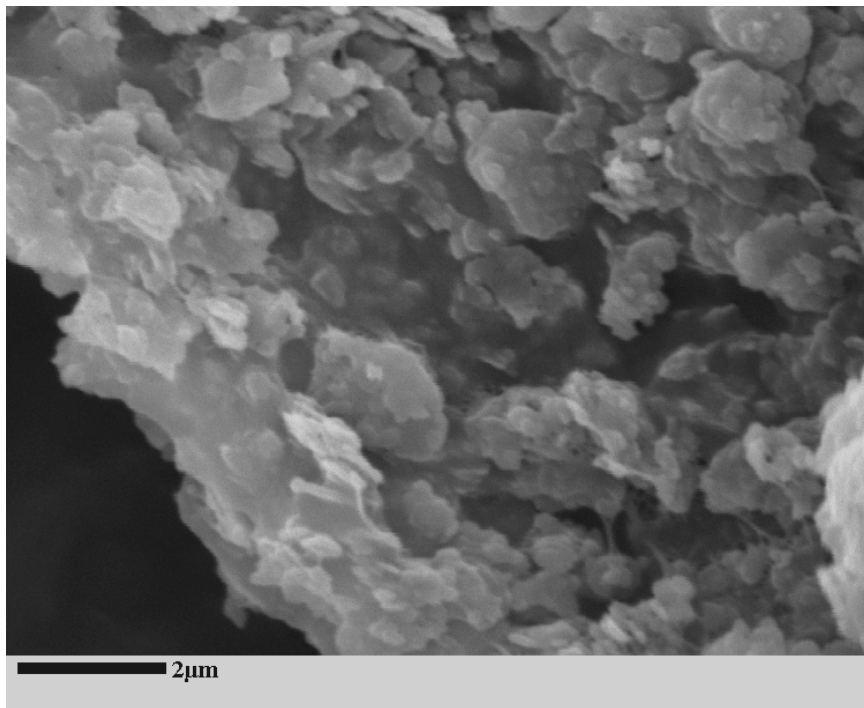


Figure 68: Microscopic surface structure of clay-cellulose (UKP) composite from SEM

6.4.2 The effects of clay-cellulose composites on paper strength and optical properties

Figure 69 shows the effects of the clay-cellulose composites on the tensile properties of paper. This data indicates that clay-cellulose composites could significantly improve paper strength properties compared to conventional papermaking clay. As the content of pure clay was increased, the tensile strength of the handsheet filled with unmodified clay was decreased significantly as shown in Figure 69. The tensile strengths of the handsheets filled with the clay-BKP composite were increased over 100 % compared to original clay at 20% dose.

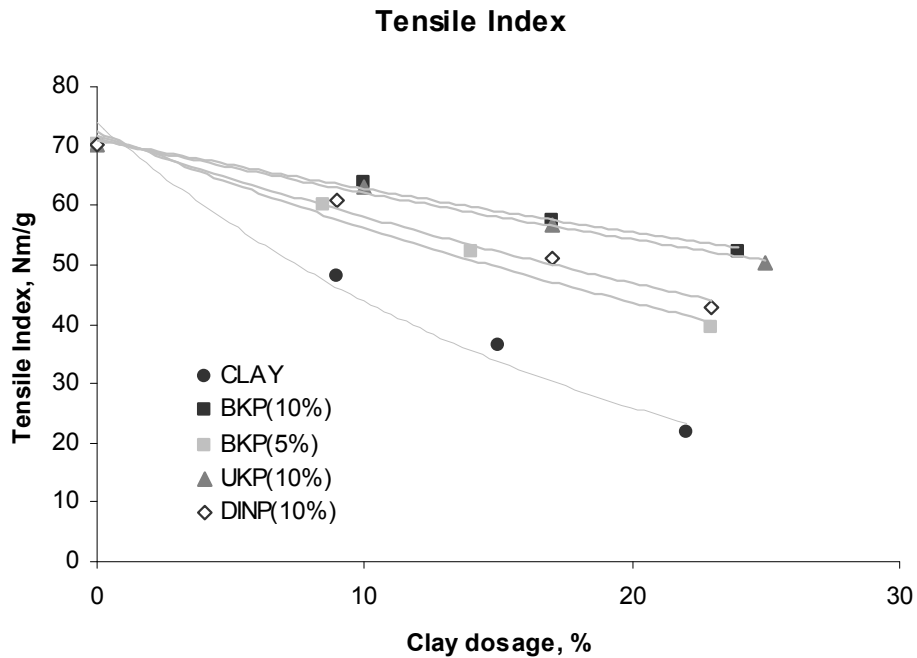


Figure 69: Tensile index as a function of clay or composite dosage for pure clay and different clay-cellulose material composites

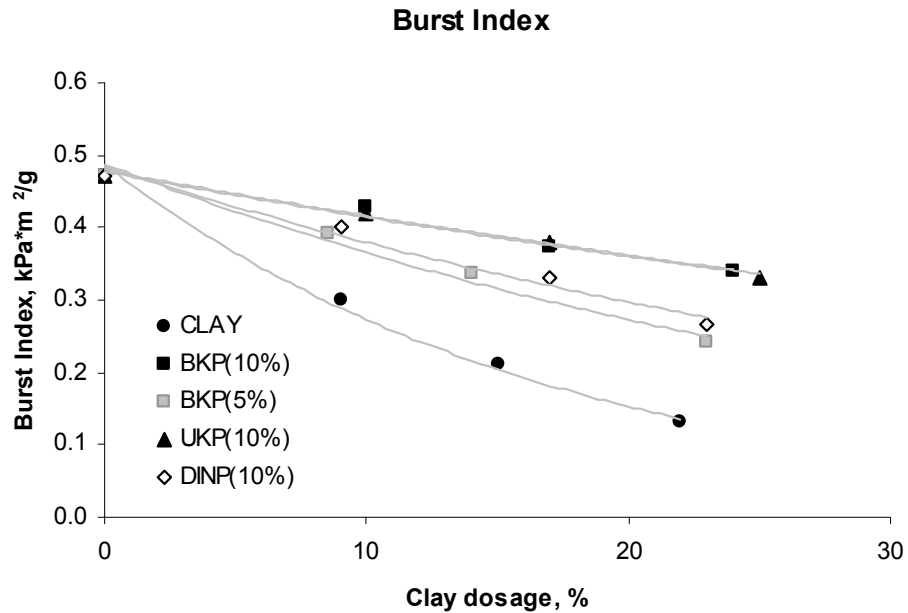


Figure 70: Bust index as a function of clay dosage for pure clay and different clay-cellulose material composites

However, as the BKP content in the composite is decreased from 10% to 5%, the tensile strength significantly decreased. The burst strength displays exactly the same pattern with the tensile strength as shown in Figure 70.

The folding strength from composites also showed a significant improvement whereas the pure clay showed a dramatic decrease (Figure 71). This significant improvement is thought to be caused by the increased bond strength between fibers and clays by composite formation and the large aggregate size of the composites, which enlarges the fiber-fiber bonding area.

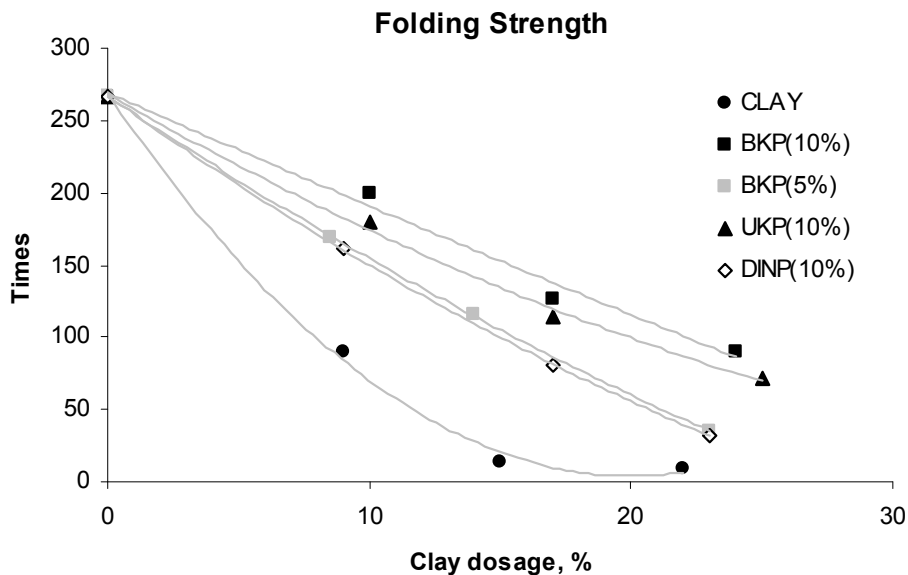


Figure 71: Folding strength as a function of clay or composite dosage for pure clay and different clay-cellulose material composites

However, due to the large size of the composite, the optical properties of the handsheets filled with composites were much lower than those with pure clay as shown in Figure 72 and 73.

As the content of composite fillers increased, the brightness decreased. Besides the large size of the composite, the light absorbing property of regenerated cellulose might also affect this result. For brightness, as the clay dosage increases, the clay coated with DINP showed the gradual decrease, which might be caused from purities in pulp material. The standard deviation of tested results was very low, which was less than 1.

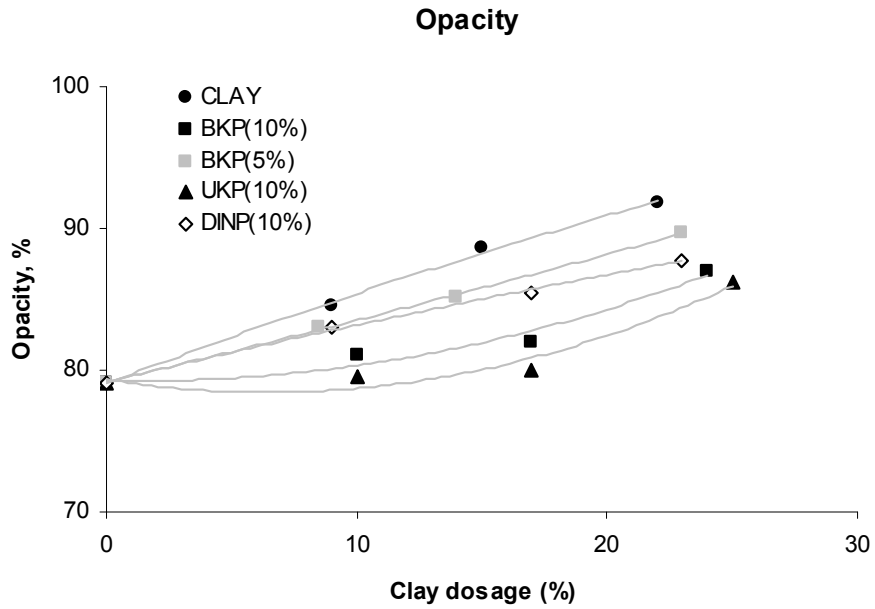


Figure 72: Opacity as a function of clay or composite dosage for pure clay and different clay-cellulose material composites

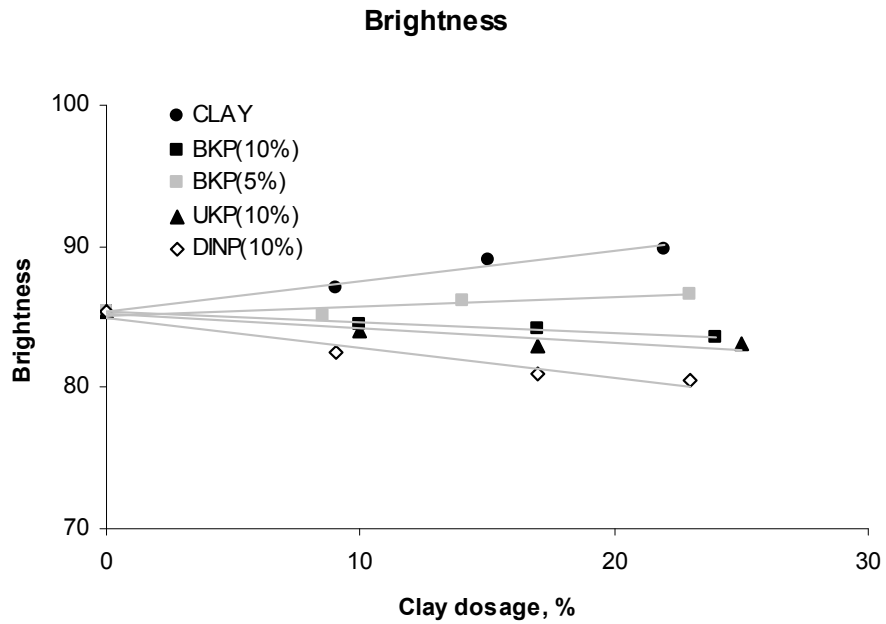


Figure 73: Brightness as a function of clay or composite dosage for pure clay and different clay-cellulose material composites

6.5 Conclusion

This study suggests a different type of clay-bonding material composites to improve the paper properties. The regenerated cellulose coated clay was simply prepared by NMMO dissolution technique. The advantage of using UKP, BKP or DINP rather than pure cellulose such as cotton or micro crystalline cellulose (MCC) is that the cost could be significantly reduced without diminishing the bonding properties with wood fibers. The morphology of the modified clay by cellulose was an aggregated fibrous type, which was investigated by SEM.

From the physical property measurements such as tensile, bust, and folding strength, the handsheet filled with modified clay was much stronger than that with unmodified clay. As cellulose content was increased, the strength improvement was significant. The main reason to increase of strength improvement is thought to be the surface coating with bonding materials and the relatively less surface area due to aggregation of fillers. Therefore, optical properties with modified clay were less than those with unmodified. For brightness, as the clay dosage increases, the clay coated with DINP showed a gradual decrease, which might be caused from impurities in pulp material.

CHAPTER 7

Experimental and Modeling Study of the Strength Properties of Clay-Starch Composite Filled Papers*

Abstract

To increase the filler content in paper without sacrificing paper properties, clay-starch composites, made from a simple precipitation method, were used in papermaking. Compared to untreated clay, the clay-starch composite filled paper improved paper tensile up to 100~200%. Contrary to untreated clays that usually reduce the ZDT (z-directional tensile strength) of papers, the clay-starch composite actually increases the ZDT. The significant improvements in the paper strengths are attributed to the formation of a fiber-starch-filler sandwich structure, which avoids direct contact between filler and fiber. The specific shear bond strength (expressed as the specific bond strength) between fillers and fibers were measured and used as the main variables for the modeling. It was also found that the fiber-fiber specific bond strength is weaker than the fiber-starch specific bond strength. The tensile strength (expressed as breaking length) was modeled by using a modified Page equation suggested by Beazley, Dennison, and Taylor (BDT). The experimental results agreed very well with the modeling results. Additionally, the stiffness of composite filled paper was modeled by calculated tensile strength.

* *This chapter has been modified from the following publication: S.Y.Yoon and Y.Deng, Experimental and modeling study of the strength properties of clay-starch composite filled papers, Ind. Chem. Res. submitted.*

7.1 Background - Theories of Paper Strength

Paper is a material with an enormously high degree of heterogeneity containing a seemingly infinite number of cracks of different dimensions. The established theories of paper strength originate mainly from the recognition of a balance between fiber strength and bond strength. For well-bonded paper, it is intuitively easy to conceive that the strength of paper must be related to the strength of the fibers as follows:

$$\sigma_p = F \cdot \sigma_f$$

Equation 13: The strength of well-bonded paper

where σ_p and σ_f are the tensile strengths of paper and fiber respectively.

The intensity function F describes the efficiency of the structure in utilizing the strength of the paper. The simplistic approach of treating paper as a two-phase composite material, where fibers make up one phase and void volume is the other phase, gives to a first approximation the following

$$\sigma_p = \frac{1}{3} \cdot V_f \cdot \sigma_f$$

Equation 14: Tensile strength of a random two-dimensional sheet

where V_f is the volume fraction of fibers.

The factor $1/3$ reflects the theoretical finding that the maximum tensile strength of a random two-dimensional sheet is equal to one third of the strength of individual

component fibers [164]. The void fraction of fibers is equal to the ratio of sheet density ρ_p to fiber density ρ_f , and thus

$$\sigma_p = \frac{1}{3} \cdot (\rho_p / \rho_f) \cdot \sigma_f$$

Equation 15: Tensile strength of a random two-dimensional sheet

Since paper in its end use is judged by its strength per unit width for a given grammage, the tensile index or the specific tensile strength σ_p^* is defined as

$$\sigma_p^* = \sigma_p / \rho_p$$

By analogy, the specific fiber strength is given by

$$\sigma_f^* = \sigma_f / \rho$$

Eq. 4 may thus be rearranged to give the following expression in terms of specific strengths

$$\sigma_p^* = (1/3) \cdot \sigma_f^*$$

Equation 16: Specific tensile strength of a random two-dimensional sheet

This equation should be expressed to describe the efficiency function F^* given by

$$\sigma_p^* = (1/3) \cdot \sigma_f^* \cdot F^*$$

Equation 17: Specific tensile strength of a random two-dimensional sheet considering efficiency function

The value of this efficiency function normally increases with beating of the fibers and with increasing intensity of wet pressing of the wet web.

Considerable effort has been spent on finding an analytical expression for an efficiency function in terms of the structure and the bonding between fibers.

Shear lag analysis which was done by Cox [164] showed when tensile failure is broken in the fiber, the tensile strength are formulated as

$$\sigma_p^* = (1/3) \cdot \sigma_f^* \cdot \left(1 - \frac{r \cdot \sigma_f}{L \cdot \tau_b}\right)$$

Equation 18: Shear lag analysis by fiber failure

When the tensile failure is occurred by bond failure (i.e. pullout), the tensile strength is formulated as

$$\sigma_p = \tau_b \cdot V_f \cdot \frac{1}{12} \cdot \frac{L}{r}$$

Equation 19: Shear lag analysis by bond failure

where r is fiber radius and τ_b is the shear strength of the matrix.

Kallmes, Bernier, and Perez (KBP) extended the fiber network theory of the load-elongation of paper to the limits of structure of failure [165]. They suggested that the tensile strength of paper is a balance between bond strength and fiber strength. They presented two expressions for the tensile strength. The first of these is for sheets in which rupture is induced by fiber failure

$$\sigma_p^* = \frac{1-f_c}{3} \cdot \sigma_f^* \cdot \left(1 - \frac{5 r \cdot \sigma_f}{6 L \cdot \tau_b} \frac{1}{RBA}\right)$$

Equation 20: KBP equation by fiber failure

where f_c is the fraction of fibers bearing no load and RBA is the relative bonded area.

The second expression gives the tensile strength of sheets when failure is induced by bond failure.

$$\sigma_p^* = \frac{\tau_b}{\rho_f} \cdot \frac{1-f_c}{10} \cdot \frac{L}{r} \cdot \mathbf{RBA}$$

Equation 21: KBP equation by bond failure

A slightly different approach to the theoretical modeling of tensile strength has been taken by Page [30] who started from the premise that tensile strength must be proportional to the fraction of fibers that are broken across the rupture zone. This may be formulated as

$$\sigma_p^* = \frac{1}{3} \cdot \sigma_f^* \cdot \frac{n_f}{n_f + n_p}$$

Equation 22: Page Equation

where n_f is the number of fibers that break at rupture and n_p is the number of fibers that pull out intact. Page then related the ratio n_p/n_f to the fiber strength and bond strength by simply assuming that

$$n_p/n_f = t/b$$

where $t_f = \sigma_f \cdot \pi \cdot r^2$ is fiber strength and $b = \tau_b \cdot \frac{L}{4} \cdot 2\pi r \cdot RBA$ is bond strength and $\frac{L}{4}$ is the mean pulled length. When Eq. 17-19 are inserted in Eq. 16, the following expression is obtained

$$\sigma_p^* = \frac{1}{3} \cdot \sigma_f^* \cdot \left(1 - \frac{5 r \cdot \sigma_f}{6 L \cdot \tau_b RBA}\right)^{-1}$$

Equation 23: Page Equation

As shown above three tensile strength models, there are only slight different views on how fiber strength and bond strength balance each other. However, limitation to the application of these tensile strength theories is the lack of data regarding fiber strength, bond strength, and relative bonded area [166].

Fiber to fiber bonding

Fiber-fiber bonding is widely regarded as one of the most important properties for the papermaker because it is principally responsible for the internal cohesion of a paper sheet [167]. Bonding is traditionally defined using two independent factors: bonded area and specific bond strength (bond strength per unit bond area) [168].

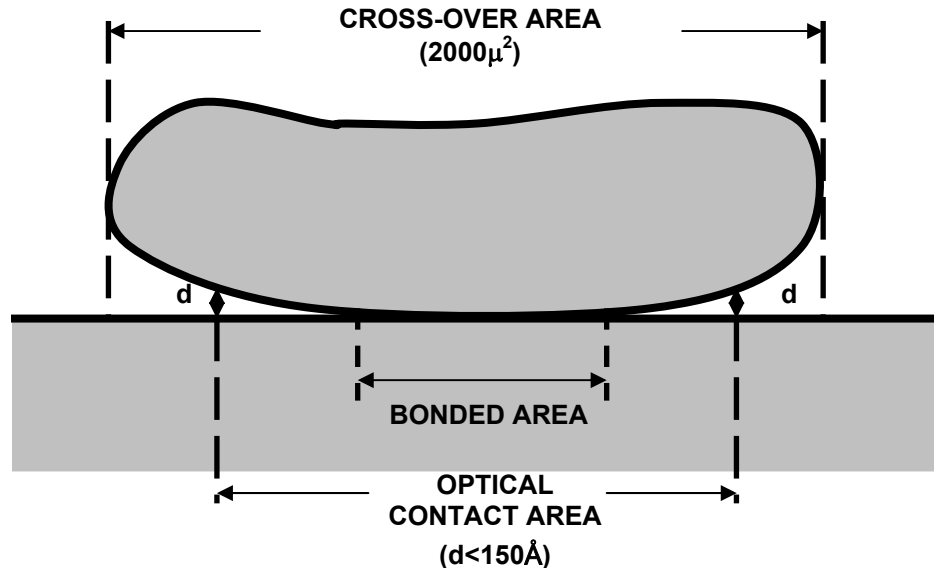


Figure 74: Areas of interest in fiber-fiber bonding

Bonded Area

As shown in Figure 74, there is considerable doubt as to whether complete bonding exists in the crossover area (about 2000 μ^2) between two fibers [169]. Page revealed that the optical contact area between two bonded fibers ranges from 50 to as much as 1000 μ^2 or more [170]. Efforts to measure bonded area by nitrogen adsorption [171] indicated that bonded area changes measured by this technique are reasonably proportional to changes in optical contact area.

Asunmaa and Steenberg [172] have shown in an electron microscopy study of interfiber bonds that areas of contact up to 100 μ^2 occur and that this contact is so intimate that is suggestive of chemical bonding. On the other hand, Jayme and Hunger [173] reported that only 10-20% of the optical contact area represents true bonding by observing the surfaces formed by interfiber bond rupture.

In order to measure the efficiency of the interfacial fiber-fiber area to transfer load, the total bonded area needs to be defined. The relative bonded area, RBA, usually characterizes the bonding degree of paper. By definition, RBA is the bonded surface area of fibers divided by their total surface area. Even though there are direct methods [174], the preparation of cross-sectional samples and their measurement such as examination of micrographs and computer analysis are quite tedious. Indirect methods are therefore usual in the measurement of RBA. They generally utilize gas adsorption or light scattering techniques. The scattering coefficient is related to the free specific surface area from which an approximation of the bonded area of a paper sheet can be derived.

$$\text{RBA} = (S_0 - S) / S_0$$

Equation 24: Calculation of RBA

where s is the specific light-scattering coefficient of the sheet and S_0 is the value corresponding to the unbonded network.

The most widely used method for measuring relative bonded area, developed by Ingmanson and Thode [175], relies on the use of light scattering coefficient and extrapolation to zero tensile strength.

Figure 75 shows the tensile strength predictions of the Page equation by changing RBA. As RBA increases by refining or wet pressing, one might see that RBA plays the one of the most important role on the tensile strength.

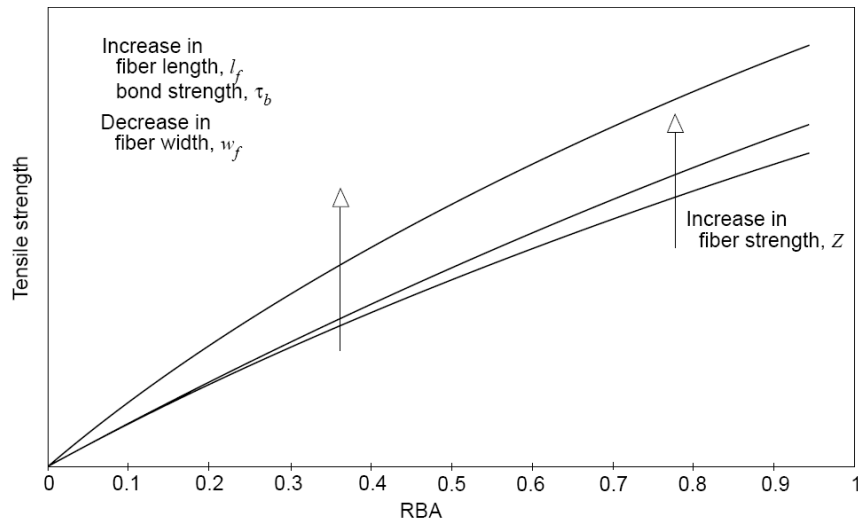


Figure 75: Predictions from Page equation for tensile strength vs. relative bonded area together with the qualitative effect of increasing fiber properties

Bond strength

The shear strength of individual fiber-fiber bonds has been determined by Davison [169], Mayhood, Kallmes & Cauley [31], and Schniewind, Nemeth & Brink [176] to be 0.4 - 1.6g (2.0×10^8 dyn/cm² to 6.9×10^8 dyn/cm²). This finding is supported by others who have measured the bond strength between a single cellulose fiber and a cellulose shive [177] or between a single fiber and cellulophane film [27]. Bonds between summerwood fibers gave higher values than those between springwood fibers, bond strength increased with pulp yield [177] and the effect of beating appeared negligible [31, 178].

Skowronski and Bichard [28] designed the delamination technique to determine fiber-fiber bond strength and specific bond strength using handsheet and proposed that bond strength increases with beating or wet-pressing due to an increase of total fiber-to-fiber bonded area, while the specific bond strength remains nearly unchanged.

An intensive study was conducted by Leach [179] to determine the effects of a dry strength additive, locust bean gum. He proposed that locust bean gum increased strength of the bonds (60%), improved sheet formation (25%), and increased number of bonds (15%); however, these conclusions involved indirect measurements plus deductive reasoning designed to separate the inherent bond strength and degree of bonded area parameters.

7.2 Introduction

For many years, the increase of filler content in paper has been driven by reducing the raw material cost and improving the paper's optical properties. However, as filler loading is increased, the paper strength, bulk, and stiffness are usually decreased. To compensate the paper strength loss with filler loading, cationic polymeric dry strength aids have been widely used. The improvement using cationic starch is limited because the maximum adsorption amount of cationic starch on wood fibers is restricted by charge saturation and thus is usually less than 0.5%. Moreover, over loading of cationic dry-strength aids will significantly increase the cost and cause fiber flocculation, resulting in a poor paper formation [70]. The un-retained cationic starch will be accumulated in the whitewater and create pitch, slime, and stickies problems.

To increase the proportion of filler without sacrificing paper properties, various methods such as preflocculation [77, 78, 81, 180], lumen loading [91-93], polymer treated fillers [82, 83], and filler-wood fine composites [84] have been explored. Although these approaches show some improvements in the paper strengths, the strength reduction at high filler level is still a challenge for papermakers. In this paper, the

fundamentals of the paper strength improvements using starch-filler composites were studied in details using a combination approach of well defined experiments and theoretical modeling.

Recently, we reported a series of filler modification methods, including starch gel-coated PCC [110], starch-coated clay by drying method [181], clay-starch composite using $(\text{NH}_4)_2\text{SO}_4$ as a precipitation agent [145], and clay-starch composite using a fatty acid as a complexation agent [182], to improve the paper strengths for high filler content papers. These methods showed dramatic improvements of tensile, burst, and folding strength without losing the optical properties compared with unmodified filled papers. In order to understand the mechanism of strength improvement using dispersed polymer-filler composites in paper, paper strength modeling in the presence of fillers should be developed. Although the tensile strength has been theoretically studied for the papers with pure wood fibers [183-185, 30], there is only limited information about the modeling study of inorganic filler filled papers [186], and there is no theoretical study about polymer-modified filler filled papers in the literature.

For an unfilled paper, Page derived his model for tensile strength [30] starting from the experimental observation that tensile strength is proportional to the fraction of fibers that break along the rupture line. This led him to the following equation for tensile strength (T)

$$\frac{1}{T} = \frac{9}{8Z} + \frac{12A\rho g}{bPL(R.B.A)}$$

Equation 25: Page equation

where

T = tensile strength of paper

Z = zero-span tensile strength of paper

A = area of average fiber cross section

ρ = density of the fibrous material

g = acceleration due to gravity

b = shear bond strength per unit bonded area

P = perimeter of the fiber cross section

L = fiber length

R.B.A. = relative bonded area of the sheet

The term b is a function of the sheet structure (formation and fiber orientation) and the fiber properties (fiber length (L) and perimeter of the fiber cross section (P)). When the type of pulp and papermaking conditions such as beating, pressing, and drying are the same for both of unfilled and filled papers, the functionality of b term affecting the sheet structure and fiber properties for filled papers (untreated clay or composite filled) can be assumed to be the same with unfilled papers. Therefore, the equation is can be written in a form as [186]

$$\frac{1}{T} = \frac{9}{8Z} + \frac{C}{b \cdot (R.B.A.)}$$

Equation 26: Simplified Page equation

where

C = collection of constants of fiber characteristics for a given pulp.

Beazley *et al.* modified the Page Equation for tensile strength to account for filler effects, herein called BDT theory [186]. If fillers are added, they reduces sheet strength in direct proportional to the surface area of it added. Therefore, they suggested the surface areas of filler and fiber available would be Equation 27 and 28, respectively.

$$\frac{kxS_c}{kxS_c + (1-x)S_f}$$

Equation 27: Available surface area of filler

$$\frac{(1-x)S_f}{kxS_c + (1-x)S_f}$$

Equation 28: Available surface area of fiber

where

S_c = specific surface area of filler

S_f = specific surface area of fiber

x = mass fraction of filler in paper

k = fraction of the filler available to interfere fiber to fiber bonding which will not be greater than 0.5 (with lightly filler papers $k \sim 0.5$ whereas with highly filled papers, where filler/filler contacts can occur, $k < 0.5$)

They proposed that the total RBA available for bonding will not be reduced since geometrically, fibers are still cross in the same way as they would with no filler presents and the RBA is apportioned between free fiber area and filler coated area able to interfere with fiber to fiber bonds, according to the relative surface area fractions of Equation 27 and 28.

Shear bond strength per unit bonded area (b) can be replaced with the sum of specific bond strength between available surface areas of filler and fibers and that between available surface areas of free fibers and fibers, which is combined with Equation 27 and 28 and substituting in Equation 26:

$$\frac{1}{T} = A + \frac{C}{\left(\frac{kb_c x S_c}{kx S_c + (1-x) S_f} + \frac{b_f (1-x) S_f}{kx S_c + (1-x) S_f} \right) (RBA)}$$

Equation 29: BDT equation

where

A = fiber strength term from the Page Equation

C = collection of the constants for a given pulp

b_c = filler/fiber specific shear bond strength per unit area

b_f = fiber/fiber specific shear bond strength per unit area

A linear relationship was found in BDT's study when the tensile strength term, was plotted against the filler specific surface area (S_c). In order to conduct the modeling

analysis using Equation 29, they assumed the specific bond strength between a filler particle and a wood fiber, b_c , is zero for unmodified inorganic fillers. Under this assumption, the effect of filler on the paper tensile strength depends solely on the filler particle size and the content of fillers in a paper sheet. Their experimental results agreed well with the modeling analysis, which indicates the small filler particles have greater effect on paper tensile strength than large filler particles or preflocculated filler aggregates [186]. Although BTD's results are important for predicting the tensile strength of a paper sheet in the presence of unmodified inorganic fillers, the validity of Equation 29 for the fillers that have strong bonding ability with wood fibers has not been known.

Because increasing the filler-fiber bonding is one of the practical solutions for improving strength of high filler contained papers, variety of polymer-modified fillers has been developed [181, 145, 182, 110]. In this study, clay was modified by starch using an ammonium sulfate precipitation method reported previously [145], and the filler-fiber specific bond strength, b_c , was directly measured using a well defined method developed in this study. The validity of BDT's equation for analyzing paper strength was tested for the papers with polymer-modified fillers.

The fiber-fiber specific bond strength, b_f , has been a subject of various theories and experimental investigations, as revealed by a great number of publications [187, 31, 177, 188, 27, 178, 28]. It has been reported that the fiber types or characteristics can affect fiber-fiber bonding. For example, single fiber crossing bond strength tests indicated that the fiber-fiber bonding ability of summerwood or springwood fibers is significantly different [177, 188, 27]. Also papermaking conditions such as refining, wet pressing and

drying conditions can affect the fiber-fiber bonding significantly [187]. Comparing to the fiber-fiber specific bond strength, b_f , only a few of studies about the fiber-filler specific bond strength, b_c , were done due to the difficulty in measuring the microscopic scale force between individual filler and fiber.

In real papermaking conditions, dry strength aids are often used to compensate for the loss of paper strength due to filler loading. Even though it has been reported from early years that bonding agents such as gum or starch can increase the bond strength between fibers [179], it has not been clearly shown how dry strength aids can affect the bond strength between the fibers or fibers and fillers. Recently, Xu *et al.* measured the delamination forces for two ply laminates where precipitated calcium carbonate (PCC) was in the ply-ply interface [189, 190].

In order to model paper strength in the presence of polymer modified fillers, variables such as the specific bond strengths of fiber-fiber and fiber-filler, the surface areas of filler and fiber were directly measured in this study. The experimental data was then used for theoretical study. Both modeling and experimental results are reported.

7.3 Experimental

7.3.1 Materials

Kaolin clay was provided by Dry Branch, Inc. and raw corn starch (B200) was provided by Grain Process Inc., respectively. Ammonium sulfate (reagent grade, $\geq 99.0\%$) was obtained from Aldrich. Bleached kraft hardwood and softwood pulps were refined in a Valley beater to a freeness of 400 CSF, respectively. Equal proportions of the two pulps were mixed, which was used as the base pulp furnish for the handsheets.

Percol-175 (medium-charge density, high molecular weight cationic poly-acrylamide retention aid) was obtained from Ciba Specialty Chemicals that was used only for retention of untreated clay. No retention aid was added if the clay-starch composites were used as the filler because of their relative large particle size and very high mechanical retention in the handsheets.

7.3.2 Preparation of clay-starch composites

The detailed preparation method was explained in our previous report [145]. Required dry clay was directly added to a 3% starch solution and the mixture was stirred until a good dispersion was obtained. The ratios of clay to starch were 1:1, 1:0.5, and 1:0.25, respectively. These clay-starch mixtures (10-15% total solid content) were cooked at 95°C for 30 minutes. Cooked clay-starch solutions were poured into a 40% ammonium sulfate solution being stirred at 500rpm. After 1 minute of stirring, the starch-clay composites were precipitated out. The resulting composites were collected on a filter paper, washed free of salt, and recollected. The final clay-starch composites were re-dispersed in water by mechanical stirring before making handsheets. The remaining ammonium sulfate solution, after filtration, can be reused by adding additional ammonium sulfate.

7.3.3 Handsheet preparation and determination of paper physical properties

The pulp was diluted to 0.5 wt% and various amounts of composites were used for handsheet making. After the addition of the composites, the slurry was stirred for 20s at

700rpm. The handsheets with a target basis weight of 60g/m² were produced according to TAPPI Test Method T 205 “Forming Handsheets for Physical Tests of Pulp”. No retention aid was used during the handsheet preparation when the composites were used as fillers. For comparison, the control handsheets were prepared using untreated clay and a cationic retention aid (Percol-175, 0.05-0.1wt% based on solid fiber weight). After wet pressing twice, all handsheets were dried at 105°C. Physical properties of the paper were measured according to standard TAPPI methods. The filler content was determined by ashing the paper in a muffler oven according to standard Tappi method T211.

7.3.4 Specific bonding strength measurement

Bond strength is defined as the average force to break a bond per unit area of a sample. Specific bond strength is defined as the force to break a bond per unit of optical surface area created by broken bonds. For a paper, the change in optical-contact area as a result of bond breakage has been calculated on the basis of the Kubelka Munk definition. However, this Kubelka Munk approach cannot be applied for our experiment because the light scattering coefficients of filler with fiber or starch are different so that optical contact area cannot be calculated.

In order to measure the specific shear bond strength between fiber and filler, the suspension of starch-coated filler was first vacuum filtered onto a membrane (Isopore™ polycarbonate membrane with an average pore size of 0.4µm), and then a thin filler disk was formed. The size of the filler disk is about 2 x 2cm and the thickness is about 1mm. This filler disk was carefully transferred onto the wet wood fine sheet (softwood :

hardwood = 1:1) made by gathering fines from the highly refined pulp and filtering using the same vacuum membrane filtration method. Then the plastic ethylene film with the 2 x 2mm square hole in the center was placed on the top of the filler disk and another wet wood fine sheet was laid above the film. The actual bonding area between fillers and fibers was fixed to be 2 x 2mm through the film hole. After conditioning at 20°C and RH 60%, both sides of a sample were fixed at the clamps in the Instron tensile tester. The tensile speed for the bond strength was set to the same as that for the handset testing. The procedure is schematically shown in Figure 76.

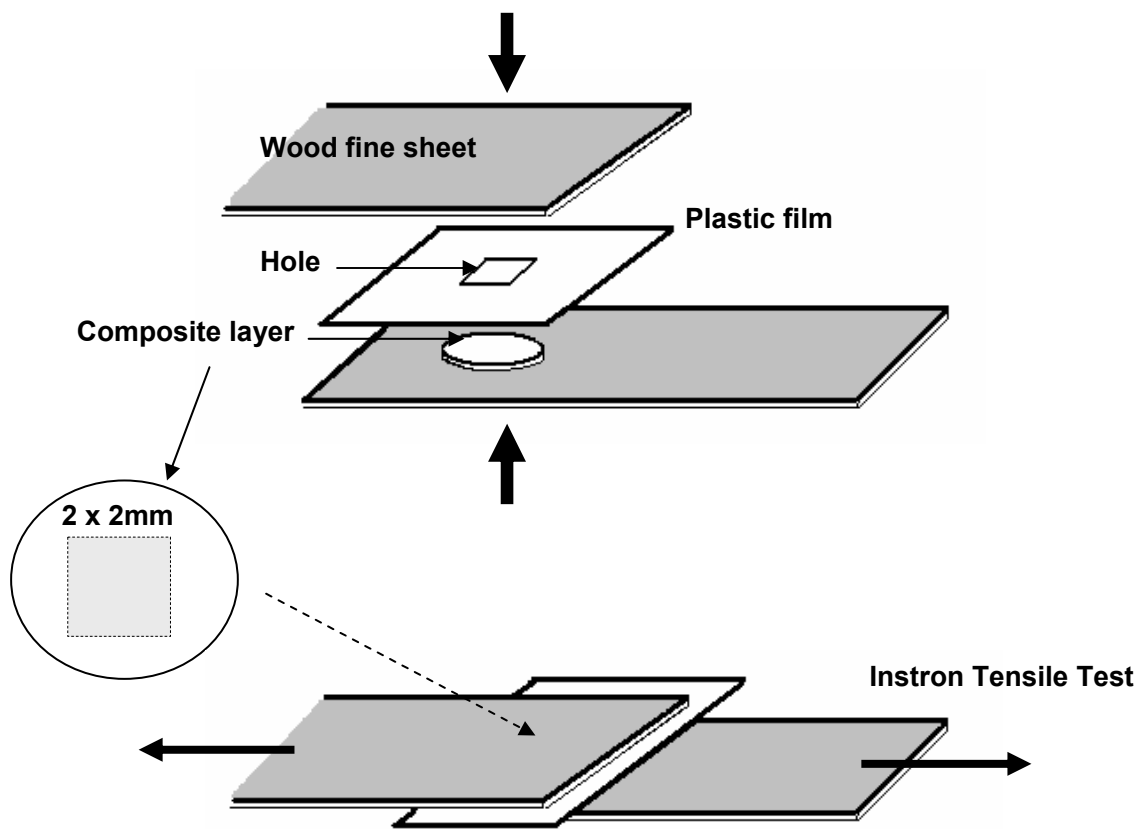


Figure 76: Schematic drawing of sample assembly and the tensile strength test

For measuring the specific shear bond strength between fibers, the handsheets (basis weight 60g/m²) made by TAPPI standard method were put on a plastic film with the same size of hole on the wet handsheet. On top of the film, the other wet handsheet was laid carefully.

Two laminated sheets as shown in Figure 76 were pressed under 90psi at 105 °C for 10 minutes using a simultaneous pressing and heating machine (PID, National Instrument). After conditioning at 20°C and relative humidity of 60%, the specific shear bond strength of the laminated sheet was tested by an Instron tensile tester. We assumed that the fillers and fibers are completely in contact because the size of wood fibers was reduced by gathering only wood fines through filtration (200mesh) to increase the bonding sites with composite fillers and pressed and dried at high temperature to allow enough bonds between fibers and composite fillers.

7.3.5 Determination of Specific Surface Area for Tensile Strength Modeling

The specific surface area of pulp, clay, and modified clay were determined by the adsorption isotherms of N₂ at 77 K by using a Flowsorb II 2300 BET surface area analyzer. Because the starch-filler composites may form dense aggregates during drying resulting in a different surface area in BET measurement, the composite particles were freeze dried overnight to hold the original size and shape after drying. The samples were degassed at 150°C for more than 20 min immediately prior to the adsorption measurements.

7.3.6 Tensile strength modeling

Skowronski and Bichard proposed that the delamination force of laminated sheets is proportional to the specific bond strength, b , and the relative bonded area, RBA[28]. Also it was found that the delamination force is linearly proportional to the internal bond strength, such as Z -direction tensile strength, ZDT , of the paper [191]. Therefore, it is reasonable to assume that ZDT has a linear relation with the bond area RBA and specific bond strength per unit area, b , in Equation 25 as shown by the following equation:

$$\frac{1}{T} = \frac{9}{8Z} + \frac{C}{b \times RBA} = \frac{9}{8Z} + \frac{D}{ZDT}$$

Equation 30: Modified Page equation

where C and D are constants.

The RBA in equation 30 is included in constant D because it is constant for clay-starch composites filled sheets. Beazley *et al.* [186] assumed that the relative bonded area, RBA, is the total bond area that includes filler-fiber and fiber-fiber and the RBA does not decrease by the filler addition because fibers still cross in the same way as they would with no filler presents as shown in Figure 77 (top). However, untreated fillers are incompressible and provide air gaps between the fibers, allowing them not to form a bond. Therefore, RBA will be decreased additionally because voids also reduce the fiber-fiber bonding area. However, for composite fillers, RBA can be assumed to be the same with

absence of fillers if handsheet making conditions and drying condition are the same, because starches coated exclusively on the filler surface are compressible and thermo-plasticized during the drying so that composite fillers are compactly bonded with wood fibers and remove air gaps as shown in Figure 77.

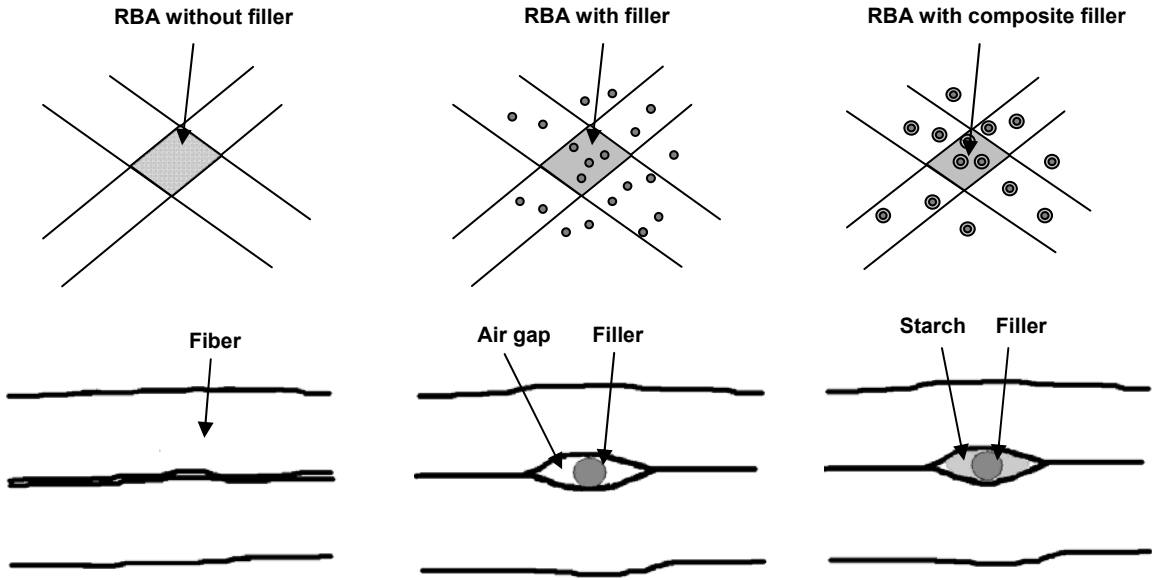


Figure 77: The relative bond area, RBA, between two fibers in the absence (left) and presence of filler (middle) or composite particles (right)

$$ZDT \propto b \cdot R.B.A. = \left(\frac{kb_c x S_c}{kx S_c + (1-x) S_f} + \frac{b_f (1-x) S_f}{kx S_c + (1-x) S_f} \right) \cdot R.B.A.$$

Equation 31: Linear relationship between ZDT and specific bond strength multiplied by RBA

Therefore, Equation 31 can be used to calculate the dimensionless force, $ZTD_{(\text{dimensionless})}$ [192]:

$$ZTD_{(\text{dimensionless})} = \frac{ZDT}{ZDT_{x=0}} = \left(\frac{k\zeta x\Delta}{kx\Delta + (1-x)} + \frac{(1-x)}{kx\Delta + (1-x)} \right)$$

Equation 32: Dimensionless ZDT

where $\zeta = b_c/b_f$ and $\Delta = S_c/S$

Equation 32 can be rewritten as

$$ZDT = ZDT_{x=0} \times \left[\frac{k\zeta x\Delta}{kx\Delta + (1-x)} + \frac{(1-x)}{kx\Delta + (1-x)} \right]$$

Equation 33: Calculation of ZDT

Therefore, Equation 25 could be rewritten after combining from Equation 30 to 33 as follows:

$$\frac{1}{T} = \frac{9}{8Z} + \frac{E}{ZDT_{x=0} \times \left(\frac{k\zeta x\Delta}{kx\Delta + (1-x)} + \frac{(1-x)}{kx\Delta + (1-x)} \right)}$$

Equation 34: Calculation of tensile strenght

where E is a constant.

The constant E can be calculated using Equation 30 because the T (tensile strength, measurable), Z (zero span tensile strength (expressed zero span as breaking

length) can be measured by TAPPI test method T231 cm-96), and ZDT (Z-Direction tensile strength) in the absence of filler.

Because now all parameters on the right side of Equation 34 are measurable, the tensile strength as a function of ZDT for the handsheets made with different fillers could be modeled. It should be nothing that the bond strength is the function of sheet structure and the fiber properties so that if different pulps or different conditions such as beating, pressing, drying are used, the derivation of Equation 34 from 25 for modeling study might not be a reasonable approach. Therefore, pulps and papermaking conditions should be kept the same for unfilled, clay filled, and composite filled sheets.

7.3.7 Stiffness Modeling from Modeled Tensile strength

Not only the tensile strength but also the stiffness could be modeled for filler containing papers. The bending stiffness relates to modulus of elasticity and thickness of a uniform sample of any material via the following formula [193]:

$$S = \frac{EI}{b} = \frac{Eh^3}{12} = A_0 h^3 \frac{\delta}{\varepsilon}$$

Equation 35: Bending stiffness

Where S : stiffness, E : modulus of elasticity, I : the momentum of inertia of the sample, h : thickness of the sample, A_0 is a constant, and b : the width of the sample. δ and ε are the stress and strain, respectively. It is known that the tensile strength of paper (T) is proportional to the elastic modulus of paper (E) and the elastic breaking strain of fibers

(ε_f), $T = E * \varepsilon_f$.³⁴ In this study, because the fibers used for all papers are the same, ε_f will be similar in all papers. Therefore, tensile strength of the paper can represent the modulus of the paper. In Equation 35, the modulus of elasticity was replaced with the maximum tensile stress (which is tensile strength) and strain relationship at breakage. It is interesting to note that all the samples tested in this study have a similar strain at failure ε' (the difference is <2% with a standard deviation of 0.19). Therefore, it is reasonable to assume ε' is a constant for all samples prepared in this study. With this approximation, Equation 11 can be written as:

$$S = \frac{EI}{b} = \frac{Eh^3}{12} A_0 h^3 \frac{\delta}{\varepsilon} \cong B_0 \frac{\delta'}{\varepsilon'} h^3 \cong C_0 \delta' h^3$$

Equation 36: Modified form of bending stiffness

where, A_0 , B_0 , and C_0 are constants, δ' is the maximum stress at breakage (Nm/g), ε' is the strain at failure. Equation 36 suggests that the stiffness S has a linear relationship with the stress at failure, or the tensile strength.

Among the bending stiffness test methods developed, Gurley and Taber stiffness are the most common for papermaking, and in many respects, Gurley method measures the same property as the Taber method [194]. In this study, the Gurley stiffness was measured (TAPPI test method T 543 pm-84) for modeling study.

7.4 Results and Discussion

7.4.1 Specific bond strength of starch-clay composites with wood fibers and their specific surface area

Figure 78 shows the dimensionless ZDT calculated using Equation 32 as a function of filler fraction in the handsheets with different ratios of filler-fiber specific bond strength ($\zeta = b_c/b_f$) and specific surface area ($\Delta = S_c/S_f$). When ζ is 0 or 0.1, which means the specific bond strength between filler and fiber does not exist or is very small, the dimensionless bond strength decreases as the filler ratio increases. These low values of ζ are typical for the papers made from unmodified inorganic fillers and were illustrated by Li *et al.* [192] using a similar approach. However, when $\zeta = 1$, the specific bond strength of filler to fiber (b_c) equals to that of fiber to fiber (b_f), and the dimensionless bond strength remains constant even as the filler content increases. This case might be applied to lumen loading or fine-filler mixtures [190]. Moreover, if ζ is bigger than 1, when filler-fiber specific bond strength is higher than fiber-fiber strength such as some polymeric filler or starch modified filler are used in paper, the dimensionless bond strength increases as the filler loading increases because the filler could act as a bonding enhancing agent if $b_c > b_f$. If the fillers are preflocculated before adding to the pulp slurry, the ratio of specific surface area of filler to fiber ($\Delta = S_c/S_f$) decreases resulting in an increase in the dimensionless bond strength although the bond strength between filler and fiber ($\zeta = b_c/b_f$) does not change.

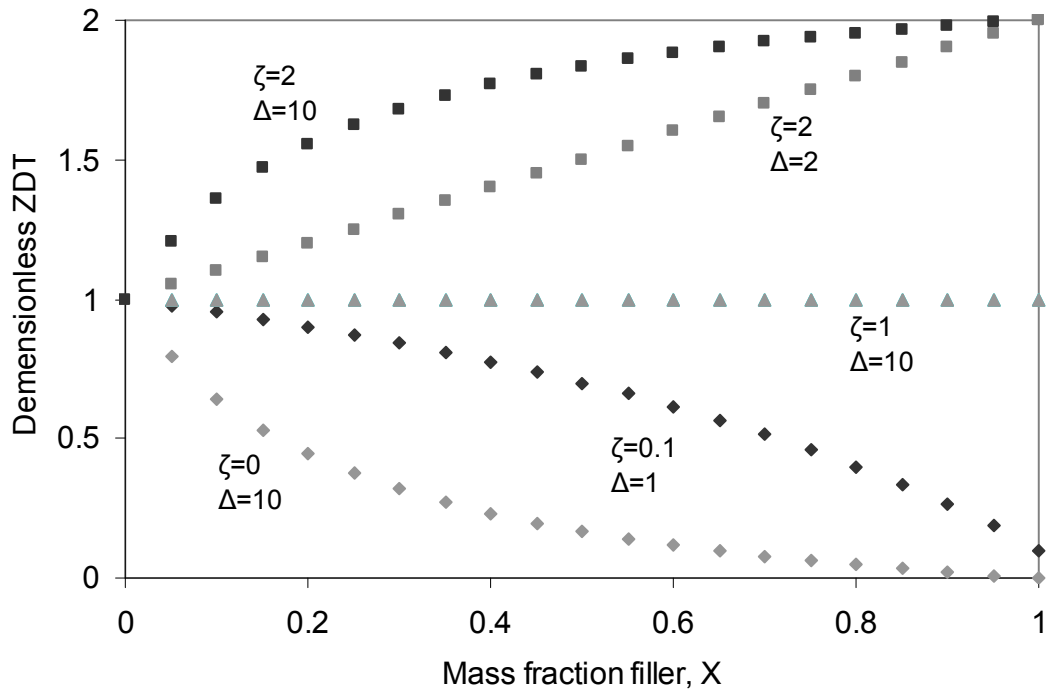


Figure 78: Calculated dimensionless ZDT as a function of filler mass fraction. Curves were calculated from Equation 32 where $\zeta = b_c / b_f$, $\Delta = S_c / S_f$ and $k=0.5$

In order to verify the theoretical calculation results, the actual specific bond strength was determined by the method shown in Figure 78. However, when the two handsheets are laminated and starch-clay composites (with a ratio of starch to clay of 0.5 to 1) were in between, the breakage always occurred between fiber-fiber rather than fiber-filler. This means that the specific bond strength between starch-clay composite and fiber is stronger than fiber-fiber bonding. Nanko [195] proposed that as a higher dosage of bonding agents, such as starch or CPAM, is treated on the fiber surfaces, the position of bond breakage shifts from fiber surfaces to the inside of the S1 layer and to the interface between the S1 and S2 interface. For these cases, it is impossible to directly measure the

specific bond strength between starch-coated fillers and wood fiber using the method proposed in Figure 78. To solve this problem, we prepared stronger sheets using wood fines, which were vacuum-filtered on a membrane filter and wet-pressed under pressure of 70psi. By using these “wood-fines papers”, the specific bond strength between filler composite film and cellulose substrate could be measured. As shown in Table 1, the specific bond strength between filler and fine was increased from 0 to $11.2 \text{ N/m}^2 \times 10^6$ as the starch ratio increased from 0 to 1.

It is well known that filler type can affect paper strength and structural properties, and the size of the filler is one of the most important factors affecting those properties. Moreover, if fillers are coated or treated with some bonding materials, the size of the filler would be changed and it becomes a critical matter affecting the paper’s properties. As shown in Figure 78, when the specific bond strength between the filler and wood fiber is identical (for example, $\zeta = 1$), the surface area can remarkably affect the internal bonding strength of the paper.

7.4.2 ZDT modeling of starch-clay composite filled handsheets

Table 7: Specific surface area of starch-clay composites and their specific shear bond strength with wood fibers

starch/clay ratio	0	0.25	0.5	1	Wood fiber (CSF 400ml)
Specific Surface Area, m^2/g	16.7	15.5	15.2	13.9	1.5
S_c/S_f	11	10.3	10.1	9.2	-
Max. Load, $\text{N/m}^2 \times 10^6$	0	4.8	7.6	11.2	5.2
b_c/b_f	0	0.9	1.4	2.1	-

After we plug the variables ζ and Δ from Table 7 into Equation 32, the ZDT values were calculated and compared with the experimental results. As shown in Figure 79, the experimental results matched very well with the calculated ZDT of the handsheet. As expected, when the specific bond strength between fillers and fibers (b_c) is bigger than interfiber bonding (b_f), ZDT was increased as the composite filler dosage was increased. Figure 79 also indicates that the model can be used for both untreated and modified clays.

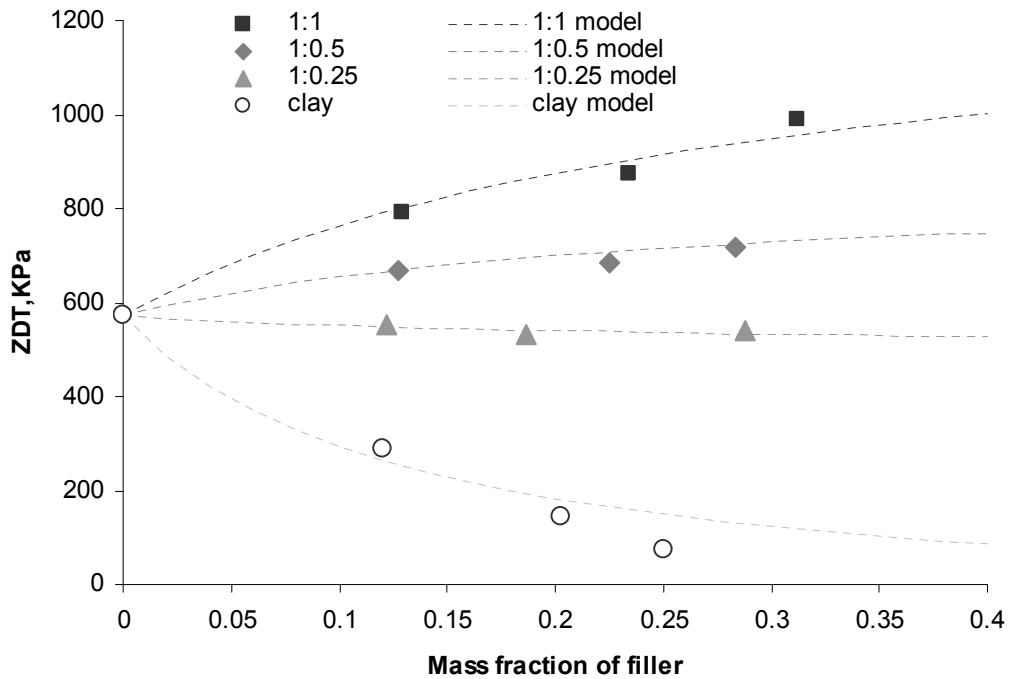


Figure 79: Calculation of ZDT based on BTD theory and comparison with tested results

7.4.3 Tensile strength modeling

For tensile strength (expressed as breaking length) modeling, one of the variables shown in Equation 34 is the zero-span tensile strength (expressed as zero-span breaking

length), Z , which can be experimentally measured using TAPPI standard method. Figure 80 shows that as the filler amount increases, the zero-span tensile strength decreases because the fraction of long fiber in the handsheet decreases.

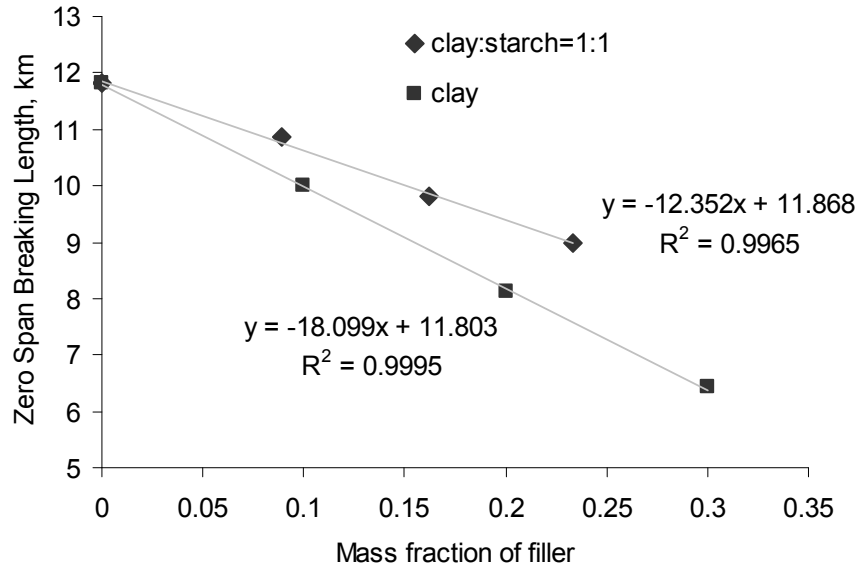


Figure 80: Zero span beaking length as a function of filler content in paper

The constant E in Equation 34 could be calculated if the zero span tensile strength Z , tensile strength T , and ZDT values are known. In this study, these three parameters were directly measured. For a filler-free sheet, the constant E in Equation 34 was calculated to be 21.5 kPa. Therefore, Equation 34 can be rewritten as

$$\frac{1}{T'} = \frac{9}{8(-18.1x + 11.803)} + \frac{21.5}{ZDT_{x=0} \times \left(\frac{k\zeta x\Delta}{kx\Delta + (1-x)} + \frac{(1-x)}{kx\Delta + (1-x)} \right)}$$

Equation 37: Tensile strength calculation

As shown in Figure 81, both experimental and calculated results indicate that the tensile strength increases as the starch amount increases. It is interesting to note from Table 7 that although the specific bond strength of filler-fibers (b_c) is double that of fiber-fiber (b_f), Figure 81 indicates that the tensile strength gradually decrease as the starch-clay composite dosage increases. The reason for this difference is because of the decrease of zero span tensile strength in the sheet as shown in Figure 80.

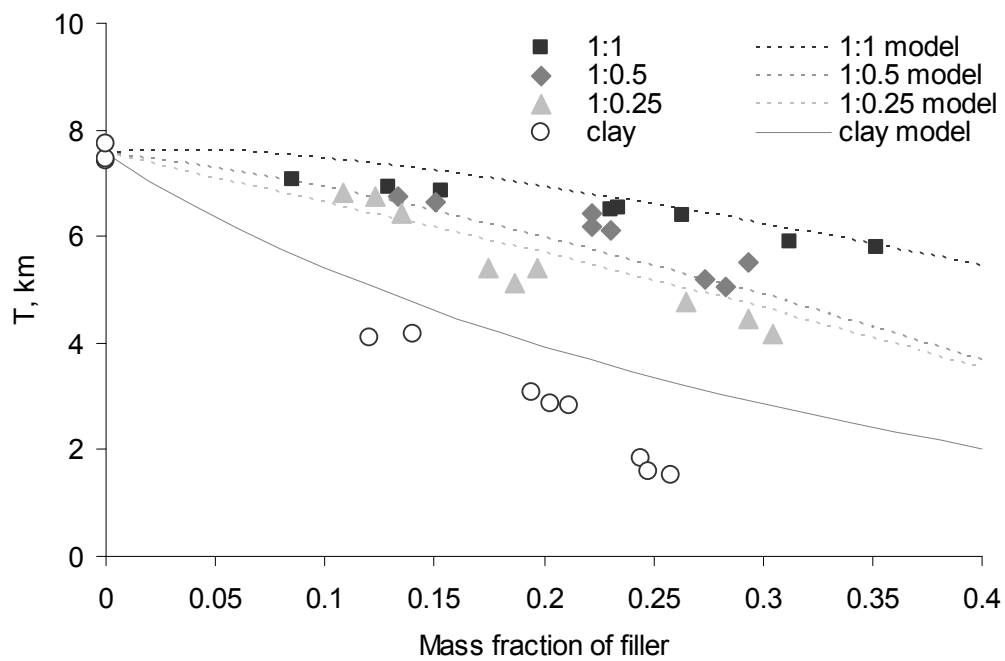


Figure 81: Experimental data (points) and modeling results (lines) of tensile strength as a function of filler dosage for different starch to filler ratios

It was noted from Figure 81 that for the papers filled with starch modified fillers, the calculated curves match with the experimental data very well. However, if pure clay was used as the filler, the calculated tensile strength is higher than experimental results.

One important reason for this difference is that a cationic polymeric retention aid (Percol 175) was used for improving the retention of pure clay on the paper sheets, but no retention aid was used for starch modified fillers because the relatively large size of modified fillers could be easily retained to fiber webs. It is well known that retention aid may cause fiber flocculation resulting in the reduction of paper formation. For the tensile model developed here, there is no consideration for the loss of strength due to fiber flocculation. Thereby a more sophisticated theory which includes the effects of fiber flocculation and sheet formation needs to be developed in the future.

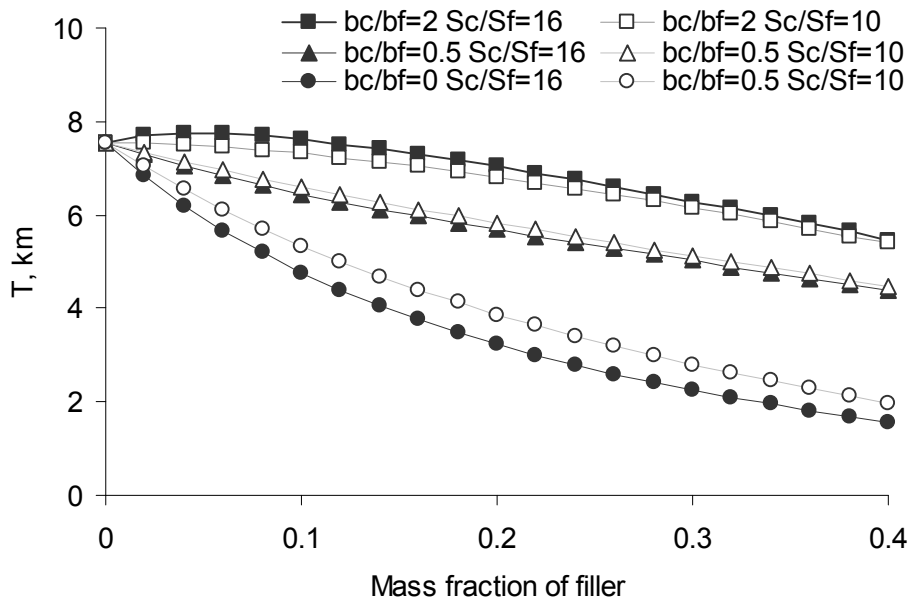


Figure 82: Calculated tensile strengths for different specific bond strength with different surface areas

According to Table 7, as the starch to clay ratio increased, the specific surface area decreased. This may raise doubts whether the improvement of tensile strength for higher starch ratios of fillers is from the increased bond strength or from the reduced surface area. Figure 82 shows the calculated tensile strengths for different specific bond strengths with different surface areas. For the fillers with high specific bond strength ($b_c/b_f=2$), the change of surface area does not affect the tensile strength much. In contrast, the bond strength is thought to be a dominant factor for the tensile strength of paper loaded with modified fillers. It is worth mentioning is that for bonding enhancing fillers ($b_c > b_f$), the tensile strength increases as the surface area increases. However, for pure clay filler, the tensile strength decreases as the surface area increases as shown in Figure 5.

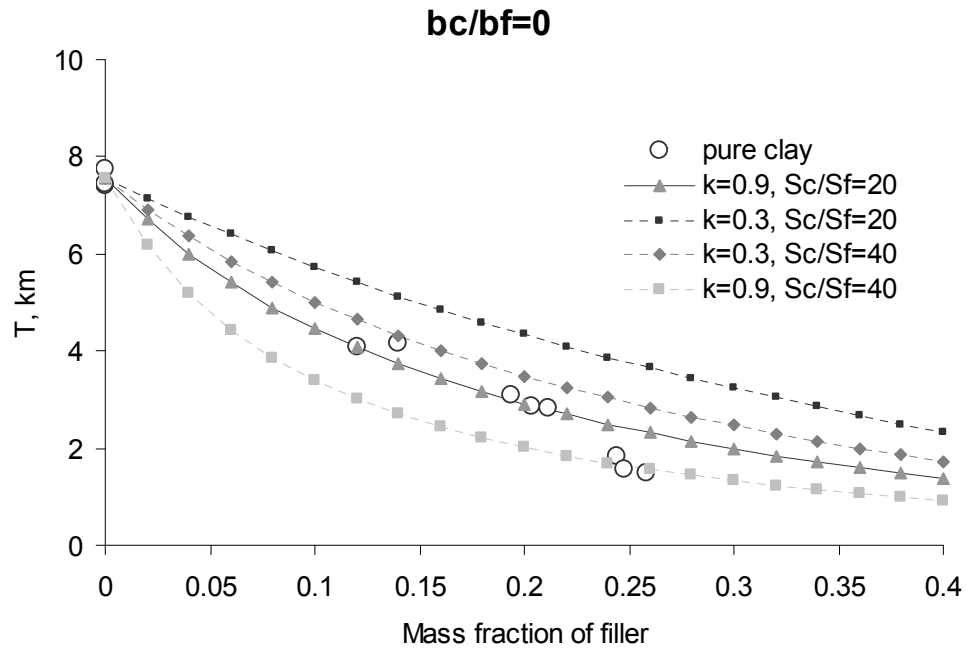


Figure 83: Theoretical tensile strength changes for different k and S_c/S_f values

The k value in Equation 34 represents the filler fraction between two contacted fibers, which strongly depends on the filler distribution in the sheets. If filler particles are located inside of contacted fibers, k increases. However, if fillers are located in the voids in a sheet, they have no contribution to k value. As shown in Figure 83, for pure fillers with b_c/b_f equaling to zero (no bonding between fillers and fibers), the tensile strength decreases as the k value changes from 0.3 to 0.9.

7.4.4 Stiffness Modeling

The stiffness of the paper sheets was modeled in Figure 84 using Equation 36. The best fitting constant, C_0 , was found to be 1.803×10^{10} (the unit is the reciprocal of Gurley stiffness), which was calculated by known tensile index and thickness of paper when the filler content was zero. As the composite filler content changes, the thickness of paper also changes. Clay-starch composites are denser materials than wood fibers so that it is evident that the thickness of composites filled sheet was lower than unfilled. It is worth noting that the higher starch ratio of composites, the less thickness was achieved as shown in Figure 85, which is the other evidence showing starch-clay composites strongly pull the fibers together. However, for untreated clay, the thickness of paper slightly increases as the clay content increases. This tendency might be explained that untreated fillers act as de-bonders preventing the consolidation of the sheet. One more possible reason will be the flocculation of fiber and clay due to the bridging mechanism of cationic polymer so that local mass distribution is not even.

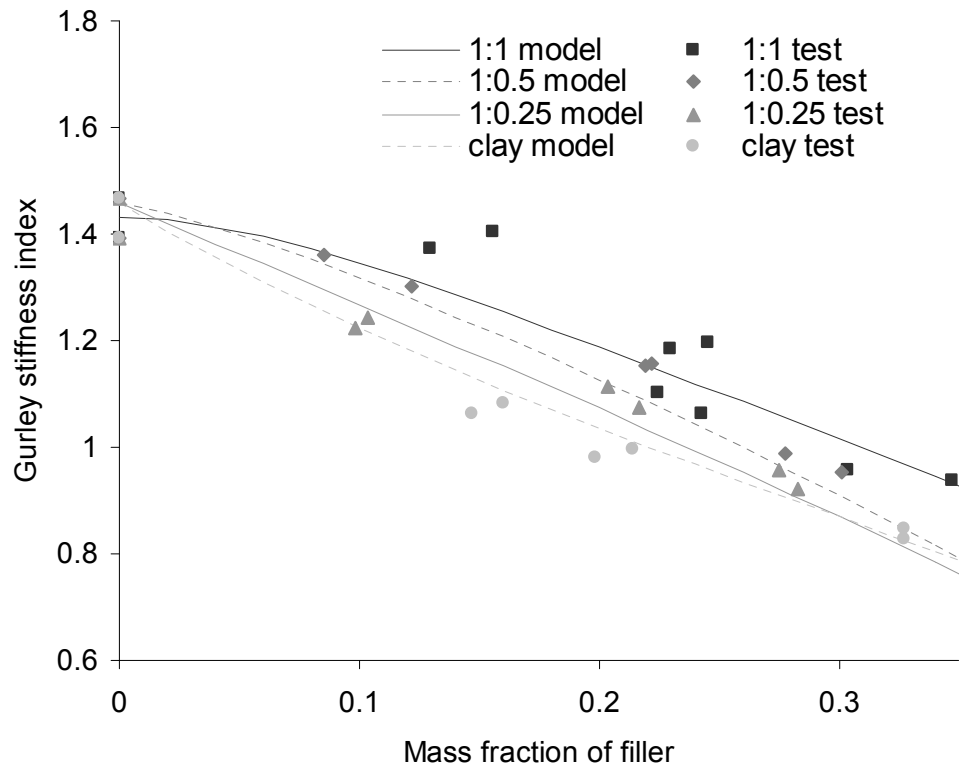


Figure 84 : Stiffness modeling for different starch to filler ratios as a function of filler dosage

The model stiffness was plotted by calculated tensile strength and thickness using Equation 36. The results indicate that the stiffness decreases as the filler amount increases for all cases including starch modified fillers. It is well known that the paper stiffness is a function of both the paper thickness (bulk) and internal bonding. The increased bonded area and specific bond strength of fillers (b_c) due to the starch coated on the fillers result in a decrease in thickness as shown in Figure 85 because the fibers will be closer to each other. Therefore, as the most dominant factor of thickness was decreased, the stiffness was decreased.

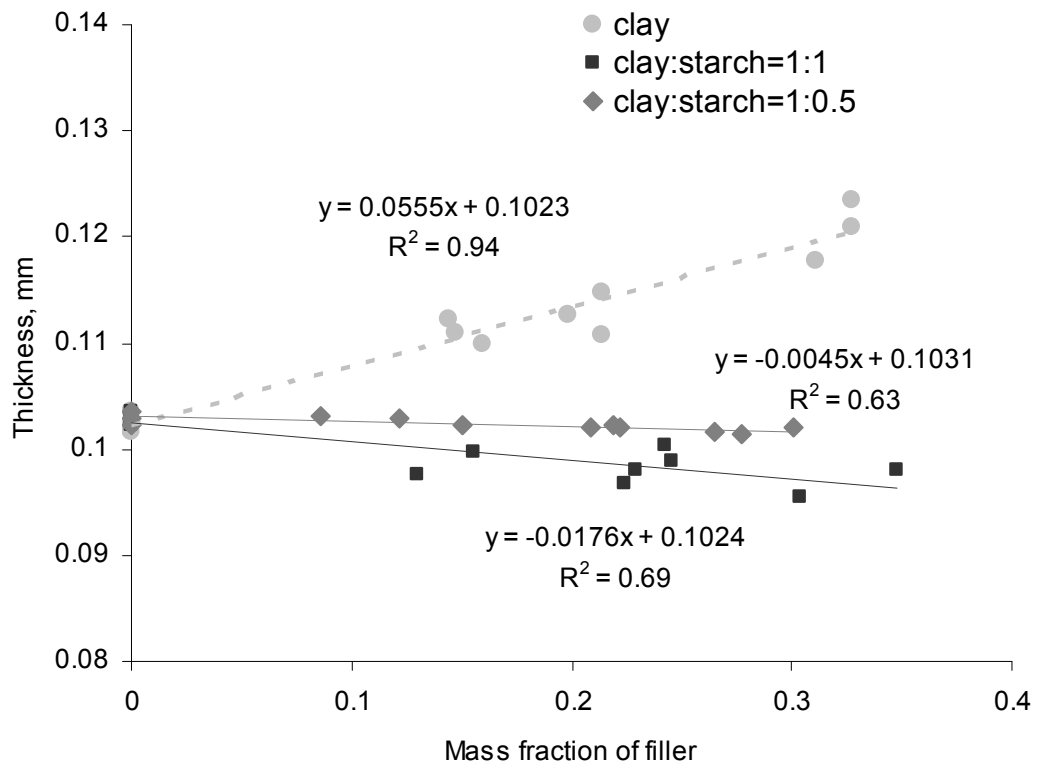


Figure 85: The change of thickness as a function of clay and composite dosage

This is further confirmed by plotting the stiffness as a function of the bond strength with a constant thickness. As shown in Figure 86, the stiffness will increase with the bond strength between fibers and fillers if the bulk remains constant.

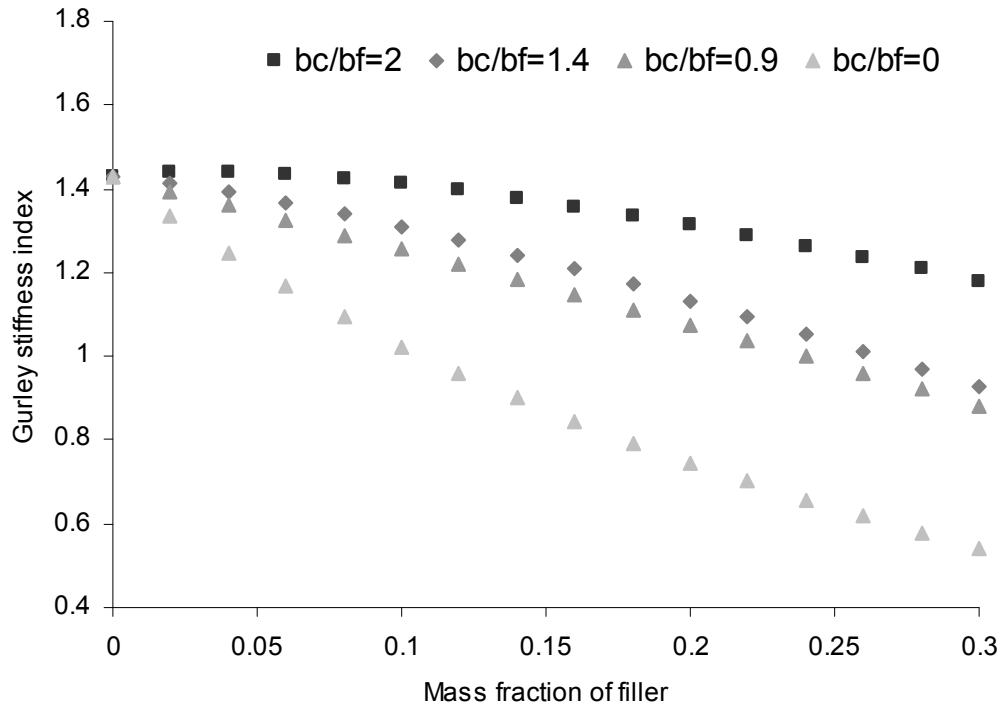


Figure 86: Effect of specific bond strength on stiffness assuming thickness is constant

7.5 CONCLUSIONS

1. This study provided a prediction method to study the tensile strength for filled paper with different filler-fiber bonding characteristics. This method in conjunction with Page's tensile strength equation and BDT theory allows one to calculate the paper tensile strength from the knowledge of specific bond strength between filler and fiber as well as filler surface area.
2. It was determined that as the starch amount on modified filler increased, the specific bond strength between the wood fiber and filler increased. It was also found that the

contribution in the strength improvement by increasing the specific bond strength between filler-fiber is more important than increasing the size of the filler aggregates.

3. The stiffness of paper was modeled using the calculated tensile strength. Even though the thickness of the paper decreases as the starch amount increases, the stiffness of paper filled with starch-clay composite is higher than that with untreated filled papers. The main reason is thought to be the increase in bond strength between fillers and fibers, which was confirmed by the stiffness modeling.

CHAPTER 8

OVERALL CONCLUSION

This dissertation reviewed the fundamental information to understand the characteristics of fibers and fillers to improve the properties of filled paper. To provide the suitable method to recover the reduction of the paper properties by filler which relates to its ability to interfere with the fiber bonding, coating the bonding materials on the filler surface was taken into consideration.

The first study involved the starch precipitation in salt solution. The clay-starch composite such prepared was used as the papermaking filler in this study. From the physical property measurements, clay-starch composites could increase the internal bonding strength (ZDT) dramatically, thereby tensile, burst, and folding strength were improved up to more than 100% at 20-30% doses compared to untreated pure clay. However, the optical properties were slightly lower than untreated clay due to the relatively large composite size. The method included many steps of mixing, cooking, precipitation, filtration, and washing, thus more simplified process is preferable.

The second study provided a method of clay-starch composite preparation by starch-fatty acid complexation. This method could also increase the internal bond strength significantly, and the tensile strength was improved up to more than 100~200% at 15% composite addition compared to untreated clay. The optical properties increased as the composite amount in sheets increased. Additionally, handsheets filled with clay-starch composites improved the water-repellant property due to the hydrophobicity of the fatty acids. The starch-fatty acid complex method in this study which is much simpler

process than the precipitation method and has more advantages for paper grades that need high filler loading, high physical strength with certain sizing requirements.

The other type of bonding material, cellulose, was considered and the cellulose-clay composite by NMMO dissolution was provided. Even though there are advantages of using low grade of cellulose materials such as UKP, BKP, and DINP, and the composites could make an improvement on the physical properties, the optical properties of composite filled sheets were less than those with unmodified.

Lastly, the tensile strength for filled paper with different filler-fiber bonding characteristics was predicted by the BDT theory and the mechanism of the improvement of composite filled sheets was studied. The main driving force to increase the paper strength was found to be the increase of the specific bond strength between the wood fiber and filler rather than the increased size of the filler aggregates. The predicted and experimented results of the tensile strength and stiffness matched well.

CHAPTER 9

FUTURE WORK

This thesis includes many areas such as wet-end chemistry, paper physics, carbohydrate chemistry to expand on and explore for future research work. Therefore, this thesis provides a good starting platform in terms of scientific work or application research. Below is a listing of possible future work.

Wet-end chemistry area

- Comparison of filler retention with conventional retention system
- Relationship between composite size and drainage or retention
- Charge characteristics of composite fillers depending on pH
- Effect of shear force on particle size and reaggregation
- Effect of the amount of different fatty acids on the AKD or rosin sizing

Paper physics area

- Microscopic shear bond strength measurement between composite fillers and fibers
- Comparison of specific bond strength designed here with other methods
- Effect of different degrees of refining on the strength of paper using composite fillers
- Effect of drying temperature on the composite filled paper
- Zero span tensile strength improvement by the composite filler method

Carbohydrate chemistry area

- Effect of molecular weight or crystallinity of cellulose or starch on the bond strength
- Different cellulose-clay composites using dissolution such as NaOH/Urea, or Phosphoric acid
- Effect of the chain length of fatty acid on complexation or solubility

APPENDIX A: COPYRIGHT PERMISSIONS

Permission from TAPPI Journal

Hello Se-Young Yoon,

I do apologize for the delay in response. But after speaking to the right person I found out that the copyright assignment form you completed was giving TAPPI the right to print your article. You actually own the rights to your paper.

If you have any other questions do not hesitate to ask.

Thank you,

Denine Phelps
TAPPI
15 Technology Parkway South
Norcross, GA 30092
Tel. 770-209-7283

From: Se-Young Yoon [mailto:Se-Young.Yoon@ipst.gatech.edu]
Sent: Thursday, March 15, 2007 4:54 PM
To: Simona Marcellus; Denine Phelps
Subject: Copyright permission

Dear Editor of TAPPI JOURNAL or to whom it may concern:

As I and my advisor (Dr. Yulin Deng) transferred the copyright of the paper we published to TAPPI JOURNAL by signing the copyright assignment form, we would like to ask your official permission to reproduce that paper in the part of my Ph. D thesis.

Following is the publication information;

“Yoon, Se-Young; Deng, Yulin, Starch-Fatty Complex Modified Filler for Papermaking, Tappi, 5 (9): 1(2006)

Thank your for kind cooperation in advance.

Se-Young Yoon

Ph.D. Candidate
Chemical & Biomolecular Engineering
Georgia Institute of Technology
500 10th street NW, Atlanta, GA
Tel: 404-894-7791

Permission from Journal of Applied Polymer Science

Dear Dr. Yoon:

Permission granted. Please provide appropriate reference to the paper in your thesis, including journal title, volume, issue and page numbers.

Thank you.

Jon Glover
Associate Publisher
Physical Sciences Journals
John Wiley & Sons, Inc.
111 River St., MS 8-02
Hoboken, NJ 07030-5774
Tel. 201-748-5721
Fax 201-748-6207
jglover@wiley.com

Wiley Bicentennial: Knowledge for Generations
1807-2007

----- Forwarded by Jon Glover/STM/Hoboken/Wiley on 03/12/2007 10:33 AM -----

Eric Baer <exb6@cwru.edu>

To JGlover@wiley.com

cc

03/12/2007 10:16 AM

Subject Fwd: Copyright permission for Ph.D thesis

Dear Jon:

Please take care of the request below for Dr. Baer.

Thanks,
Mariah

Begin forwarded message:

From: Se-Young Yoon <Se-Young.Yoon@ipst.gatech.edu>
Date: March 10, 2007 9:07:18 PM EST
To: exb6@po.cwru.edu
Subject: Copyright permission for Ph.D thesis

Dear Dr. Eric Baer (Editor of Journal of Applied Polymer Science):

As I and my advisor transferred the copyright of the paper we published to JAPS by signing the copyright assignment form, I would like to ask your official permission to put that paper into the part of my Ph. D thesis.

Following is the publication information;

“Yoon, Se-Young, Deng, Yulin, Clay-Starch Composites and Their Application in Papermaking, Journal of Applied Polymer Science, 100 (2): 1032 (2006)”

Thank your for kind cooperation in advance.

Se-Young Yoon

Ph.D. Candidate
Chemical & Biomolecular Engineering
Georgia Institute of Technology
500 10th street NW, Atlanta, GA
Tel: 404-894-7791
Fax: 404 894 4778

REFERENCES

1. Kouris, M. (1996). "Dictionary of Paper " 5th ed: TAPPI PRESS. Atlanta, GA. p.215.
2. Alen, R. (2000). "Chpater1: Structure and Chemical Composition of Wood." Forest Products Chemistry. Vol. 3: Fapet Oy. Jyvaskyla, Finland.
3. Fengel, D., and Wegener, G. (1983). "Wood- Chemistry, Ultrastructure, Reactions." Walter de Gruyter & Co. Berlin. p6.
4. Scott, W.E. (1996). "Principles of Wet-End Chemistry." TAPPI Press. Atlanta, GA. p.11.
5. Beck, M.W. (1998). "The importance of wet end equipment and its influence on retention." Retention of Fines and Fillers During Papermaking, ed. J.M. Gess: TAPPI PRESS. Atalanta, GA. p.129-158.
6. Fengel, D., and Wegener, G. (1979). "Hydrolysis of Polysaccharides with Trifluoroacetic Acid and Its Application to Rapid Wood and Pulp Analysis." Hydrolysis of Cellulose: Mechanism of Enzymatic and Acid Catalysis ed. J. Brown, R.D., and Jurasek, L. Vol. 181: ACS. p145-158.
7. Sjöström, E. (1993). "Wood Chemistry: Fundamentals and Applications, 2nd ed." Academic Press. San Diego (CA).
8. Smook, G.A. (1997). "Handbook for Pulp & Paper Technologists, 2nd edition, ." Angus Wilde Publications Inc. Bellingham, WA, 1997. p.17.
9. Billmeyer, F.W. (1962). "Textbook of Polymer Science ": Wiley Interscience. Newyork. 146.
10. Haas, D.W., Hutfiord, B. F., and Sarkane, K. V. (1967). "Kinetic study on the alkaline degradation of cotton hydrocellulose." J. Appl. Polymer Sci., **11**: 587-600.
11. Barzyk, D., Page, D. H., and Ragauskas, A.(1997) "Carboxyl Acid Groups and Fiber Bonding". in Transactions of 11th Fundamental Research Symposium Cambridge: Pira International: p. 893-908.
12. Adler, E. (1977). "Lignin chemistry-past, present and future." Wood Sci. Technol., **11**: 169-218.
13. Salmén, L. (1985). "Cellulose chemistry and its applications." Mechanical properties of wood fibres and paper, ed. T.P.a.H.Z.S. Nevell: Ellis Horwood Limited. England. pp. 505-530.

14. Hafrén, J., Fujino, T., Itoh, T., Westermark, U. and Terashima, N. (2000). "Ultrastructural changes in the compound middle lamella of *Pinus thunbergii* during lignification and lignin removal " Holzforschung, **54**(3): 234-240.
15. Côté, W.A., Jr. (1967). "Wood Ultrastructure: an atlas of micrographs." University of Washington Press. Seattle, USA.
16. Petri, K., and Yongzhong, Y.(1997) "Fiber Properties and Paper Fracture – Fiber Length and Fiber Strength". in The Fundamentals of Papermaking Materials, Transactions of the 11th Fundamental Research Symposium. Cambridge: Pira International: p. p.521-545.
17. Page, D.H., EI-Hosseiny, F., Winkler, K. (1977). "Elastic modulus of single wood pulp fibers." Tappi, **60**(4): 114.
18. Page, D.H., EI Hosseiny, F., Winkler, K., and Rain, R. . (1972). "The mechanical properties of single wood pulp fibers. Part1. A new approach." Pulp and Paper Magazine of Canada, **73**(8): T198-T203.
19. Page, D.H., Seth, R. S., and EI Hosseiny, F.(1985) "Strength and Chemical Composition of Wood Pulp Fibers". in Transactions of the Eight Fundamental Research Symposium Oxford: Pira International: p. p.77.
20. Berthold, J.a.S., L. (1997). "Effects of Mechanical and Chemical Treatments on the Pore Size Distribution in Wood Pulps Examined by Inverse Size-Exclusion Chromatography." J. Pulp Paper Sci., **23**(6): 245-253.
21. Stone, J.E., and Scallan, A. M. (1968). "A Structural Model for the Cell Wall of Water-Swollen Wood Pulp Fibers Based on their Accessibility to Macromolecules." Cellulose Chem. Technol., **2**(3): 343-358.
22. Thorpe, J.L., Mark, R. E., Eusufzai, A. R. K., and Perkins, R. W. (1976). "Mechanical Properties of Fiber Bonds." Tappi, **59**(5): 96-100.
23. Misovec, P., Krkoska, P. . (1987). "Investigation of the Bonding Strength of Pulp Fibers." Papir a Celuloza, **42**(3): 16-20.
24. Page, D.H.(1989). in Fundamentals of Papermaking. London: Pira International: p. p.18.
25. Rutulainen, E., Niskanen, K., and Nilsen, N. (1998). "Paper Physics." Papermaking Science and Technology, ed. J. Gullichsen, and Paulapuro, H.: Fapet Oy. Jyvaskylan, Filand. p. 62.
26. Smook, G.A. (1997). "Handbook for Pulp & Paper Technologists, 2nd edition, ." Angus Wilde Publications Inc. Bellingham, WA, 1997. p.205.

27. Mohlin, U.-B. (1974). "Cellulose Fiber Bonding." Svensk Papperstidn., **77**: 131-177.
28. Skowronski, J., and Bichard, W. (1987). "Fibre-to-Fibre Bonds in Paper. Part 1. Measurement of Bond Strength and Specific Bond Strength." J Pulp Paper Sci, **13**(5): J165-J169
29. Nordman, L.(1954) "Bonding in Paper Sheets. " in Transactions of the Ist Fundamental Research Symposium. Cambridge: FRC.
30. Page, D. (1969). "A Theory for the Tensile Strength of Paper." Tappi, **54**(4): 674-183
31. Mayhood, C.H., Kallmes, O. J., and Cauley, M. M. (1962). "The mechanical Properties of Paper Part2. Measured Shear Strength of Individual Fiber to Fiber Contacts." Tappi, **45**(1): 69-73
32. Pruett, R.J., and Pickering, Jr. S. M. (2006). "Kaolin." 7th ed. Industrial Minerals and Rocks, ed. J.E. Kogel, Trivedi, N. C., Barker, J. M., and Krukowski, S. T.: Society for Minding, Metallurgy, and Exploration. Littleton, Colorado.
33. Krogerus, B. (1999). "Papermaking Chemistry." Papermaking Science and Technology, ed. J. Gullichsen, and Paulapuro, H.: Fapet Oy. Jyvaskyla, Filand. 117-149.
34. Drage, G., and Tamms, O. (2000). "Kaolin." Pigment Coating and Surface Sizing of Paper, ed. E. Lehitnen. Vol. 11: Fapet Oy. Helsinki, Filand. p68-93.
35. Neimo, L.(1985) "Internal sizing of printing paper " . in PAPEX-85 International Conference and Exhibition Leatherhead, England: PIRA.
36. Brown, R. (1998). "Particle Size, Shape and Structure of Paper Fillers and Their Effect on Paper Properties." Paper Technology, **39**(2): 44-48.
37. Kubelka, P., and Munk, F.,Z. (1931). "Ein beitrag zur optik der farbanstriche." Tech. Physik, **12**: 593.
38. Schott, H. (1971). "Adhesion of Montmorillonite Clay to Cellulose and Effect of Particulate Fillers on Mechanical Properties of Paper." Tappi, **54**(5): 748-753.
39. Fineman, I., Bergenblad, H., and Pauler, N. (1990). "Influence of Fillers on the Pore Structure of Paper." Papier, **44**(10A): 39-51.
40. Maron, S.H., Lando, J. B. (1974). Fundamentals of Physical Chemistry: Macmillan. 775-799.

41. Gill, R.A. (1989). "The Behavior of On-Site Synthesized Precipitated Calcium Carbonate and Other Calcium Carbonate Fillers on Paper Properties." Nord.Pulp Pap.Res.J, **4**(2): 120.
42. Gill, R., and Scott, W. (1987). "The Relative Effects of Different Calcium Carbonate Filler Pigments on Optical Properties." Tappi, **70**(1): 93-99.
43. Brown, R. (1983). "The Effect of Particle Size and Shape of Paper Fillers on Paper Properties." Wochenbl. Papierfabr., **111**(20): 737-740.
44. Fairchild, G.H. (1992). "Increasing the filler content of PCC-filled alkaline papers." Tappi, **75**(8): 85-90.
45. Brown, R. (1996). "Physical and Chemical Aspects of the Use of Fillers in Paper." 2nd ed. Paper Chemistry, ed. J.C. Roberts: Blackie. London. 194-230.
46. Norell, M., Johansson, K., and Persson, M. (1999). "Papermaking Chemistry." Papermaking Science and Technology, ed. L. Neimo. Vol. 16: Fapet Oy. Helsinki, Filand. 42-81.
47. Bleier, A., and Goddard, E.D. (1980). "Flocculation of aqueous silica suspensions using cationic polyelectrolytes " Colloids and Surfaces, **1**(3/4): 407.
48. Yoon, S., and Deng. Y. (2004). "Flocculation and Reflocculation of Clay Suspension by Different Polymer System under Turbulent Conditions." J. Colloid & Interf. Sci., **278**(1): 139.
49. Doiron, B.E. ("Retention of Fines and Fillers During Papermaking." Retention Aid Systems, ed. J. M.Gess: TAPPI Press. Atlanta. 159-176.
50. Wagberg, L., and Lindstrom, T. (1987). "Flocculation of Cellulosic Fibers by Cationic Polyacrylamides with Different Charge Densities." Nord.Pulp Pap.Res.J, **4**: 152-160
51. Fan. A., T., N.J., and Somasundaran, P. (2000). "A Study of Dual Polymer Flocculation." Colloids and Surfaces A: Physicochemical and Engineering Aspects, **162**: 141-148
52. Yoon, S., *A Study on flocculation kinetics and shear resistance of polymer induced clay flocculation and its preflocculation effect on paper sheets* 2003, Institute of Paper Science and Technology: Atlanta
53. Iivessalo-Pfaffli, M., S. (1977). "in Puukemia." ed. W.Jensen: Polytypos. Turku, Filand. 400.
54. Swerin, A., Risinger, G. and Odberg, L. (1997). "Flocculation in Suspension of Microcrystalline Cellulose by Microparticle Retention Aid System." J. Pulp Paper Sci., **23**(8): J374-381

55. Thomas, R., J. (1991). "in Wood Structure and Composition." ed. M.L.a. I.S.Goldstein. Vol. chapter 2: Marcel Dekker. New York, U.S.A.
56. Lindstrom, T.a.G.-N., G. (1984). "Network Flocculation and Fractionation of Latex Particles by Means of a Polyethyleneoxide-Phenolformaldehyde Resin Complex." J. Colloid Interaction Sci., **97**: 62.
57. Pelton, R.H., Allen, L.H., and Nugent, H.M. (1981). "Novel Dual-Polymer Retention Aids for Newsprint and Ground Specialities." Tappi J., **64**(11): 89.
58. Goto, S.a.P., R. (1999). "The Influence of Phenol Cofactor on the Properties of Calcium Carbonate Flocs Formed with PEO." Colloid and Surfaces, A : Physicochemical and Engineering Aspects, **155**: 231-239.
59. Xiao, H., Pelton, R. and Hamielec, A. (1996). "Retention Mechanism for Two-Component Systems Based on Phenolic Resins and PEO or New PEO-Copolymer Retention Aids." J. Pulp Pap. Sci., **22**(12): J475-J485.
60. Tam Doo, P.A., Kerekes, R.J. and Pelton, R.H. (1984). "Estimates of Maximum Hydrodynamic Shear Stress on Fiber Surfaces in Papermaking." J. Pulp Paper Sci., **10**(4): J80.
61. Smith, D.K.W., and Kitchener, J.A. (1978). "The strength of aggregates formed in flocculation " Chemical Eng. Sci., **33**: 1631.
62. Gregory, J. (1988). "Polymer Adsorption and Flocculation in Sheared Suspensions." Colloid and Surfaces, **31**: 231-253.
63. Sikora, M.D.a.S., R.A. (1981). "The Shear Stability of Flocculated Colloids." Tappi, **64**(11): 97.
64. Hedborg, F.a.L., T. (1996). "Some Aspects on the Reversibility of Flocculation of Paper Stocks." Nordic Pulp Paper Res. J., **11**(4): 254.
65. Farnwood, P.R., Dodson, C.T.J. and Lowen, P.R.(1993) "Forming and formation of paper". in Proc. 10th Fund Res.Symp. Oxford: p. 183
66. Marton, J. (1996). "Dry-strength additives." Paper Chemistry, ed. J.C. Roberts: Chapman & Hall. New York. 63-75.
67. Bobacka, V., Nasman, J., and Eklund, D. . (1998). "Interactions between cationic starch and anionic trash of a peroxide-bleached TMP at different salt concentration." J. Pulp & Paper Sci., **24**(3): 78.
68. Hubbe, M.A.(1999) "Difficult Furnishes ". in TAPPI Papermakers Conference. Atlanta: p. 1353-1367.

69. Brouwer, P.H. (1996). "Starches for Surface Sizing and Wet-End Addition,1." Woch. f. Paper, **124**(1): 19.
70. Roberts, J.C., Au, C.O., Clay, G.A., and Lough, C. . (1987). "Study of the Effect of Cationic Starch on Dry Strength and Formation Using Carbon-14 Labeling." J. Pulp Paper Sci., **13**: J1-J8
71. Eklund, D., and Lindstrom, T. (1991). "Paper Chemistry - An Introduction." DT PAPER SCIENCE. Grankulla, Finland. 299.
72. C.E.Farley.(1993) "role of electrokinetics in papermaking". in Papermakers Conference Proceedings. Atlanta (TAPPI PRESS: p. 1.
73. Aloï, F.G. (1998). "Retention of Fines and Fillers During Papermaking." Retention in Neutral and Alkaline Papermaking, ed. J.M. Gess: TAPPI Press. Denvers, USA. p. 63.
74. Triksak, R.M.(1991). in TAPPI Papermakers conference: TAPPI PRESS: p. 236.
75. Odberg, L., Tanaka, H., and Swerin, A. (1993). "Kinetic Aspects of the Adsorption of Polymers on Cellulosic Fibers." Nordic Pulp Paper Res. J., **8**(1): 6.
76. Koethe, J., and Scott, W.(1993) "Polyelectrolyte Interactions with Papermaking Fibers: Mechanism of Surface Charge Decay". in TAPPI Papermakers Conference Proceedings: TAPPI PRESS: p. 569.
77. Brooks, K., and Meagher, J. . (1982). "Increasing Role of Calcium Carbonate in the Paper Industry." Paper, **198**: 25-27
78. Hayes, A.J. (1985). "Forty Percent Filler-Loaded Paper: Dream or Reality?" Paper Technology and Industry **26**: 129
79. Smith, D.E., *Producing Dispersion of Preflocculated Fillers for Use in Papermaking*, in *U. S. Pat. 4295933*. p. 1981.
80. Mabee, S., and Harvey, R.(2000) "Filler Flocculation Technology – Increasing Sheet Filler Content Without Loss in Strength or Runnability Parameters". in TAPPI Papermakers Conference: TAPPI Press: p. pp. 797-810.
81. Mabee, S.W.(2001) "Controlled Filler Preflocculation: Improved Formation, Strength and Machine Performance". in TAPPI Papermakers Conference Cincinnati, OH: TAPPI Press: p. 1129
82. Gill, R.A., *Cationic Polymer Modified Filler Material, Process for Its Preparation and Method for Its Use in Papermaking*, in *Can. Pat. .* 1995.
83. Kuboshima, K. (1982). "Part 1. Highly Filler-Containing Paper." High Perform Paper Soc (Jpn), **21**: 31-38.

84. Aho, O., Silenius, P., Pitkanen, M., and Hietanen, S. , *Filler and a Process for the Production thereof*, in *Can. Pat.* . 2002. p. .
85. Gill, R.A., *Cationic Polymer-Modified Filler Material, Process for Its Preparation and Method for its Use in Papermaking*. 1992: USA.
86. Novak, J., Stark, K, and Eichinger, R. (1987). "The influence of Filler Pretreatment on Paper." Paper (London), **207**(3): 22-24.
87. Park, S.H., and Shin, D.S. . (1987). "Effects of the Preflocculated Domestic Fillers on the Strength and Optical Properties in Highly-Filled Papermaking." J. Korean Tappi, **19**(3): 44-61
88. Koper, G.J.M., Vanerek, A. and Van De Ven, T.G.M. (1999). "Poly(Polypylene Imine) Dendrimers as Retention Aid for the Depositon of Calcium Carbonate on Pulp Fibers." J. Pulp & Paper Sci., **25**(3): 81-83.
89. Vanerek, A., Alince, B and Van De Ven T.G.M. (2000). "Interaction of Calcium Carbonate Fillers with Pulp Fibers : Effect of Surface Charge and Cationic Polyelectrolytes." J. Pulp & Paper Sci., **26**(9): J317- 322
90. Dunham, A., Jakubowski, R., Govoni, S. and Pruszynski, P. .(1999) "Filler Retention – Recent Challenges and Possible Solution". in TAPPI Papermakers Conference: p. 1327-1334.
91. Green, H.V., Fox, T. J., and Scallan, A. M. . (1982). "Lumen-Loaded Paper Pulp." Pulp Paper Can., **83**: 203 1982.
92. Middleton, S.R., and Scallan, A. M. . (1985). "Lumen-Loaded Ppaer Pulp: Mechanical of Filler-to-Fiber Bonding." Colloids Surf, **16**: 309-332
93. Miller, M.L., and Paliwal, D. C. . (1985). "Effects of Lumen-Loading on Strength and Optical Properties of Paper." J. Pulp Paper Sci., **11**: 84.
94. Jenkins, P.J.a.D., A. M. (1996). "Application of small-angle neutron scattering to the study of the structure of starch granules." Polymer, **37**: 5559-5568.
95. Jenkins, P.J., Cameron, R. E., and Donald, A. M. (1993). "A uiversal feature in the structure of starch granules from different botanical sources " Starch, **45**: 417-420.
96. Wu. H. C. H. and Sarko, A. (1978). Carbohydr. Res., **61**(7-25).
97. Wu. H. C. H. and Sarko, A. (1978). Carbohydr. Res., **61**: 27-40.
98. Wurzburg, O.B. and C.D. Szymanski. (J. AGR. FOOD CHEM., **18**: 997 1970.
99. Mizuno, A., M. Mitsuiki, and M. Motoki. (J. Agric. Food Chem., **46**: 98 1998.

100. Tester, R.F.a.M., W. R. (1990). "Swelling and gelatinisation of cereal starches. 1. Effect of amylopectin, amylose, and lipids." Cereal Chem, **67**: 551-557.
101. Dunnill, P., and Lilly, M. D. (1967). Process. Biochem, **2**(7): 13.
102. P. R. Foster, P.D., and M. D. Lilly. (1971). Biotechnol. Bioeng., **13**: 713.
103. Chan, M.Y.Y., Hoare, M. and Dunnill, P. . (1986). "The Kinetics of Protein Precipitation by Different Reagents." Biotechnol. Bioeng., **28**(3): 387-393.
104. Foster, P.R., Dunnill, P., and Lilly, M. D. (1976). "The Kinetics of Protein Salting-Out: Precipitation of Yeast Enzymes by Ammonium Sulfate." Biotechnol. Bioeng., **18**: 545-580.
105. Khairy, M., Morsi, S. and Sterling, C. (1963). "Crystallization in Starch." J. Polymer Sci. Part A, **1**: 3547-3559.
106. Samec, M. (1936). Kolloid-Beih., **43**: 272.
107. Frank, H.S., and W.-Y. Wen. (1957). "Structural Aspects of Ion-Sovent Interaction in Aqueous Solutions: A Suggested Picture of Water Structure." Discussions Faraday Soc., **24**: 133.
108. Cushing, M.L., and Schuman, K. R. (1959). Tappi, **42**: 1006
109. Gaspar, L.A., in *TAPPI Ann Mtg Proc* p. 89 1982.
110. Zhao, Y., Hu, Z., Ragauskas, A. and Deng. Y. (2005). "Improvement of Paper Properties Using Starch-Modified Precipitated Calcium Carbonate Filler." Tappi, **4**(2): 3-7.
111. Hernandez, H.R., Bana, A. N., Greif, D. S., and Thornton, D. S. , in *U.S. Pat.* . 1977.
112. Hu, Z., and Deng, Y. . (2004). Powder Tech., **140**: 10.
113. Kiyoshi, K., Yasunori, N., Yashiro, O., and Kazuto, T. , U.S.P. 6190633, Editor. 2001.
114. Mathur, V.K., in *Int. Pat. Applic. WO 01/14274*. 2001.
115. Katz, J.R., and Itallie, T. B. . (1930). Z. physik. Chem., **A150**: 90.
116. Bear, R.S. (1942). "The Significance of the "V" X-Ray Diffraction Patterns of Starches." J Am Chem Soc: 1388-1392.
117. Bear, R.S. (1944). "Complex Formation between Starch and Organic Molecules." J. Am. Chem. Soc., **66**: 2122 1944.

118. Senti, F.a.W., L. (1946). "Oriented Filaments of Amylose and Alkali Amylose." J Am Chem Soc, **68**: 2407-2408.
119. Mikus, F.F., Hixon, R. M., and Rundle, R. E. . (1946). "The Complexes of Fatty Acids with Amylose." J. Am. Chem. Soc., **68**: 1115 1946.
120. Rundle, R.E., and French, D. (1943). "The Configuration of Starch and the Starch-Iodine Complex. 2. Optical Properties of Crystalline Starch Fractions." J Am Chem Soc, **65**: 558-561.
121. rundle, R.E., and French, D. (1943). "The Configuration of Starch in the Starch-Iodine Complex. 3. X-Ray Diffraction Studies of the Starch-Iodine Complex." J Am Chem Soc, **65**: 1707-1710.
122. Rundle, R.E. (1947). "The Configuration of Starch in the Starch-Iodine Complex. 5. Fourier Projections from X-Ray Diagrams." J Am Chem Soc, **69**: 1769-1772.
123. Rundle, R.E., and Baldwin, R. R. (1943). "The Configuration of Starch and the Starch-Iodine Complex, I. The Dichroism of Flow of Starch-Iodine Solutions." J. Am. Chem. Soc., **65**: 554-558.
124. Talyor, T.C., and Nelson, J. M. . (1920). "Fat Associated with Starch." J Am Chem Soc, **42**: 1726-1738.
125. Talyor, T.C., and Sherman, R. (1933). "Carbohydrate-Fatty Acid Linkings in Corn Alpha Amylose." J Am Chem Soc, **55**: 258-264.
126. Schoch, T.J. (1938). "Absence of Combined Acid in Cereal Starches." J Am Chem Soc, **60**: 2824-2825.
127. Lehrman. (1942). "The Nature of the Fatty Acids Association with Starch. The Adsorption of Palmitic Acid by Potato and Defatted Corn and Rice Starches." J Am Chem Soc, **64**: 2144-2146.
128. Biliaderis, C.G., and Galloway, G. (1989). "Crystallization Behavior of Amylose V Complexes: Structure-Property Relationships." Carbohydr. Polym., **189**: 31-48.
129. Rundle, R.E. (1943). "The Configuration of Starch in the Starch-Iodine Complex. IV. An X-Ray Diffraction Investigation of Butanol-Precipitated Amylose." J Am Chem Soc, **65**(11): 2200-2203
130. Yamashita, Y. (1965). "Single Cryeta16 of Amylose v Complexes." J Polym Sci, Part A, **3**: 3251-3260.
131. Schoch, T.J., and Williams, C. B. (1944). "Adsorption of fatty acids by the linear component of corn starch." J Am Chem Soc, **66**: 1232

132. Godet, M.C., Buleon, A., Tran, V., and Colonna, P. (1993). "Structural Features of Fatty Acid-Amylose Complexes." Carbohydrate Polymers, **21**: 91-95.
133. Biliaderis, C.G., and Tonogai, J. R. (1991). "Influence of Lipids on the Thermal and Mechanical Properties of Concentrated Starch Gels." J. Agr. Food. Chem., **39**: 833-840.
134. Godet, M.C., Bizot, H., and Buleon, A. (1995). "Crystallization of Amylose-Fatty Acid Complexes Prepared with Different Amylose Chain Lengths." Carbohydr. Polym., **27**: 47-52.
135. Karkals, J.a.M., S., Morrison, W. R., and Pethrick, R. A. (1995). "Some Factors Determining the Thermal Properties of Amylose Inclusion Complexes with Fatty Acids " Carbohydr. Res., **268**: 233-247.
136. Kowblansky, M. (1985). "Calorimetric Investigation of Inclusion Complexes of Amylose with Long-Chain Aliphatic Compounds Containing Different Functional Groups." Macromolecules, **18**: 1776-1779.
137. Raphaelides, S., and Karkalas, J. (1988). "Thermal Dissociation of Amylose-Fatty Acid Complexes." Carbohydr. Res., **172**: 65-82.
138. Fanta, G.F., Shogren, R. L., and Salch, J. H. (1999). "Steam Jet Cooking of High-Amylose Starch-Fatty Acid Mixture. An Investigation of Complex Formation." Carbohydr. Polym., **38**: 1-6.
139. Fanta, G.F., and Eskins, K. (1995). "Stable Starch-Lipid Compositions Prepared by Steam Jet Cooking." Carbohydr. Polym., **28**: 171-175.
140. Karkals, J., and Raphaelides, S. . (1986). "Quantitative Aspects of Amylose-Lipid Interactions." Carbohydr. Res., **157**: 215-234.
141. Lebail, P., Buleon, A., Shiftan, D., and Marchessault, R. H. (2000). "Mobility of Lipid in Complex of Amylose-Fatty Acids by Deuterium and 13C Solid State NMR." Carbohydr. Polym., **43**: 317-326.
142. Snape. C. E., M., W. R., Maroto-V, M., Karkalas, J., and Pethrick, R. A. . (1998). "Solid State 13C NMR Investigation of Lipid Ligands in V-Amylose Inclusion Complexes." Carbohydr. Polym., **36**: 225-237.
143. Veregin, R.P., and Fyfe, C. A. (1987). "Investigation of the Crystalline "V" Amylose Complexes by High- Resolution 13C CP/MAS NMR Spectroscopy " Macromolecules, **20**: 3007-3012.
144. Godet, M.C., Tran, P., Colonna, P., and Buleon, A. (1995). "Inclusion/ Exclusion of Fatty Acids in Amylose Complexes as a Function of the Fatty Acid Chain Length." Int. J. Biol. Macromol., **17**: 405-408.

145. Yoon, S., and Deng, Y. . (2006). "Clay-starch composites and their application in papermaking." J. Appl. Polym. Sci., **100**(2): 1032-1038
146. D. S. Jackson, C.C.-O., R. D. Waniska, and L. W. Rooney. (1988). "Characteristics of Starch Cooked in Alkali by Aqueous High-Performance Size-Exclusion Chromatography." Cereal Chem, **65**(6): 493-496.
147. Greenwood, W.B.a.C.T. (1972). "The Conformation of Amylose in Alkaline Salt Solution." Carbohydr. Res., **21**: 229-234.
148. Biermann, C.J. (1993). "Essentials of Pulping and Papermaking." Academic Press. San Diego, California. p. 190.
149. Bown, R. (1998). Paper Technology, **39**(2): 44.
150. Hubbe, M.A., and Gill, R.A., (2004) "Filler particle shape vs. paper properties - A review". in TAPPI Paper Summit- Spring Technical and International Environmental Conference Atlanta: TAPPI PRESS: p. 141-150.
151. Washburn, E.W. (1921). "The dynamics of capillary flow." Phys. Rev., **2**(17): 273-283.
152. Rosenau, T., Potthast, A., Sixta, H., and Kosma, P. . (2001). "The Chemistry of Side Reactions and Byproduct Formation in the System NMMO/Cellulose (Lyocell Process)." Prog. Polym. Sci., **26**: 1763-1837.
153. Rosenau, T., Potthast, A., Sixta, H., and Kosma, P. (2002). "Radicals derived from N-methylmorpholine-N-oxide(NMMO):structure, trapping, and recombination reactions." Tetrahedron, **58**: 3073-3078.
154. Rosenau, T., Potthast, A., Adorjan, I., Hofinger, A., Sixta, H., Firgo, H., and Kosma, P. (2002). "Cellulose Solutions in N-methylmorpholine-N-oxide(NMMO) -Degradation Processes and Stabilizers." Cellulose, **9**: 283-291.
155. Rosenau, T., Potthast, A., Hofinger, A., Sixta, H., and Kosma, P. (2002). "Instabilities in the System NMMO/Water/Cellulose (Lyocell Process) Caused by Polonowski Type Reactions." Holzforschung, **56**: 199-208
156. Rosenau, T., Potthast, A., Kosma, P., and Chen, C. I. . (1999). "Autocatalytic Decomposition of N-methylmorpholine-N-oxide Induced by Mannich Intermediates." J. Org. Chem., **64**: 2166-2167.
157. Turbak, A.F., et al., in *U.S. Patent*. p. 1981.
158. Cuculo, J.A. and S. Hudson, M., in *U.S. Patent*. p. 1983.

159. Hattori, M., Koga, T., Shimaya, Y., and Saito, M. (1998). "Aqueous calcium thiocyanate solution as a cellulose solvent, structure and interactions with cellulose." Polym J, **30**: 43-48.
160. Hattori, M., Shimaya, Y., and Saito, M. (1998). "Solubility of dissolved cellulose in aqueous calcium- and sodium thiocyanate solution." Polym J, **30**: 49-55.
161. Johnson, D.C., and Nicholson, M.D., *Solvent system for polysaccharides in U.S. Patent*. 1978, Institute of Paper Science and Technology.
162. Graenacher, C., and Sallman, R., *Cellulose solution and process of making same*, in *U.S. Patent*. 1939.
163. Johnson, D.L., *Process for strengthening swellable fibrous material with an amine oxide and the resulting material*, in *U.S. Patent*. 1969.
164. Cox, H.L. (1952). "The elasticity and strength of paper and other fibrous material." Br. J. Appl. Phys., **3**(3): 72-79.
165. Kallmes, O., Bernier, G., and Peres, M. (1977). "Mechanistic theory of the load-elongation properties of paper (2) characteristics of fiber characteristics of fibers taken into account " Paper Technology, **18**(7): 222.
166. Ruvo, A.D., Fellers, C., and Kolseth, P. (1986). "Descriptive Theories for the Tensile Strength of Paper." Paper-Structure and Properties, ed. J.A.B.a.P. Kolseth: Marcel Dekker, INC. New York. 267-279.
167. Retulainen, E., Ebeling, K., . . (1993). "Fibre-fibre bonding and ways to characterize the bond strength." Appita **46**, **46**(4): 282-288.
168. Nordman, L.S.(1957) "Bonding in Paper Sheets". in Transactions of the Second Fundamental Research Symposium Cambridge,, London, U.K.: British Paper and Board Makers Association: p. 333.
169. Davison, R.W. (1972). "The weak link in paper dry strength." Tappi, **55**(4): 567-573.
170. Page, D.H. (1960). "A theory for tensile strength of paper." Paper Tech., **1**(4): T165.
171. Stone, J.E. (1963). Pulp Pap. Mag. Can., **64**(12): T528.
172. Asunmaa, S., and Steenberg, B. (1958). "Beaten pulps and the fibre-to-fibre bond in paper." Sven. Papperstidn, **61**(18b): p.686-695.
173. Jayme, G., and Hunter, G. (1962). "Formation and Structure of Paper ", ed. F. Bolam: BPBMA. London. 135-170.

174. Yang, C.-F., A. R. K. Eusufzai, R. Sankar, R. E. Mark and R. W. Perkins. (1978). "Measurements of Geometrical Parameters of Fiber Networks." Sven. Papperstidn, **81**(13): 426-433.
175. Ingmanson, W.a.E.T. (1959). "Factors Contributing to the Strength of a Sheet of Paper II: Relative Bonded Area." Tappi, **42**(1): 83-93.
176. A. P. Schniewind, L.J.N., and D. L. Brink. (1964). "Fiber and Pulp Properties 1. Shear Strength of Single-Fiber Crossings." Tappi, **47**(4): 244-248.
177. McINTOSH, D.C. (1963). "Tensile and Bonding Strengths of Loblolly Pine Kraft Fibers Cooked to Different Yields." Tappi, **46**(5): 273-277
178. Mohlin, U.-B. (1975). "Cellulose Fibre Bonding Part3. The Effect of Beating and Drying on Interfibre Bonding." Sven. Papperstidn, **78**: 338-341.
179. Leech, H.J. (1954). "An Investigation of the Reasons for Increase in Paper Strength When Locust Bean Gum is Used as a Beater Adhesive." Tappi, **37**(8): 343
180. Riddell, M.C., Jenkins, B., Rivers, A., and Waring, I. . (1976). "Developments at Paper Mills. ." Paper Technology, **17**: 76-85.
181. Yan, Z., Liu, Q., Deng, Y., and Ragauskas, A. (2005). "Improvement of Paper Strength with Starch Modified Clay." J. App. Poly. Sci., **97**(1): 44-50
182. Yoon, S., and Deng, Y. (2006). "Starch-Fatty Complex Modified Filler for Papermaking." Tappi, **5**(9): 1-9
183. Garg, P., and Scott, W. E.(2001) "Potential Application of Predictive Tensile Strength Models in Paper Manufacture: Part 1 - Development of a Predictive Tensile Strength Model from the Page Equation". in TAPPI Papermakers Conference Cincinnati, OH: TAPPI Press: p. 829.
184. Gorres, J., Amri, R., Wood, J. R., and Karnis, A. (1995). "The shear bond strength of mechanical pulp fibers." J. Pulp Paper Sci., **22**(5): J161
185. Krkoska, P., Olos, P., Misovec, P., and Pirozek, J. (1989). "Paper Characterization of pulp fibres. V. Modification of Paper Fomula for describing tensile strength of paper by funtional fibre parameters." Cellulose Chem. Technol., **23**: 609
186. Beazley, K.M., Dennison, S. R., and Talyor, J. H. (1979). "Influence of Mineral Fillers on Paper Strength: Its Mechanism and Practical Means of Modification." Preprints ESPRA European Meeting, 11th: 217
187. Dasgupta, S. (1994). "Mechanism of paper tensile-strength development due to pulp beating." Tappi, **77**(6): 158-166.

188. Mohlin, N.H.a.U.-B. (1975). "Cellulose Fibre Bonding Part 2. Influence of pulping on interfibre bond strength." Sven. Papperstidn, **78**: 295-299.
189. Xu, Y., Chen, X., and Pelton, R. (2005). "How polymers strengthen filled papers." Tappi, **4**(11): 8-12.
190. Xu, Y.a.P., R. (2005). "A new loo at how fines influence the stregh of filled papers." J. Pulp Paper Sci., **31**(3): 147-152
191. Koubaa, A., and Koran, Z. (1995). "Measure of the Internal Bond Strength of Paper/ Board." Tappi, **78**(3): 103-111.
192. Li, L., Collis, A., and Pelton, R. . (2002). "A New Analysis of Filler Effects on Paper Strength." J. Pulp Paper Sci., **28**(8): 267-273
193. Carson, F.T., Worthington, V. (1952). "Stiffness of Paper." J. Research of the National Bureau of Standards, **49**: 385-391.
194. Verseput, H.W. (1969). "Precision of the Tabler Stiffness of Paper." Tappi, **52**: 1136-1141.
195. Nanko, H.(2003) "Bond Strength Enhancement Mechanism of Cationic Starch and Cationic Polyacrylamide". in International Paper Physics Conference. Victoria, BC, Canada: TAPPI Press: p. 127.